

**EVALUATION OF PERFORMANCE AND EMISSION PARAMETERS OF
CI ENGINE FUELLED WITH POLANGA BIODIESEL BLENDS USING
ANN MODELING**

by

ABHISHEK SHARMA

SAP ID.: 500024039

COLLEGE OF ENGINEERING STUDIES

**IN PARTIAL FULFILLMENT OF THE DEGREE OF
DOCTOR OF PHILOSOPHY**

Under the Guidance of

Dr. P.K. SAHOO
Sr. Associate Professor
UPES

Dr. R.K. TRIPATHI
Associate Professor
UPES

Dr. L.C. MEHER
Scientist-D, DRDO

Submitted to



UNIVERSITY OF PETROLEUM AND ENERGY STUDIES

DEHRADUN

OCTOBER, 2015

CERTIFICATE

The thesis entitled “**Evaluation of Performance and Emission parameters of CI engine fuelled with polanga biodiesel blends using ANN modeling**”, being submitted by **Abhishek Sharma** to the University of Petroleum and Energy Studies for the award of the degree of Doctor of Philosophy is a bonafide research work carried out by him. He has worked under our supervision, and has fulfilled the requirements for the submission of this thesis, which has attained the standard required for a Ph.D. degree from the University. The content of the thesis, in full or parts have not been submitted to any other Institute or University for the award of any other degree or diploma.

(Dr. P. K. Sahoo)
Senior Associate Professor
Department of Mechanical Engineering
College of Engineering Studies
University of Petroleum and Energy Studies,
Dehradun, Uttarakhand 248007,
India

(Dr. L. C. Meher)
Scientist-D
DRDO Army Biodiesel Programme,
DIBER Project Site
Military Farm Road Old Bowenpally
Secunderabad-500011 (AP)

(Dr. R. K. Tripathi)
Associate Professor,
Department of Aerospace Engg.
University of Petroleum and Energy Studies,
Dehradun, Uttarakhand 248007,
India

DECLARATION

I, Abhishek Sharma, student of Ph.D. hereby declare that the thesis titled **“Evaluation of Performance and Emission parameters of CI engine fuelled with polanga biodiesel blends using ANN modeling”** which is submitted by me is my own work and that, to the best of my knowledge and belief, it contains no material previously published or written by another person, nor material which has been accepted for the award of any other degree or diploma of the University or other Institute of higher learning, except where due acknowledgment has been made in the text.

(ABHISHEK SHARMA)

SAP ID: 500024039

ACKNOWLEDGEMENTS

I am extremely grateful to my supervisors Professor Dr. P.K. Sahoo, Professor Dr. R.K. Tripathi and my external supervisor Dr. L.C. Meher for their valuable guidance, ever helping attitude, critical and encouraging comments throughout the completion of this research work.

I am highly thankful to Dr. Kamal Bansal, Dr Rajnesh Garg and all FRC members of UPES for guiding me and also helping me with so many ideas.

I wish to sincerely thank to Dr. Harshdeep Sharma, Associate Professor, Galgotias University, Greater Noida, for his valuable research input and continuous support which have been of great assistance in pursuit of this work.

I am also grateful to my dear friends Mr. Yashvir Singh, Mr. Amit Sharma (UPES), Mr. Deepak Kumar. In addition, I also appreciate the help of lab assistant Mr. Pradeep Kumar and during my research work.

My sincere thanks also go to all other colleagues and the management of the Ideal Institute of Technology, Ghaziabad for contributing to the success of this research in one way or the other.

Due to the preoccupation with the priorities for the research project my parents (Dr. Ram. C. Sharma and Dr. Vasundhra Sharma), also my parents-in-law Mr. S.N Pandey and Bharti Pandey, I also thankful especially my beloved wife Prateeksha were deprived of the privileges and prerogatives which God has bestowed on them. Their patience and kind understanding & cooperation have always been a moral booster for me. I would like to thank my children, Anya and Abhiraj for his selfless support and love.

Last but not the least, I sought inspiration and I owe a great deal to my father Late Shri Sonpal Sharma and my grandmother Late Smt Kashmeri Devi who have unquestionably given their ears for the primrose path in my life. They have taught me, he that ventures not fails not and made me able to face the world. It was my father's and my grandmother's wishing to see me with a doctorate degree. I would prefer to pay homage by dedicating my thesis to my late father and grandmother under whose careful protection I have been able to enjoy my life.

I would like to apologize to those whose names do not figure here, but have helped me during the tenure of my research.

(Abhishek Sharma)

CONTENTS

	Page No.
CERTIFICATE	i
DECLARATION	ii
ACKNOWLEDGEMENTS	iii
CONTENTS	v
EXECUTIVE SUMMARY	x
LIST OF FIGURES	xiii
LIST OF TABLES	xvi
LIST OF SYMBOLS	xviii
LIST OF ABBREVIATIONS	xix
CHAPTER 1	
INTRODUCTION	1-13
1.1 Energy Scenario: Indian Perspective	1
1.2 Energy usage and Environment	2
1.3 Diesel Engines and need of Alternative fuel	3
1.4 Vegetable Oil: Alternative fuel for diesel Engines	4
1.5 Biofuels Policy: Government of India	5
1.6 Polanga “Calophyllum Inophyllum”: An alternative diesel Fuel	7
1.7 Artificial neural networks (ANN) Approach	7
1.7.1 Artificial network operations	9
1.7.2 Training an artificial neural network	11
1.8 Research Objectives	12
1.9 Organization of Thesis	12

CHAPTER 2	LITERATURE REVIEW	14-39
2.1	Introduction	14
2.2	Reviews of available Literature	14
2.2.1	Biodiesel production from vegetable oils	14
2.2.2	Diesel Engine trials and analysis of the results using biodiesel as a fuel	21
2.2.3	Analysis of results and prediction using ANN	32
2.3	Problem statement	38
CHAPTER 3	SYSTEM DEVELOPMENT AND METHODOLOGY	40-79
3.1	Introduction	40
3.2	Production of Polanga (<i>Calophyllum Inophyllum</i>) biodiesel	40
3.2.1	Transesterification for production of Polanga biodiesel	41
3.2.2	Biodiesel production optimization from Polanga oil	42
3.3	Physico-Chemical characterization of Polanga biodiesel	43
3.3.1	Kinematic viscosity measurement	44
3.3.2	Density measurement	44
3.3.3	Calorific value measurement	45
3.3.4	Oxidative stability measurement	45
3.4	Preparation of fuel blends for Engine trial	46
3.5	Selection of diesel Engine for experimental trial	47
3.5.1	Development of Engine test rig	47
3.5.2	In-cylinder pressure	50
3.5.3	Temperature measurement	51
3.5.4	Emission measurement	51

3.5.5 Data acquisition system	54
3.5.5.1 Engine Test Express V5.76	55
3.5.6 Engine test cycles	55
3.6 Testing procedures and the details of the measured parameters	55
3.7 Selection of Engine test parameters	57
3.7.1 Measurement of operating parameters of the test Engine	58
3.7.2 Measurement methods	58
3.7.3 Accuracies and uncertainties of the Experimental results	59
3.7.4 Calibration of instruments	60
3.7.5 Procedure to ensure accuracy of measurement	61
3.8 Artificial neural networks (ANN) Model	62
3.8.1 ANN back propagation algorithm	68
3.8.2 Normalization process for input and output data	69
3.8.3 Training process design	69
3.8.4 Post-training analysis	71
3.8.5 ANN model for variable injection timing	73
3.8.6 ANN model for variable injection pressure	76
3.9 Optimization of Engine parameters	78
CHAPTER 4	RESULTS AND DISCUSSION
	80-130
4.1 Introduction	80
4.2 Physico-Chemical properties of Polanga biodiesel and its blends	80
4.3 Results of Engine trials with varying Injection Timing and Pressure	82
4.3.1 Brake thermal efficiency (BTE)	82
4.3.2 Brake specific fuel consumption (BSFC)	83

4.3.3 Peak cylinder pressure (Pmax)	85
4.3.4 Exhaust gas temperature (EGT)	86
4.3.5 Carbon monoxide (CO)	88
4.3.6 Un-burnt hydrocarbon emission (UHC)	90
4.3.7 Oxides of nitrogen emissions (NOx)	91
4.3.8 Smoke Opacity	93
4.3.9 Carbon dioxide (CO ₂)	94
4.4 ANN modeling of Engine operating parameters	96
4.4.1 Brake thermal efficiency (BTE)	97
4.4.2 Brake specific fuel consumption (BSFC)	99
4.4.3 Exhaust gas temperature (EGT)	101
4.4.4 Peak cylinder pressure (Pmax)	102
4.4.5. Oxides of nitrogen (NOx)	104
4.4.6 Smoke	106
4.4.7 Unburned hydro carbon (UHC)	107
4.4.8 Carbon mono oxide (CO)	109
4.4.9 Carbon dioxide (CO ₂)	110
4.5 Validation of ANN model	112
4.6 Multi-objective optimization of Engine parameters	114
4.6.1 Performance parameters	117
4.6.2 Emission constituents	122
4.6.3 The multi-objective optimization Engine performance and emission constituents	127

CHAPTER 5	CONCLUSION	131-135
5.1 Future scope of work		135
REFERENCES		136-149
APPENDIX		150-164

EXECUTIVE SUMMARY

The endeavour of this study is to analyze the emission and performance characteristics of a single cylinder; four stroke diesel engine using a Polanga biodiesel blends as fuel. The assortment of Polanga biodiesel is based on a widespread review of literature which indicated that this is relatively unexplored fuel for a diesel engine. The experimental investigation is followed by a computational study consisting of modelling using artificial neural network and optimization for forecasting the best possible emission and performance parameters constituents of the diesel engine. The experimental investigation is conducted on a Kirloskar make single cylinder, four stroke diesel engine using Polanga biodiesel blends with diesel as a test fuel. The exhaust emissions and performance characteristics are assessed by operating the diesel engine at altered predetermined fuel injection timings of 15, 19, 23, 27 and 31°bTDC and changed fuel injection pressures of 160 bar, 180, 200, 220 and 240 bar at varying load from zero to full load in steps of 20 percent increments. The exhaust emission constituents measured are unburnt hydrocarbons (UHC), carbon monoxide (CO), carbon dioxide (CO₂), smoke opacity and oxides of nitrogen (NO_x). The performance parameters are brake specific fuel consumption (BSFC), brake thermal efficiency (BTE) and exhaust gas temperature (EGT). The experimental study accomplished provides a very large number of results. But, it is impossible to select the input parameters such as injection timing, injection pressure and blend for obtaining best exhaust emissions and performance and from the diesel engine. Hence, an appropriate computational study is required to be carried out to meet the goal of finding the best grouping of the input parameters under different specific priorities. ANN is used to obtain the output parameters using different input parameters. ANN

modelling is a very complex technique which is capable of modelling different functions and processes. In this study, ANN modelling is developed using the neural network feature of MATLAB (R2010a).

After then developed ANN model is validated using a different set of input conditions. The selected input variables are: Engine fuel injection timing of 17, 21, 25, 29°bTDC, 100% engine load (3.5Kw.), Polanga biodiesel blend B25 and fuel injection pressure of 180 bar for variable injection timing model. For variable fuel injection pressure model the selected input variables are: fuel injection timing of 23°bTDC, full engine load (3.5Kw.), Polanga biodiesel blend B25 at different fuel injection pressure of 170, 190, 210 and 230 bar. The results obtained through the developed models are compared with those obtained experimentally. The percentage error for all the parameters lies between in the range of 0.47 to 4.58. Also the variation in error for all the parameters is negligible. The mean percentage error for Engine performance parameters BTE, BSFC and EGT are ± 1.85 , ± 2.35 and ± 2.57 % respectively. On the other side mean percentage error for Engine emission parameters UHC, NO_x, CO₂ and CO are ± 1.78 , ± 2.57 , ± 2.79 and ± 2.56 % respectively. The mean percentage error for variable fuel injection timing is $\pm 2.39\%$ and for variable fuel injection pressure is $\pm 2.17\%$. Thus this ANN model depicts the Engine performance and emission parameters quite efficiently and hence can be used as an assessment tool for single cylinder diesel engine when using Polanga based biodiesel as a test fuel.

After ANN modelling has found the best working tool for diesel engine, after then best Engine operating conditions from the point of view of minimizing BSFC, maximising BTE, EGT and proportion of emission from exhaust gas is need to requiried. Thus, multi-objective optimization of Engine exhaust emission and engine

performance characteristics is carried out to find optimum fuel injection timing, fuel injection pressure and Polanga biodiesel blend percentage at full engine load using genetic algorithm (GA) technique for single cylinder Kirlosker make test diesel engine. MATLAB genetic algorithm (GA) toolbox is used for optimization in this study. From this study, it can be observed that B20 Polanga blend shows performance characteristic closest to diesel fuel with all respects. At higher fuel injection timing particularly of 28° bTDC should be the mode of operation when the diesel engine is fuelled with Polanga biodiesel blends. Also, higher fuel injection pressure of 226 bars is preferable for Polanga biodiesel blends due to its relatively higher viscosity of test fuel. The exhaust emission assessment shows that the Polanga biodiesel blend B40 gives least harmful exhaust emissions amongst all the Polanga biodiesel blends. Further, at a higher injection timing of 31° bTDC and injection pressure of 240 bars reasonably reduction of exhaust emissions is observed for B40 blend. The optimal solution for performance parameters is obtained by fuel injection timing 24° bTDC, 233 bar fuel injection pressure and B27 Polanga biodiesel blend. For exhaust emission constituents, one of the optimal solutions is obtained by 19° bTDC fuel injection timing, 231 bar fuel injection pressure and B19 biodiesel blend. Finally optimal solution when different weightages to engine performance and emission parameters is assigned then output are: fuel injection timing 25° bTDC, 235 bar injection pressure and B31 Polanga biodiesel blend.

LIST OF FIGURES

Figure	Page No.
Fig. 1.1: A Basic Artificial Neuron	9
Fig. 1.2: A Simple Neural Network Diagram	10
Fig. 1.3: Simple Network with Feedback and Competition	11
Fig. 3.1: Polanga (<i>Calophyllum inophyllum</i>) seeds and oil	41
Fig. 3.2: Mineral polanga (<i>Calophyllum inophyllum</i>) and Biodiesel	43
Fig. 3.3: Various blends of polanga biodiesel and diesel	47
Fig. 3.4: The Test Engine	48
Fig. 3.5: Three hole injector and the spray cone	49
Fig. 3.6: The eddy current type dynamometer	50
Fig. 3.7: Exhaust gas analyzer and smoke meter	53
Fig. 3.8: The Data Acquisition System	54
Fig. 3.9: Layout of engine test rig	57
Fig. 3.10: Representation of feed forward network for single hidden layer	62
Fig. 3.11: Flow chart for the development and training of ANN network model	63
Fig. 3.12: Different transfer functions	64
Fig. 3.13: Block diagram for training using Levenberg–Marquardt algorithm: E_{k+1} is the current total error, and E_k is the last total error.	71
Fig. 3.14: Predicted and experimental results for testing sets of parameters	72
Fig. 3.15: Schematic representation of ANN model for variable injection timing	74
Fig. 3.16: Network architecture for variable Injection timing	75

Fig.3.17: Schematic representation of ANN model for variable IPs	77
Fig. 3.18: Network architecture for variable Injection pressure	78
Fig. 4.1: Variation of BTE with Injection timing	82
Fig. 4.2: Variation of BTE with Injection pressure	83
Fig. 4.3: Variation of BSFC with Injection timing	84
Fig. 4.4: Variation of BSFC with Injection pressure	84
Fig. 4.5: Variation of Pmax with Injection timing	85
Fig. 4.6: Variation of Pmax with Injection pressure	86
Fig. 4.7: Variation of EGT with Injection timing	87
Fig. 4.8: Variation of EGT with Injection pressure	88
Fig. 4.9: Variation of CO with Injection timings	89
Fig. 4.10: Variation of CO with Injection pressure	89
Fig. 4.11: Variation of UHC with Injection timings	90
Fig. 4.12: Variation of UHC with Injection pressure	91
Fig. 4.13: Variation of NOx with Injection timing	91
Fig. 4.14: Variation of NOx with Injection pressure	92
Fig. 4.15: Variation of smoke opacity with fuel Injection timing	93
Fig. 4.16: Variation of smoke emission with Injection pressure	94
Fig. 4.17: Variation of CO ₂ with Injection timings	95
Fig. 4.18: Variation of CO ₂ with Injection pressure	96
Fig. 4.19: Predicted and experimental results for testing sets of BTE parameters	98
Fig. 4.20: Predicted and experimental results for testing sets of BSFC parameters	100

Fig. 4.21: Predicted and experimental results for testing sets of EGT parameters	102
Fig. 4.22: Predicted and experimental results for testing sets of Pmax parameters	104
Fig. 4.23: Predicted and experimental results for testing sets of NOx parameters	105
Fig. 4.24: Predicted and experimental results for testing sets of Smoke	107
Fig. 4.25: Predicted and experimental results for testing sets of UHC parameters	108
Fig. 4.26: Predicted and experimental results for testing sets of CO parameters	110
Fig. 4.27: Predicted and experimental results for testing sets of CO ₂ parameters	112
Fig. 4.28: Optimization tool problem definition screen	119
Fig. 4.29: MATLAB program showing optimization of engine performance	120
Fig. 4.30: Pareto front for optimization of performance parameters	121
Fig. 4.31: Optimization tool problem definition screen	124
Fig. 4.32: MATLAB program showing optimization of engine emission	125
Fig. 4.33: Pareto front for optimization of emission constituents	126
Fig. 4.34: MATLAB editor	127
Fig. 4.35: Pareto front for optimization of both engine performance and emission	128

LIST OF TABLES

Table	Page No.
Table 3.1: List of equipments and standards used for biodiesel property measurements	46
Table 3.2: Engine specification	49
Table.3.3: Injector specification	49
Table 3.4: Technical Specifications of Exhaust gas analyzer and Smoke Meter	52
Table 3.5: Accuracies and uncertainties associated with various measurements	60
Table 4.1: List of equipment	80
Table 4.2: Properties of Polanga biodiesel and its blends	81
Table 4.3: Comparison between Polanga and Jatropha properties	81
Table 4.4: Correlation coefficients for BTE using different learning algorithms	97
Table 4.5: Correlation coefficients for BSFC using different learning algorithms	99
Table 4.6: Correlation coefficients for EGT using different learning algorithms	101
Table 4.7: Correlation coefficients for Pmax using different learning algorithms	103
Table 4.8: Correlation coefficients for NOx using different learning algorithms	105
Table 4.9: Correlation coefficients for smoke using different learning algorithms	106
Table 4.10: Correlation coefficients for UHC using different learning algorithms	108
Table 4.11: Correlation coefficients for CO using different learning algorithms	109
Table 4.12: Correlation coefficients for CO2 using different learning algorithms	111
Table 4.13: Validation of ANN Model	113
Table 4.14: Upper and Lower Bounds for Constraints	117

Table 4.15: Polynomials for Engine Performance Parameters	118
Table 4.16: Optimal set of solution for Engine Performance Parameters	122
Table 4.17: Polynomials for Engine Performance Parameters	123
Table 4.18: Optimal set of solution for Engine Emission Parameters	126
Table 4.19: Optimal set of solution for different weightages Engine Parameters	130

LIST OF SYMBOLS

%	percent
η	η kinematic viscosity
°C	degree Celsius
°F	degree Fahrenheit
Cal	calorie
cm	centimeter
cSt	centistokes
g	gram
hr	hour
j	joule
kCal	kilocalorie
Kg	kilogram
Kw	kilowatt
L	liters
m	meter
mm	millimeter
min	minutes
MJ	mega joule
ml	milliliters
mg	milligram
RPM	revolutions per minute
W	Watt
wt	wieght

LIST OF ABBREVIATIONS

ASTM	American Society for Testing and Materials
ADC	Analogue to digital converter
ANN	Artificial neural network
aTDC	After top dead centre
BBM	Bold basal medium
BIS	Bureau of Indian standards
BDC	Bottom dead centre
B10	Fuel blend with 10 % Polanga biodiesel
B20	Fuel blend with 20 % Polanga biodiesel
B30	Fuel blend with 30 % Polanga biodiesel
B40	Fuel blend with 40 % Polanga biodiesel
B100	Polanga biodiesel
bTDC	Before top dead centre
BP	Brake power
BTE	Brake thermal efficiency
BSFC	Brake specific fuel consumption
BFGS	Quasi-Newton back propagation
CA	Crank angle
CCD	Central composite design
CFPP	Cloud filter plugging point
CN	Cetane number
CNG	Compressed natural gas
CO	Carbon mono oxide

CO ₂	Carbon dioxide
CV	Calorific value
EGT	Exhaust gas temperature
FAME	Fatty acid methyl esters
FFA	Free fatty acid
FID	Flame ionization detector
HSD	High speed diesel
IARI	Indian Agricultural Research Institute
IEA	International energy agency
IT	Fuel injection timing
IP	Fuel injection pressure
LM	Levenberg Marquardt
min	FPP flat plate photobioreactor
MJ	GC Gas chromatograph
MSE	Mean square error
NO _x	Oxides of nitrogen
P _{max}	Peak cylinder pressure
R	Correlation coefficient
RSM	Response surface methodology
LM	Levenberg Marquardt
SD	Standard deviation
SCG	Scaled conjugate gradient learning algorithm

CHAPTER 1

INTRODUCTION

1.1 ENERGY SCENARIO: INDIAN PERSPECTIVE

The modernization of human civilization from rural societies to affluent urban ones was made possible through the employment of modern technology based on multitude of scientific advances all of which is driven by energy [1]. Globalization and rapid economic growth have resulted in the exhaustive use of energy resources worldwide. In this race, resurging India with rapid economic growth and a large human population is putting huge pressure on global energy supply and environmental sustainability.

Indian per capita energy consumption with 2010 as the baseline is 3.72 times less than global average, but its rate of growth is 2.47 times higher than the global growth rate, making it one of the most energy consuming country [2]. On a cumulative basis, Indian primary energy consumption pie in the global chart has increased from 3.69% in 1990 to 5.62% in 2010 making it the second fastest energy consuming country of the world after China [2, 3]. Hence, it is very much expected that the energy requirements of India are supposed to increase many folds to reach the global average level in the years to come [4, 5].

India needs an abundant and sustainable energy supply in the foreseeable future to maintain an economic growth momentum and a progressive social transformation without jeopardizing the environment. Unfortunately, it has not able to diversify its

energy sources whose sustainability and environmental effect are a factor of great concern. Indian energy sectors are highly dependent on exhaustible energy resources like fossil fuels.

The total primary energy requirement of India, 42.3% is met through coal, 23.6% through oil, 24.5% through renewable sources and the rest through others [6]. The contribution of non-renewable energy like coal and oil towards total primary energy requirements in India has alarmingly increased since last ten years, partly due to installation of a large number of Mega thermal power projects running on coal, natural gas and oil and an exponential increase in terms of numbers as well as variations of automobile fleet that was made available for a billion plus market. Although, coal is mostly indigenous, oil is not. Without any substantial increase in domestic crude oil production over the years and the lack of diversification of energy sources compounded with rapid economic growth has led to an increase in import of crude oil [7, 8]. This heavy dependence of India on non-renewable resources results in faster resource depletion, environmental degradation and a huge economic burden for import of expensive fossil fuels resulting in widening trade deficit [9].

1.2 ENERGY USAGE AND ENVIRONMENT

As discussed earlier, the impact of renewable energy on the environment is minimal. For example, electrical power generation from solar energy does not hamper environment, but if the same electricity is generated from coal fired thermal power plants, it leads to emission of poisonous gases like CO, SO_x and NO_x along with fly ash slurry and several other water, soil and air pollutants resulting in environmental degradation [10].

It is evident that our present energy consumption pattern both at the national and global level is predominantly dependent on non-renewable resources in general

and fossil fuels (coal, oil, natural gas etc.) in specific. This reliability leads to environmental degradation. In order to save the environment, either of the following must be done.

- Reduction in energy consumption.
- A shift in the present sources of energy from more polluting to less polluting and from non-renewable to renewable sources.

As the bulk of the world population today is devoid of basic amenities of life, hence for inclusive, sustainable growth and progressive social transformation, the latter option must be implemented.

1.3 DIESEL ENGINES AND NEED OF ALTERNATIVE FUEL

Projection results for the 30-year period from 1990 to 2020 show that the demand of fossil-fuel will almost increase three times and hence engine emissions create a serious problem. The major cause for high pollution levels, in spite of the stringent emission standards that have been enforced, is the increasing energy demand for all sectors and most extensively the increase in the use of IC engines for mobility and power [11, 12]. As elaborated in the previous sections, a major chunk of imported crude oil derivatives is used as fuel in internal combustion engines. The most popular petroleum fuels are gasoline and diesel, used as motor fuels in spark ignition and compression ignition engines respectively. Amongst them, compression ignition engines have shown their usefulness in power and transportation sectors because of more ruggedness and efficiency and hence play a pivotal role in rural as well as urban Indian economy [13]. With respect to usage, diesel engines are largely favored across a wide spectrum of activities like automotive application, small and decentralized power generation, the prime mover for farm and agricultural machineries, small scale industrial prime mover and so on. Therefore, in Indian context, diesel consumption is

always disproportionately higher than gasoline. It was observed that diesel to gasoline consumption ratio was 4.80 in 2005 which was dropped to 4.31 in 2012. This indicates that the consumption of gasoline is increasing at a faster rate than the consumption of diesel. Still, diesel consumption in India is nearly four and half times higher than gasoline.

Therefore, even a partial substitution of mineral diesel by any renewable and carbon neutral alternative fuel can have a significant positive effect on the economy and environment in terms of reduction in carbon footprints and dependence on imported crude oil. In the light of the apprehensions about the continuing availability of the diesel, stringent environmental norms and impacts due to extensive use in the fast growing Indian economy have necessitated the search for a renewable substitute of diesel [14].

1.4 VEGETABLE OIL: ALTERNATIVE FUEL FOR DIESEL ENGINES

Vegetable oils are the plant origin bio-fuels generally obtained from resins and plant seeds. Because of being a part of the carbon cycle, the vegetable oils are carbon neutral. Moreover, these oils are extensively found all over the country with special penetration in rural areas. Certain characteristics like renewable background, higher lubricity, high cetane rating, low sulfur content, non-toxic nature, bio-degradability, superior anti-corrosion properties, etc. make these fuels a promising alternative for diesel engine application [15-18]. However, there are certain constraints regarding its usage for CI engines. The major problem with these oils is their higher viscosity than diesel. The high viscosity is attributed due to unsaturated fatty acids and high molar masses of vegetable oils. At high engine temperatures, the polymerization of unsaturated fatty acids occurs due to which cross-linking leads to the gumming. When CI engines are allowed to run using vegetable oils, fuel injectors turn out to be choked

after a small number of hours. The higher viscosities of vegetable oil cause poor atomization of fuel, which lead to unfinished combustion of fuel and hence carbon deposition on the valve seat and injector which causes serious engine fouling. Due to incomplete combustion of fuel, incompletely burnt fuel runs down the engine walls and weakens the engine lubricating oil [15]. Therefore, vegetable oils are not recommended for direct diesel engine application. However, there are several methods like dilution, pyrolysis, transesterification and engine hardware modification with which oil can be used in compression ignition engines. Amongst these methods, transesterification has been established as the best method for use of vegetable oils in diesel engines. Transesterification is a chemical process in which the triglycerides of the vegetable oils are converted into mono-alkyl esters and glycerol in the presence of a catalyst. The vegetable oil alkyl esters are popularly known as bio-diesel and have properties very similar to mineral diesel [14].

1.5 BIOFUELS POLICY: GOVERNMENT OF INDIA

In light of the need for diversification of energy supply as discussed earlier, Indian Government has taken a lot of initiative on the front of wind and solar energy harnessing projects. However, a formal National Policy on Biofuels to explore the non-edible vegetable oils and other bio-origin oils as alternative fuels was approved by the Government of India in December 2009. It encouraged the use of alternative fuels to supplement transport fuels (diesel and petrol for vehicles) and planned a target of bio-fuel blending up to 20 % (both bio-ethanol and biodiesel) latest by the year 2017. In this context, the Government of India initiated the National Biodiesel Mission (NBM) which recognized *Jatropha Curcas* for biodiesel production.

The Planning Commission of India had set a motivated, target of covering 11.1 to 13.3 million hectares of land for *Jatropha Curcas* cultivation by the closing stages of

the 11th Five-Year Plan [18]. The central government of India and several state governments are providing financial motivations for carrying plantations of *Jatropha Curcas* and other non-edible oilseeds. A number of public institutions, state agricultural universities, cooperative sectors and state biofuel boards are also sustaining the bio-fuel mission in a different manner [19]. However; Government of India had two major constraints in its bio-fuel policy. Firstly, only non-edible oils were allowed to be used as fuel as India is non self-sufficient in edible oil production, rather it imported 40% of its total edible oil requirements in 2012 [20]. Secondly, only those non-edible oil species which can grow in waste and barren lands with drought conditions are preferred as diversion of arable lands for energy crop production may impinge food production.

On the lines of the above constraints, Indian government's motivated plan of producing adequate biodiesel to meet its mandate of 20 percent biodiesel blending by 2012 was not realized. Excessive dependence on *Jatropha Curcas* to produce biodiesel, lack of sufficient feed stocks, absence of exploration of other suitable oilseeds for biodiesel production and lack of comprehensive research and development activities have been some of the major stumbling blocks cited officially by Government agencies for the above mentioned failure [21-23].

As cited in the previous paragraph, lack of sufficient feedstocks and excessive dependence on *Jatropha curcas* were some of the reasons for the initial setback of NBM. Therefore, exploration of other potential non-edible oil feedstocks for biodiesel production and an integrated research and development approach to address the multifaceted dimensions of biodiesel production and usage may supplement Government's bio-fuel policy and also increase the feedstock availability substantially. In this context, the present research work deals with one such less

popular non-edible vegetable oil feedstock known as “*Calophyllum Inophyllum*” to evaluate its potential as an alternative diesel engine fuel.

1.6 POLANGA: AN ALTERNATIVE DIESEL FUEL

Polanga is a perennial angiosperm. Its full botanical name is “*Calophyllum Inophyllum*” [24]. It is a non-edible oil seed. The tree bearing polanga seeds are medium sized and it grows well in exposed sea sands or deep soil. The rainfall requirement for this tree is 750–5000 mm/year. The expansion rate of the Polanga tree is 1.1m height per year in favourable locations. This plant is widely found in South-East Asia, East Africa, Australia and India [25-28].

Polanga tree yields 100-200 fruits/kg with each fruit having one large brown seed of 2-4 cm diameter. A single, large seed is surrounded by a shell (endocarp) and a thin, 3-5 mm layer of pulp. The oil obtained from the seed is thick and tinted green. About 2000 kg/ha oil yield has been reported [27-30]. Looking at its omnipresence throughout the Indian coastline, it seems that its natural production potential is no less than *Jatropha curcas*. High oil content, extensive availability, non-edible nature, low water requirement, growth on non-arable lands, etc. makes this oil seed highly suitable for fuel applications in diesel engines. An integrated research and development approach to evaluate the potential of this oil seed to be a true alternative to mineral diesel is to be assessed.

1.7 ARTIFICIAL NEURAL NETWORKS (ANN) APPROACH

The researchers involved in engine development and modification generally want to identify the emission and performance of a CI engine using various proportions of blends, for changed fuel injection timings and at altered fuel injection pressures. This requirement can be fulfilled either by conducting large numbers of engine tests or by modelling and simulation of the diesel engine operation. Testing the

diesel engine under all probable operating conditions using various fuel blends are expensive and time consuming. On the other hand, the development of precise models of CI engine fuelled with blended biodiesel is too complicated due to the intricate nature of the various processes concerned. Thus, engine exhausts emissions and performance can be modelled by means of artificial neural networks.

ANN is a relatively new method in computing and provides more refined computation of data. Artificial Neural Networks are basically a simple tool based on the neural configuration of the human brain. Computers do things well, like performing complex math or keeping ledgers. But computers fail in identifying even elementary patterns. For eliminating such problem, advances in genetic research assure a primary understanding of the human philosophy of thinking mechanism. In engineering some problem patterns are very complex, for example, the ability to identify individual face patterns from distinct angles [31]. ANN does not use conventional computer programs, but engages the large parallel networks for guiding of those networks to solve definite particular situations.

The elementary processing component of an ANN is a neuron. Basically, a biological neuron collects input data from some sources, merges them in some way, executes a nonlinear process on the outcome, and then gives final output. All natural neurons have the similar four basic modules viz., synapses, soma, dendrites and axon [32]. Similarly, the basic unit of ANN, the artificial neurons, simulates the four basic objectives of natural neurons. Figure 1.1 shows an elementary representation of a neuron. In Figure 1.1, x_n represents the different inputs given to the neural network. Each of the inputs is modified by multiplying an associated weight represented by w_n . The product of the processed inputs is first operated by a summation function and

then feed through a transfer or activation function to produce an output via an algorithm, and finally the result.

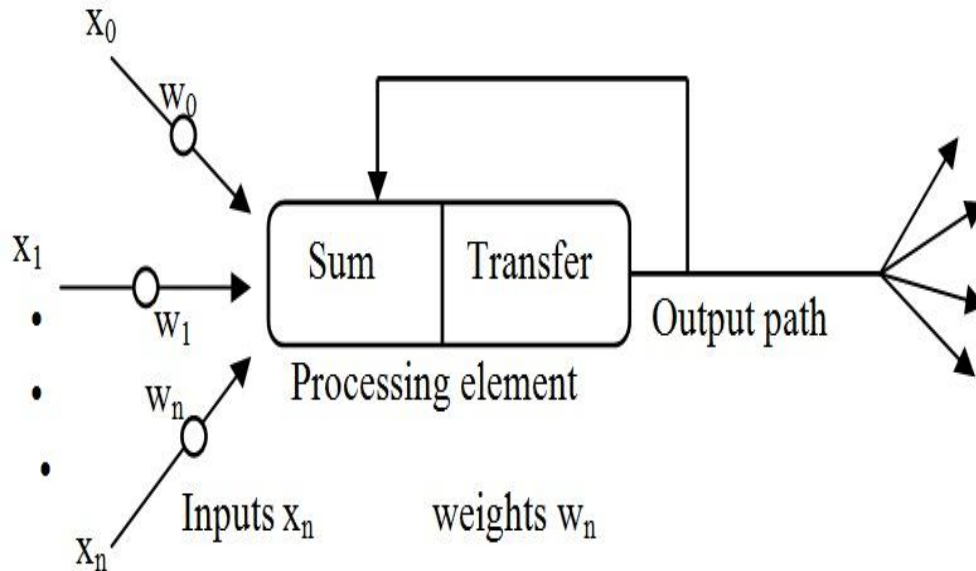


Fig.1.1: A Basic Artificial Neuron

The addition of an activation function increases the time sensitivity of the summation function [33]. The ANN processing element is further prepared for the output of ANN transfer function. This output is considered as an input to the further processing in the ANN network. All ANN networks are fabricated from this basic block of the processing element or the neuron.

1.7.1 ARTIFICIAL NEURAL NETWORK OPERATIONS

Another part of the task of using ANN networks, involves around the countless of ways the individual artificial neurons can be gathered together. This gathering happens in the living human brain also in such a way that instruction can be treated with an interactive, dynamic and self-organizing way.

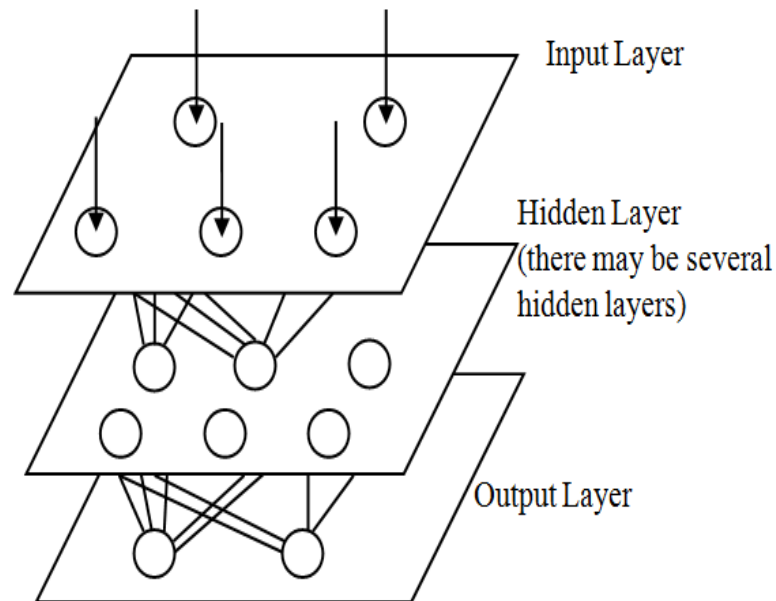


Fig. 1.2: A Simple Neural Network Diagram

This gathering occurs by constructing layers which are connected to each other [34]. Fundamentally, all ANN's have a same structure as shown in Figure 1.2. A fully functional ANN is thus comprised of different interconnected layers having artificial neurons operated by the summation and transfer functions.

Although there are applications where the problem can be modeled by using the single layer network, or even one neuron, most advanced applications require ANN's that contain a minimum of three basic layers viz., input layer, hidden layer, and output layer. The neurons in the input layer receive the data either from data files or directly from sensors in real-time applications. The output layer sends the instructions directly to a secondary program, or to devices such as the mechanical controlling system. The internal hidden layers lie between input and output layers which may contain a number of neurons in various interconnected structures.

One of the important feature of these networks is the feed forward way of communication from one neuron present in the input or upper layer to another one present in different layer which may be hidden or output layer [35]. The operation of

the neural network is largely affected by the method in which these neurons are interlinked. These connections may either cause the summing mechanism of the next neuron to add or subtract. The feedback mechanism is an example of such connection where the result of one layer goes back to a previous layer (Figure 1.3).

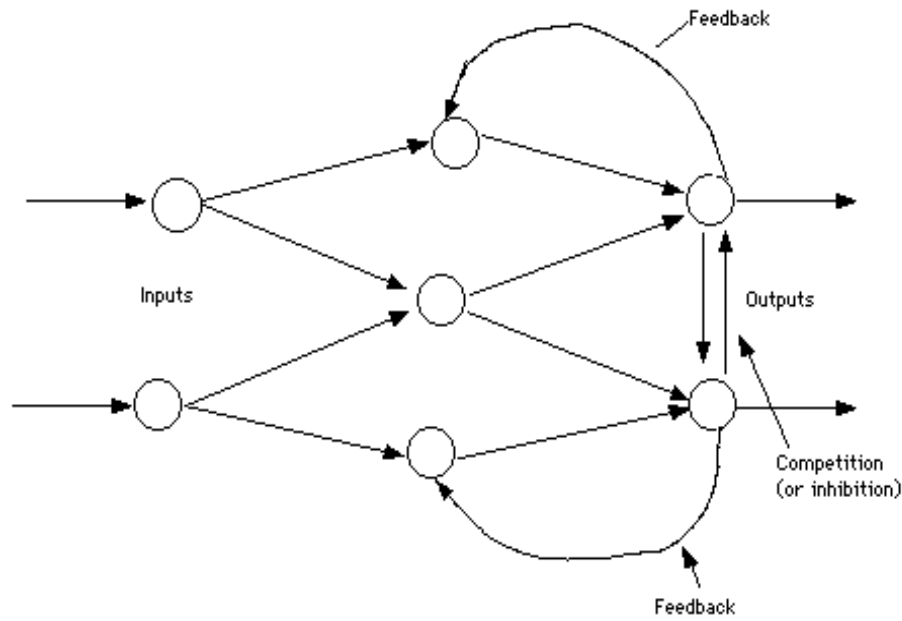


Fig.1.3: Simple Network with Feedback and Competition

1.7.2 TRAINING AN ARTIFICIAL NEURAL NETWORK

After an ANN has been planned, then ANN is ready for training procedure. The preliminary weights are elected randomly for initiating the training of the network. Thereafter, the learning or training of network starts. There are basically only two methods for training the ANN networks; supervised and unsupervised. In case of supervised training of network engrosses a mechanism of providing the ANN network with the most wanted output by grading the ANN network's performance. On the other hand, unsupervised network training, network has to formulate the inputs without outside help [36]. Mostly ANN networks employ supervised training.

Artificial neural systems do precise individual demands. The ANN system requires a number of conditions to be met. These conditions are:

- A data set that can specify the application.
- A sufficient data set for both training and testing of ANN.
- Assessments of transfer and activation functions and the learning methods.
- Ample processing power (some of the engineering applications require real-time process).

Once these above conditions are met, artificial neural networks are able to solve even the typical problems where conventional programming techniques show inefficiency.

1.8 RESEARCH OBJECTIVES

The present work is focussed on the development of Artificial neural network algorithm for modelling of performance, emission parameters of CI engine fuelled with Calophyllum inophyllum (Polanga) biodiesel and diesel blends. The simulated results of the developed ANN model are validated and compared with experimental data. Optimization of performance and emission parameters of the developed model is obtained using MATLAB.

1.9 ORGANIZATION OF THESIS

The thesis starts with an introduction giving a concise close importance of various biodiesel as an optional fuel for diesel engine and the application of ANN in performance and emission evaluation. Chapter 2 presents a logical and complete review of the literature on the use of various edibles and non-edibles vegetable oils and their biodiesel as alternate fuels for diesel engines. The literature review includes few available studies related to artificial neural network. The experimental test rig used to conduct the study and the developed ANN model is explained in Chapter 3. Chapter 4 deals with the results of the trial experiments study carried out on the test

setup of a single cylinder diesel engine using diesel oil, Polanga biodiesel blends with diesel as a test fuels. The results of modelling through ANN for engine exhaust gas emissions and performance are explained in this chapter. At the end of this chapter optimization process was carried out. Chapter 5 gives the concluding remarks of this study.

CHAPTER 2

LITERATURE REVIEW

2.1 INTRODUCTION

As discussed in the earlier section, an integrated research and development approach has to be implemented to assess the potential of “Calophyllum Inophyllum” as alternative diesel fuel. Therefore, the existing quantum of research work in the domain like biodiesel production optimization from vegetable oil sources, physico-chemical and fuel property characterization, application in engines to evaluate performance and emission with the ANN modeling need to be studied as a review of literature. In this context, a comprehensive literature review of various national and International journals was carried out. Some of the important outcomes are summarized below.

2.2 REVIEWS OF AVAILABLE LITERATURE

2.2.1 BIODIESEL PRODUCTION FROM VEGETABLE OILS

Some important properties of palm biodiesel blends with diesel were measured by Benjumea et al. [37] as per ASTM standards. To predict, Kay’s mixing rule at three different distillation curve T10, T50 and T90 are adopted to calculate heating value, density, cetane index and cloud point, whereas fuel viscosity was obtained by Arrhenius mixing rule. The very low deviation was found when certain suitable mixing rules were adopted for biodiesel. There was large cetane number of biodiesel as compared to other using ASTM D4737.

Sahoo et al. [38] produced biodiesel by transesterification in the presence of a catalyst. It was observed that transesterification process was influence depending upon the temperature, quality of catalyst, reaction time and verity of alcohol with the molecular ratio to the oil. Another mode of production of biodiesel from other filtered non-edible Karanja, Jatropha, and Polanga oil were also explained in this research. Chakraborty et al. [39] evaluated some relevant properties, the prospect of terminalia oil for biodiesel production. The fatty acid results of oil extorted from terminalia was found more suitable with respect to other seed oils tried. Terminalia oil contained 28.7% linoleic acid, 32.9% palmitic acid and 31.4% oleic acid. The kinematic viscosity and calorific value of terminalia oil were 25.50 cSt and 37.40 MJ/kg respectively, and lie within acceptable limits of the EN 14214 standard. However, the flashpoint of terminalia was found 90 °C which is relatively lesser than the required standard for diesel engine. Finally, these fuel properties conformed that biodiesel obtained from terminalia seed fulfil breathing biodiesel properties.

Kaya et al. [40] extracted peanut seed oil 50% wt/wt, by solvent extraction process. Transesterification was used to produce biodiesel from peanut. The viscosity of biodiesel was close to diesel while, the calorific value was about 6% less than as compare to diesel. Peanut biodiesel contained heating value of up to 8.4%, which is lower to diesel. Other important properties like flash point, kinematic viscosity, pour point, iodine number, cetane number, cloud point and density of peanut oil and its biodiesel were found out and compared to diesel fuel, EN and ASTM biodiesel standards which showed that peanut biodiesel had relatively closer to fuel properties to diesel.

Chen et al [41] studied the possibility of biodiesel production from vernicia Montana oil. High cold filter plugging point of 11°C, 94.9% weight of ester content and

oxidative stability of 0.3 hours at 110°C for the biodiesel. Also, Tung oil biodiesel exhibited high density of 903 kg/m³ at 15°C, kinematic viscosity of 7.84 mm²/s at 40°C, and iodine value of 163.1 g I₂/100 g. The properties of the Tung biodiesel blended with palm oil, canola had better resulted to suit the category of biodiesel fuel were found to get better by blending with palm oil and biodiesel to suit the category of biodiesel fuel.

Lee et al [42] used a mixture of CaO-MgO catalyst for transesterification process of non-edible *Jatropha* biodiesel production. They found the optimum level of biodiesel production by 97.55% by taking ratio of 35:77 of methanol/oil molar ratio with the catalyst of quantity 3.60 by weight percentage for 3.34 hr. At 155.77°C. For statistically evaluate and optimize the biodiesel production process using RSM with the central composite design (CCD).

Omar et al. [43] by using heterogeneous transesterification produced biodiesel from waste cooking palm oil to a maximum biodiesel yield of by the process by which produced 79.8% maximum biodiesel yield at the most favorable methanol to oil molar ratio ¼ 28:1, catalyst ¼ 2.8 wt.%, time of reaction ¼ 88 min and temperature of reaction ¼ 114.5°C.

Wu et al. [44] produced biodiesel using alkaline transesterification from camelina seed oil. Four main process conditions reaction time, methanol quantity, catalyst concentration and reaction temperature were studied. The order to consider significant factors for biodiesel production were catalyst concentration > reaction temperature > reaction time > methanol to oil ratio. The best biodiesel yield was found a ratio of methanol to oil in 8:1, a time for the reaction of 70 min, a temperature of 51°C, and a concentration of catalyst of 1 wt.%. The properties of the optimized biodiesel were kinematic viscosity, density etc. The optimized biodiesel from camelina oil met the

appropriate EN 14214 and ASTM D6571 biodiesel standards and could be used as an alternate fuel for diesel engines.

Atadashi et al [45] explored the production of biodiesel from high free fatty acid containing feedstocks to bring their properties close to mineral diesel. The properties of the biodiesel produced closely matched the corresponding ASTM standards and the cost of production was reported to be 25% less as compared to refined low FFA feedstocks.

Wang et al. [46] studied the feasibility of biodiesel production from *Datura stramonium* L. oil (DSO). The research work found an optimum yield of 87% using a two-step catalyzed reaction conditions. The fuel properties of DSO biodiesel were also evaluated. As compared to *Jatropha* and beef tallow biodiesel, DSO biodiesel shows the best value of kinematic viscosity 4.34 cST and cold filter plug point (-5.1°C).

Ilham et al. [47] proved that, with the help of supercritical dimethyl carbonate process triglycerides and fatty acids of oil were successfully converted into biodiesel. In this work, optimization of the supercritical dimethyl carbonate method was discussed to include all essential key parameters such as the FAME yield, pressure, time, reaction temperature, oxidation stability, tocopherol content, fuel properties, degree of denaturation, and thermal decomposition. The most favorable condition for this method was obtained at 42:1/300°C /20MPa /20min.

Yucel [48] Response surface methodology with a combination of CCD was utilized to optimize the production parameters of biodiesel using pomace oil. Reaction time, molar ratio of methanol to oil, reaction temperature and biocatalyst content were selected as the variables and the response was the yield of pomace biodiesel in this work. The best conditions for the transesterification was established to be: alcohol/oil

molar ratio of 5.3:1, chemical reaction temperature of 40 °C, reaction time of 24 hours and catalyst of 5.8% w/w. Under the given optimal conditions Pomace biodiesel yield was obtained 92.77%. Also biodiesel yield was increased up to 93.83% by adding up the water (1% w/w) in the reaction zone under the above best possible conditions.

Uzun et al. [49] performed the transesterification process of waste frying oils in different conditions using alkali-catalyst to find out the effect of methanol/oil molar ratio, catalyst concentration, reaction temperature, reaction time, purification type and catalyst type on biodiesel production yields. The best conditions obtained were reaction time 30 min., NaOH of 0.5% wt, methanol to oil ratio 7.5, reaction temperature 50°C and hot distilled water purification. From experimental results, 96% biodiesel yield with ~97% ester content was obtained. The specifications of prepared biodiesel were, according to required standards of ASTM D 6751 and EN 14214.

Silitonga et al. [50] investigated biodiesel characterization and production from Ceiba pentandra seed oil. Two step acid–base transesterification was used for production. The results found that property of C. pentandra methyl ester fell within the suggested biodiesel standards (EN 14214 and ASTM D6751). The study also suggested that biodiesel-diesel blending improved the properties of fuel like viscosity, density, oxidation stability, calorific value and flash point.

Chammoun et. al. [51] identified Oilseed radish as a potential biodiesel as an energy crop for the southern U.S. The fatty acid summary of this oil showed more intensity of erucic acid C23:1, which was dangerous to human health issues. This oil was converted to biodiesel by transesterification process. Fuel properties were analyzed free and total glycerol, including fatty acid profile, sulphur content, acid number, cold filter plugging point and water content. After transesterification process all fuel

properties of this biodiesel were found to meet up ASTM biodiesel standards and can also for use in engine as a fuel.

Atapour et al. [52] used frying oil as a cheap feedstock for producing biodiesel from alkali-catalyzed transesterification. The design of experiments was performed using a double 5-level-4-factor CCD tied with response surface methodology in order to study the effect of factors on the yield of biodiesel and optimizing the reaction conditions. The factors studied were: reaction temperature, the molar ratio of methanol to oil, catalyst concentration, reaction time and catalyst type (NaOH and KOH). A quadratic model was suggested for the prediction of the ester yield. The p value for the model fell below 0.01 (F-value of 27.55). Also, the R² value of the model was 0.8831 which indicated the acceptable accuracy of the model. The optimum conditions were obtained as follows: reaction temperature of 65°C, methanol to oil molar ratio of 9, the NaOH concentration of 0.72% w/w, reaction time of 45 min and NaOH as the most effective catalyst. In these conditions the predicted and observed ester yields were 93.56% and 92.05%, respectively, which experimentally verified the accuracy of the model. The fuel properties of the biodiesel produced under optimum conditions, including density, kinetic viscosity, flash point, cloud and pour points were measured according to ASTM standard methods and found to be within specifications of EN 14214 and ASTM 6751 biodiesel standards.

Kilic et al. [53] investigated the optimization and production process for biodiesel from castor oil by the transesterification process using alkaline-catalyst by full factorial design method. The experiment was conducted for the assessment of different a process variables. Catalyst concentration, methanol/oil molar ratio and effects of temperature were evaluated according to the 23 CCD. For determining the effect of purification techniques on biodiesel yield, various purification techniques

were applied after transesterification reaction. The model was generated to forecast biodiesel yield and with the experimental results this procedure provided a common yield of greater than 91% biodiesel production.

Yun et al. [54] simulated a biodiesel production navigator plant using WCO with enzyme-catalyzed having production ability of 6482 tons/yr. Five main reactions were useful to represent the transesterification of the production. The results were found good agreement with the actual data. Based on the simulation of the existing process, five optimization processes were proposed centre of attention on saving of energy and recovery of methanol. For heat exchange networks pinch technology was also developed. During the all optimizations process, the biodiesel quality was kept good order of more than 98.5%.

Hwai et al. [55] discovered crude *Calophyllum inophyllum* (Polanga) oil as a possible feedstock for biodiesel production. The above mentioned oil had a high acid value which is 59.30 mg KOH/g. Therefore, the degumming, esterification, neutralization and transesterification process were carried out to decrease the acid value to 0.34 mg KOH/g. The optimum yield was obtained at 10:1 methanol to oil fraction with 1 wt. % and NaOH catalyst at 50°C for 2 h. On the other hand, the *C. Inophyllum* biodiesel properties fulfilled the specification of ASTM D6751 and EN 14214 biodiesel standards. After that, the *C. Inophyllum* biodiesel, diesel blends were tested to evaluate the engine emission and performance characteristic. The performance and emission of 10% *C. Inophyllum* biodiesel blends (CIB10) gave a satisfactory result in diesel engines as the brake thermal increased 2.30% and fuel consumption decreased 3.06% compared to diesel. Besides, CIB10 reduced CO and smoke capacity compared to diesel. Briefly, *C. Inophyllum* biodiesel could become an alternative fuel in the future.

Following major findings were obtained as an outcome of an exhaustive review of available literatures in the field of biodiesel production from vegetable oils.

1. With some exceptions, most of the non-edible oils have high free fatty acid contents leading to a two stage transesterification process to produce biodiesel.
2. The energy consumption in two stage transesterification is higher. Therefore, optimization of process parameters is most important for high FFA non-edible oil seeds for commercial scale production.
3. However, most of the process optimization was confined to the final stage only with % yield as the response and not both the stages of transesterification.
4. In many reported cases the final biodiesel sample produced did not comply with the designated standards of ASTM/EN/ISO, etc. resulting in further addition of additives and post-processing.

In the light of the above review, it may be stated that production of biodiesel from *Calophyllum inophyllum* oil with optimized process parameters and the subsequent compliance with the corresponding international standards may prove the suitability of this oil as a true alternative to mineral diesel.

2.2.2 DIESEL ENGINE TRIALS AND ANALYSIS OF THE RESULTS USING BIODIESEL AS A FUEL

Rehman et al. [56] carried out investigations to study the properties of blends Karanja biodiesel with diesel 20% to 80% by vol. Diesel engine tests were performed to plan the comparative measurement of the BTE, torque, BSFC and emissions smoke, NO_x, CO and to evaluate the behavior of the diesel engine. From experiments drop in exhaust emissions with an increase in BTE, torque, and reduction in BSFC were found when using blends of B20 and B40.

Sahoo et al. [57] prepared biodiesel from Polanga by a triple stage transesterification process. After than Polanga biodiesel blends with diesel was tested on diesel engine for its use as an alternative fuel of diesel. Polanga biodiesel fuel blends (20B, 40B, 60B, 80B, and 100B) were used to conduct experiments on diesel engine at varying engine speed and load. The engine performance parameters BSFC and BTE and engine emission parameters such as CO, NO_x, CO₂, HC, and O₂ were measured. The most favorable engine functioning state based on lesser BSFC and higher BTE was observed at full load for B100. As of lower exhaust emission approach the neat Polanga biodiesel was found to be the best fuel as compared to diesel fuel.

Raheman et al. [58] evaluate the performance of Mahua biodiesel blends with diesel. The properties of these fuels were found to be similar to diesel and to both the European and American standards. The diesel engine performance parameters such as EGT, BTE and BSFC and engine exhaust emissions such as NO_x, CO and smoke density were measured to calculate the behavior of the diesel engine when run on mahua biodiesel. The decrease of BSFC and exhaust emissions together with increased BTE found for B20 biodiesel blend. In this way B20 is a more appropriate optional fuel for single cylinder diesel engine and it also help in controlling environmental pollution.

Lapureta et al. [59] collected and analyzed the published work in reputed scientific journals about diesel engine exhaust emissions when run on biodiesel as an alternate fuel. On the basis of engine performance evaluation the main compromise was found for an increase in BSFC due to the heat loss. In the next sections, the exhaust emissions from biodiesel and diesel fuels were analyzed, paying special attention to NO_x and UHC exhaust emissions.

Nabi et al. [60] produced Karanja methyl ester (KME) by transesterification process. The properties of KME and its blends were measured by ASTM and EN14214 standard. The gas chromatography of B100 shows that a maximum of 97.5% methyl ester was generated from Karanja oil. The Engine experiment results showed that engine emissions were decreased for all biodiesel blends, including smoke, CO and engine noise, but slightly enhance in NO_x emission was occurring as compared to diesel, also engine noise reduced by 2.5 dB when using B100.

Nabi et al. [60] produced Karanja methyl ester (KME) by transesterification process. The properties of KME and its blends were measured by ASTM and EN14214 standard. The gas chromatography of B100 shows that a maximum of 97.5% methyl ester was generated from Karanja oil. The results showed that the engine emissions were reduced for all blends, including smoke, CO and engine noise, but slightly increased NO_x was observed as compared to diesel, engine noise was reduced by 2.5 dB when using B100.

Sukumar et al. [61] conducted experiments on DI diesel engine, with varied fuel injection pressures from 200- 240 bar using high linolenic linseed oil methyl ester. Injection pressure of 240 bar gave better results. BTE was same to diesel and a drop in smoke, CO, and UHC emissions were also observed with slightly increase in NO_x emissions.

Sayin et al. [62] used methanol-blended diesel fuel to assess the impact of fuel injection timing on the emissions parameters of a four-stroke CI engine. The engine tests were carried out for three altered fuel injection timings (150, 200 and 250 CA bTDC). CO₂, NO_x emissions and BSFC were found to increase, but CO, smoke opacity, UHC emissions and BTE decreased with blending. At retarded injection timing (150 CA bTDC), CO₂ and NO_x emissions decreased.

Baiju et al. [63] utilized Karanja biodiesel as an alternative diesel fuel. It was found that methyl esters generated slightly more power than ethyl esters. However, the emission characteristics of both the esters were approximately same. It was suggested that both esters of Karanja oil could be used as an alternative fuel for CI engines without any major hardware modification.

Bajpai et al. [64] conducted experiments on non-edible straight vegetable oil Karanja blends (5%, 10%, 15%, and 20%) having high viscosity 27.84 cSt at constant engine speed. The BSFC, BTE, and engine exhaust emissions were selected to determine the optimum biodiesel fuel blend. A fuel blend of 10% showed a higher value of BTE at 60% engine load. Also, this blend obtained the lowest emission characteristics.

Sahoo et al. [65] ran a three cylinder Escort make tractor engine using non-edible Polanga, Karanja and Jatropha. Experimental data were obtained under part/full load at different engine speeds from 1200-2200 rpm. The best power output was obtained for 50% jatropha biodiesel blend with diesel. BSFC for the all biodiesel blends was increased with increasing blending and decreased with engine speed. A fall in smoke level was observed for all the biodiesels and their blends.

Canakci et al. [66] predicted the engine exhaust emissions and performance using neural networks at various engine speeds and full engine load conditions. For ANN network, engine speed, environmental and fuel properties were selected as the input layer parameters, and Pmax, emissions and BTE were used as output parameters. For all the ANN networks, the learning algorithm was used BP with a single hidden layer. This network produced average R^2 values of 0.99.

Godiganur et al. [67] used biodiesel of Mahua oil and its blends on a water cooled, turbocharged, CI engine at constant 1500 RPM under variable load. An increase in the percentage of biodiesel decreased the HC, CO emission but increased the BSFC and

NO_x emission of biodiesel. BSEC reduce and BTE of the engine slightly amplified when the engine operates on 20B as compare to diesel fuel.

Qi et al. [68] observed that biodiesel produced from soya bean shows the same combustion stages as in diesel. At full engine loads, the P_{max} of soya bean biodiesel and diesel was same. However, the peak rate of pressure rise and the peak of HRR were lower. A significant reduction in NO_x, HC, CO, and smoke was observed at full engine load with soya bean biodiesel.

Sahoo et al. [69] experimentally accessed, the use of Jatropha, Polanga and Karanja biodiesel and their blends in a single cylinder diesel engine. P_{max}, time of occurrence of P_{max}, HRR and ignition delay was selected as engine parameters. It was found that Polanga biodiesel gave maximum P_{max}, the ignition delays was less for Jatropha biodiesel as compared to neat Polanga and Karanja biodiesel.

Buyukkaya et al. [70] conducted experimental tests using Rapeseed biodiesel and its blends to estimate the engine parameters. The Rapeseed biodiesel generates less smoke and CO emissions but increased BSFC by 11%. All combustion characteristics of rapeseed biodiesel and its blends is very much close to diesel fuel.

Qi et al. [71] observed a significant reduction of CO and smoke using soybean based biodiesel. However, a small increment in BSFC and NO_x and reduction in BTE was also observed. It was concluded that Soyabean biodiesel could be partially used as an alternate fuel.

Kannan et al. [72] investigated the mixture of waste cooking palm oil methyl ester, ethanol and diesel as a potential biodiesel. This mixture of diestrol fuel was tested on a DI diesel engine at a varying fuel injection pressure and fuel injection timing and the engine characteristics were obtained. Maximum BTE of 31.4% was obtained at

fuel injection pressure of 240 bar. A reduction in NO_x, smoke, CO₂ and CO was observed for test fuel. A small increment in UHC was also observed.

Ganapathy et al. [73] conducted experiments using Jatropha biodiesel and diesel and observed its effect on BSFC, BTE, P_{max}, HRR_{max}, HC, CO, smoke density and NO emissions. It was seen that an advance in fuel injection timing reduced the HC, CO, BSFC and smoke and increased the P_{max}, BTE, NO_x emission.

Murlidharan et al. [74] carried out experiments to estimate the engine performance, combustion characteristics and emission of a 4 stroke, VCR CI engine fuelled with the WCO. An improvement in performance as well as emissions parameters was observed.

Sayin et al. [75] used COME as biodiesel with different fuel injection pressures in the range of 18- 24 MPa at an interval of 2 MPa at a stable engine speed and changed engine loads. The BSEC and BSFC using COME biodiesel were more than that of diesel while the BTE is lesser than that of diesel. Increase in fuel injection pressure resulted in increased BSFC and BTE.

Chauhan et al. [76] evaluated the performance parameters BTE, BSFC, power output. The emission parameters such as CO₂, CO, UHC, NO_x and smoke opacity for different fuels and compared these with diesel results. The BTE of Jatropha biodiesel and its blends were lesser than diesel and BSEC were found to be high. On the other hand, CO, HC, smoke and CO₂ were lower. Engine NO_x emissions on Jatropha biodiesel were slightly more than diesel. The experimental results commit that biodiesel derived from Jatropha could be a good alternative for diesel engine and can be used in a conventional diesel engine without any alteration.

Dhar et. al. [77] investigated various engine parameters using biodiesel from Neem oil. BSFC and NO_x were found to be higher than diesel whereas HC and CO

emissions were less. The combustion was slightly delayed in biodiesel blends as compared to diesel. HRR for every biodiesel blends were nearly same to diesel. Fuel combustion time for Neem biodiesel blends was found to be lesser than diesel.

Ozener et al. [78] conducted tests on soya bean biodiesel and its blends. The results showed that, compare to diesel, soya biodiesel produced 1-5% lower torque and 2-8% increase in the BSFC. Conversely, biodiesel reduced CO approx (28–46%) and HC, but the NO_x and CO₂ emissions amplified slightly. Above results point out that soya bean biodiesel could be used without any engine amendment.

Selvam et al. [79] conducted experiments with pure beef tallow biodiesel. A decrease in BTE and an increase in BSFC was observed for all the biodiesel blends. A reduction in smoke, carbon mono-oxide and unburnt hydrocarbons and an increase in NO_x was observed for all the blends of biodiesel.

Murcak et al. [80] experimentally investigated the performance of the DI diesel engine for various fuel injection timings using ethanol-diesel as a test fuel. The test fuel blends were prepared by mixing ethanol of 5 to 20 percent by volume. Experimental studies show that maximum engine power was obtained for 10B ethanol-diesel blends at 3100 RPM and 45° bTDC fuel injection timing. The maximum torque was obtained for 10B fuel blends at 1400 RPM and 25° bTDC fuel injection timing. The least BSFC was obtained for 20B blends at 1210 RPM and fuel injection timing of advance of 36° bTDC.

Shivalakshmi et al. [81] conducted experiments on diesel engine using diethyl ether with biodiesel. It was observed that CO emissions and smoke emissions at all engine loads were decreased while NO_x and HC emissions increased.

Shehata et al. [82] studied the effect of biodiesel fuel with and without EGR system. Biodiesel fuels were prepared from palm oil, flax oil and cottonseed oil. Biodiesel

fuels gave a little less BP, BTE and slightly more BSFC as compared to diesel. At same condition, diesel test fuel produced more CO than the biodiesel fuel due to less O₂ content. As EGR was increased, CO emission boosted while NO_x dropped due to decrease in flame temperature and O₂ in fresh air. However, engine wall temperature for diesel fuel was more than the biodiesel. Biodiesel fuels gave maximum P_{max} than diesel. The position of P_{max} was, 14° after TDC for Palm, 12° after TDC for cotton, 20° after TDC for diesel fuel and 11° crank angle after TDC for flax biodiesel.

Mufijur et al. [83] studied the possibility of Jatropha as a probable biodiesel fuel in Malaysia. The end results showed that the viscosities of B10 and B20 were very closer to diesel. Oxidation stability of B10 and B20 met the European specifications of 20 hours, for that reason, only B10 and B20 were used to evaluate engine emission and performance. As compared to diesel, the reduction in BP was 4.69% for B10 and 8.87% for B20 blends. It was also seen that BSFC rise as the volume of biodiesel increased. Compared to diesel, a decrease in HC of 3.74% and 10.35% and CO emission of 17% and 26% were obtained for B10 and B20 blends. On the other hand, the increase in NO_x emission was found about 4% and 7% while using B10 and B20. As an end result B10 and B20 can be used in a diesel engine devoid of any engine modifications.

Chen et al. [84] manufactured Jatropha biodiesel and prepared various blends with diesel to assess the deviations in the fuel properties of various test fuels. Correlations find between fuel properties, CV, plugging point, kinematic viscosity, density, and oxidation stability of the Jatropha diesel blends. The combustion tests of the blends were performed on a diesel engine. Higher BTE and lower BSFC were clearly observed with full load condition.

Chauhan et al. [85] Transesterified Karanja oil and found the properties within tolerable limits of significant standards. The performance parameter was calculated such as BTE of Karanja biodiesel blends having compositions of 5B, 10B, 20B, 30B and 100B with diesel. BTE was found 3-5% less with respect to diesel for Karanja biodiesel blends. Also, emission parameters such as CO, CO₂, UBHC and smoke opacity were less for Karanja biodiesel blends. The combustion analysis was done using Pmax and HRR with respect to crank angle. Pmax and HRR were lower for Karanja biodiesel. The final results from the experiments recommended that fuel blends from Karanja biodiesel could be used for diesel engine and in future especially used for small and medium size diesel engine.

Liaqat et al. [86] used three blends of fuels mixture of coconut biodiesel with diesel B0, B5, and B15. These test fuels were tested to find the performance and emission parameters of diesel engine test at full load, at varying engine speed. As results of examinations, there was a decrease in torque and BP, while the amplify in BSFC as compared to diesel. The exhaust gas emissions result was lower HC, CO and, high CO₂ value and NO_x emissions were found to be high as compared to diesel.

Ozer Can et.al. [87] conducted experiments on a single cylinder, four-stroke, CI engine with biodiesel blended with WCO. It was observed that blending with WCO resulted in increased BSFC and reduced in BTE. Also, the NO_x emissions increased by 8.7%.

Labeckas et al. [88] Experimental study was conducted with a 4-cylinder, DI diesel engine to find the effects of ethanol namely E5, E10, E15 blends. A new approach revealed an important role of the oxygen molecule. The influence of the fuel, O₂ on maximum HRR, maximum Pmax, NO_x, emissions, smoke opacity and CO from the exhaust. Engine fuelled with blend E15 the engine developed the brake BTE of 36%,

at rated 2200 RPM engine speed. The addition of the ethanol to diesel reduced the NO_x and the HC emissions.

Rizwanul Fattah et al. [89] carried an experimental investigation of the mixing antioxidant addition effect on engine emission and performance characteristics. For conducting experiments biodiesel was produced by the transesterification process using KOH as a catalyst. Experimental tests were carried out on a 2.5 liter, 55 KW, 4 cylinder diesel engine at full load condition at varying engine speed. The engine performance results show that B20 showed 1.36% lower mean brake power and 4.90% higher BSFC with compared to diesel. The addition of antioxidants boosts BP and trim down BSFC slightly. Emission results showed that B20 amplified NO_x but reduced CO and HC emission. By adding antioxidants NO_x emission reduced by 1.7–3.7%, but both CO and HC emission increased as comparison to B20, but the level were below the diesel emission level. In this way B20 blended with antioxidants could be used in diesel engines without any major modification.

S.M. Ashrafur Rahman et. al. [90] reviewed for finding the effect of fuel injection timing on a diesel engine. For experimental investigation alcohol, biodiesel, diesel and other another fuels were used for review. From the review it was concluded that for diesel fuel, advancement in fuel injection timing resulting lower HC and CO emission but it increased NO_x emission was found. Also, advancement in fuel injection timing increased BTE and reduced BSFC was observed from the literature review. Biodiesel blends with diesel produced more CO and HC emission, but reduction of NO_x emission was observed when the fuel injection timing was retarded. From literature review it was also observed that advancement in fuel injection timing shows the higher the EGT with increase the percentage biodiesel in test blends.

Hwai Chyuan Ong et al. [91] experimentally investigated the CI engine performance and emissions run on *Jatropha*, *Ceiba pentandra* and *Polanga*. Engine testing was performed using biodiesel blends 10B, 20B, 30B and 50B at full engine load condition. A 10B blend showed the best engine performance such as engine torque, engine power, BSFC and BTE among the all tested blends. All biodiesel blends also showed an appreciable fall in CO, CO₂ and smoke opacity with a very less increase in the engine NO_x.

As an outcome of the elaborative review of existing technical literatures regarding the engine trial results of biodiesel derived from a wide range of vegetable oil feedstocks and its blends, the following conclusions are made.

1. Depending upon the feedstocks, some of the biodiesel showed improved brake thermal efficiency and reduced brake specific fuel consumption with increased biodiesel volume fraction in the test fuel where as some others exhibited exactly opposite trend. Therefore, engine performance using biodiesel directly depends upon the property of the corresponding feedstock and the transesterification process.
2. Most of the literatures agreed on the common denominator that emissions of carbon or nitrogen increased. However, the same was not linear. In many cases even, reduction in oxides of nitrogen was reported.
3. Almost all the literatures indicated an increase in cylinder pressure for lower volume fraction of biodiesel in the test fuels irrespective of the feedstocks. This led to shorter combustion duration, increased in-cylinder temperature and lower exhaust temperatures reported in many cases. However, at higher volume fractions of biodiesel some literatures indicated a reduction in peak in-cylinder pressure, whereas others indicated minimal change in the peak in-cylinder pressure. Therefore, the

combustion phenomena using biodiesel are highly sensitive to the nature of the feedstock and transesterification process which actually determines the fuel properties.

4. To increase in volume fraction of biodiesel, reduction in the combustion heat release was reported in major cases. However, in some cases a marginal increase was reported at lower blends.

5. Increased heat release in the diffusion phase, smoother engine operation, etc. are some of the major conclusions in most of the literatures.

In light of the above reviews it may be concluded that comprehensive engine trials to evaluate performance, emissions and combustion studies on diesel engines fuelled with *Calophyllum inophyllum* biodiesel is absent in the literature. Therefore, exhaustive engine trials using *Calophyllum inophyllum* biodiesel at various proportions and the subsequent analysis may provide a clear picture regarding the suitability of the seed oil as an alternative fuel to diesel.

2.2.3 ANALYSIS OF RESULTS AND PREDICTION USING ANN

Erol et al. [92] used ANN model, to predict out the engine exhaust emissions and performance of diesel engine with respect to throttle position, fuel injection pressure, RPM of the engine. Engine trial has been taken on 100, 150, 200 and 250 bar fuel injection pressures at 50, 75 and 100% throttle positions of the engine. Engine torque, power, BMEP, BSFC, fuel flow rate, and exhaust emissions CO₂, SO₂, smoke and NO_x have been measured. The BP learning algorithm was used with single and two hidden layers, and transfer-function, logistic sigmoid have been applied for developed the ANN network. Engine RPM, throttle position and fuel injection pressure were used in the input layer for ANN network; exhaust emission and performance characteristics of the engine were taken as an output layer parameter of ANN

network. From result the values of R^2 were about 0.9998 for the training data set, and 0.998 for the testing data set; values of RMS were lesser than 0.01; and mean percentage errors were lesser than 8.7.

Canakci et al. [93] explored the utilization of the ANN method for predicting the engine exhaust-emission and performance values of biodiesel fueled diesel engine at full load at a constant 1500-rpm. ANN network was developed in which the heat of combustion, molecular weight, specific gravity of fuel, viscosity, cetane number and C/H ratio for every test blends were used as in the input layer parameter of ANN network, while in ANN outputs layer the BSFC, EGT and exhaust gas emissions were taken. The ANN network average yielded values were (R^2) 0.991 and the mean percentage errors were lesser than 4.2 for the training data set. For testing data set the average values of R^2 were about 0.992 and the average mean percentage errors were lesser than 5.7.

Ghobadian et al. [94] prepared model for a diesel engine run on WCO biodiesel fuel. Using ANN network prediction of BP, torque, engine exhaust emissions and BSFC of the diesel engine was carried out. An ANN model was developed using the Back-Propagation algorithm and MLP was used for non-linear mapping between the input layer and an output layer of the network. It was seen that the ANN network generates good correlation coefficient (R) 0.9497, 0.998, 0.939 and 0.998 for the torque, BSFC, HC, emissions and CO respectively.

Mustafa Canakci et al. [95] experimentally analyzed the performance and emissions of a 4 stroke SI engine running on ethanol petrol blends of 0B, 5B, 10B, 15B and 20B. An ANN network was developed in which BP, torque, BSFC, BTE, volumetric efficiency and emission as an output layer parameters and blends of ethanol with gasoline and engine RPM as an input layer parameters. An ANN network gives a

good correlation coefficient (R) in the span of 0.971-1. Also the values of MRE were in the range of 0.47–5.56%, and RMSE were found to be very small.

G. Najafi et al. [96] studied the use of ANN to predict BP, exhaust emissions, BSFC, and torque of modified diesel engine operated with a mixture of CNG and diesel separately at different engine loads and speeds. Experimental results show that the mixtures of diesel and CNG fuel gives improved engine emission and performance characteristics as compared with diesel. For the ANN modelling, the BP algorithm was found to be the most favourable choice for training the ANN network. It was noticed that the ANN network was good to predict the engine exhaust emissions and performance with a best correlation coefficient R of 0.9885, 0.9848, 0.9577, and 0.9944 for the engine BSFC, engine torque, EGT and NO_x correspondingly.

R. Manjunatha et al. [97] developed an ANN model for diesel engine. The experimental investigations were carried out on a diesel engine using blends of Pongamia, Neem and Jatropha oils. The performance parameters such as BP, BTE, BSFC, volumetric efficiency, EGT was measured along with regulated exhaust emissions of HC, CO and NO_x. The multilayer perceptron ANN network was used for nonlinear mapping between input layer and output layer of ANN network. The values of R (Regression Coefficient) for exhaust gas emissions were obtained 0.991, 0.952 and 0.994 for CO, NO_x, and HC respectively.

Shivakumar et al. [98] investigated the effect of fuel injection timing on the emissions and performance for a 4 stroke stationary single cylinder, VCR diesel engine run on WCO biodiesel blends with diesel. An ANN network was used to predict the diesel engine emission and performance parameters. The developed model predicted the values quite well and mean error was within limits.

Çay et al. [99] developed an ANN model based on standard back propagation algorithm for a 4 cylinder, 4 stroke methanol based engine. The proposed model predicted the performance parameters well within 3.9% of the testing data.

Ismail et al. [100] developed an ANN model for a small diesel engine driven by blends of various biodiesel with diesel fuels. ANN model was used to predict engines output responses CO₂, CO, UHC, NO, CAD P_{max}, P_{max}, HRR_{max}, and CuHRR. Four engine input operating parameters RPM, torque, biodiesel fuel types and fuel mass flow rate were used as the for ANN modelling. An ANN modelling results were validated against with experimental data.

H. Sharon et al. [101] produced biodiesel of veg and non-veg fried oil by transesterification process. Experiments than conducted using these biodiesel and their B25, B50, B75 blends with diesel on DI diesel engine which showed better emission for B75. An ANN network was shaped with engine power and biodiesel blends as input layer and BSFC, HC, NO_x, BTE, CO and smoke as in the output layer. The SIMULINK network for the trained ANN was generated to forecast the fuel performance and emissions. The ANN network gives a good correlation coefficient of 0.9979 and 0.998 for B15, B30, B60 and B90.

M. H. Shojaeefard et al. [102] experimentally investigated the performance and emission characteristics of a heavy-duty CI engine. In this study engine load, engine speed on power, BSFC, peak pressure, NO_x, CO, CO₂, HC and soot emissions were predicted using ANN network. The tests were performed at various fuel injection timings, loads and speeds. Multi-objective optimization with respect to engine emissions level and engine power was used in order to determine the optimum load, speed and injection timing. For this goal, a fast and elitist non-dominated sorting

genetic algorithm II (NSGA II) was applied to obtain maximum engine power with minimum total exhaust emissions as a two objective functions.

Thomas Renald et. al. [103] conducted a progression of experiments on engine with small modification using LPG and diesel mixture. The major parameters of the LPG jet injector were optimized by the CFD technique by utilizing a CFD code. Engine changes in the performance and emission levels by the of the jet parameters were observed and analyzed. Ultimately, an ANN model was developed to forecast the emission levels using the jet parameters, load and the % of LPG consuming for experiments. It was found that the predicted results provided good correlation with the experimental values.

Vinay Kumar. D et al. [104] conducted experiments on a single cylinder diesel engine whose combustion elements were coated with an experimental thermal barrier coating material made from Lanthanum Zirconate. Biodiesel was prepared from Pongamia Pinnata oil through transesterification process. A large numbers of experiments were carried out on the engine with and without thermal barrier coating using diesel and biodiesel fuels. Performance and emissions data from the experiments were used to train the network with the load, fuel type and coating being the input layer and the BSFC, BTE, CO, HC and NO_x emissions being the output layer. Results showed that the coating of engine components with lanthanum zirconate TBC resulted in improved engine efficiency with reduced emissions. ANN model was tested for its accuracy to predict the performance and emissions of the engine with the correlation coefficient values of 0.998 for both the training and testing data with a mean square error of 0.002 and a mean relative error of 6.8%.

Yusuf Cay [105] created ANN network modelling for a SI engine to predict the BSFC, effective power and EGT of the engine. For training and testing the ANN

network used to develop for a 4 cylinder, 4 stroke gasoline engine operated at different engine torques and speeds. The study proved that the ANN modelling could be used for accurate prediction of performance and other parameters of I/C engines.

Shiva Kumar et al. [106] conducted experiments on C. I engine using Pongamia as a fuel at various fuel injection timings and compression ratios. An ANN method was developed with compression ratio, blend percentage, load and fuel injection timings as the input layer variables. MRE values were found to be less than 10%.

Patel et al. [107] studied the effect of injection timing, injection pressure, compression ratio and load on the performance of a single cylinder CI engine. The experimental tests were carried out at five different fuel injection timings (20°, 22°, 23°, 24°, 25° CA bTDC), five injection pressure (140 , 160, 180, 200, 220 bar) and five compression ratio (18, 17, 16, 15, 14). The ANN model with standard BP algorithm was observed to be the best choice for training the ANN.

Kannan. G.R et. al. [108] proposed ANN model for diesel engine fuelled with waste cooking palm oil based biodiesel. Among the various networks tested, the network with two hidden layers and 11 neurons gave better correlation coefficient for the prediction of engine performance, emission and combustion characteristics.

Sumit Roy et al. [109] explored the potential of ANN to predict the exhaust emissions and performance of a 4 stroke CRDI engine under changing EGR strategies. An ANN network was prepared to forecast BTE, BSFC, CO₂, smoke and NO_x with load, fuel injection pressure, fuel injected per cycle and EGR used as input parameters for the ANN network. This ANN model was capable of forecasting the emissions and performance output of the engine with outstanding correlation coefficients within the range of 0.988-0.998, percentage error in the range of 1.11-4.58%.

Sumit Roy et. al. [110] modelled the emission and performance parameters of a 4 stroke CRDI engine under CNG-diesel dual-fuel using ANN. The developed ANN model was capable of predicting the emission and performance parameters with commendable accuracy as observed from correlation coefficients within the range of 0.99832-0.99998.

Kamyar Nikzadfar et al. [111] conducted experiments with injected fuel mass, injection timing, inlet air pressure and temperature, exhaust pressure, fuel rail pressure and exhaust gas recirculation rate (EGR) as input variables. The data were then used to train a feed forward neural network. Comparison between experimental data and simulated results showed about 6% error in prediction of the outputs. The engine performance and emission were then analyzed using both graphical and statistical methods to study how different input parameters can influence the engine emissions and performance.

2.3. PROBLEM STATEMENT

In the light of the exhaustive and valuable literature review and the subsequent analysis, the problem statement of the present research was devised. The present work intends to deal with the effect of fuel injection timing and injection pressure on engine performance parameters such as BSFC, BTE, EGT and exhaust emissions in case of bio-diesel from Polanga (*Calophyllum inophyllum*) oil and its blends for their use as a substitute fuel of diesel in a light duty four stroke diesel engines. Also, from the literature survey, it has been observed that ANN modelling with *Calophyllum inophyllum* on CI engine does not exist. The present work involves modelling and optimization of C.I. Engine performance and operating parameters for Polanga using ANN networks. On the basis of this valuable information, the following objectives are envisaged for the present research work.

1. A comprehensive engine trial will be carried out to assess the performance and emission behaviours of actual diesel engine fuelled with Polanga biodiesel and its blends and its comparison with the baseline diesel operation.
2. The ANN model for evaluation of emission and performance parameters of CI engine fuelled with *Calophyllum inophyllum* (Polanga) biodiesel and diesel blends has been developed. The simulated results of the developed ANN model are validated and compared with experimental data.
3. Optimization of performance and emission parameters of the developed model is obtained using MATLAB.

CHAPTER 3

SYSTEM DEVELOPMENT AND METHODOLOGY

3.1 INTRODUCTION

This chapter gives a detailed systematic execution of the experimental facilities required for Polanga (*Calophyllum inophyllum*) oil, preparation of various blends of the Polanga biodiesel and its characterization, the test engine's characteristics and specifications, and also describes the test rig and instrumentation. The details of measured parameters, data acquisition system and application software are also provided. After the experimental work, efforts are made to develop an ANN model by testing different learning algorithms with different network structures obtained by altering number of neurons and number of layers, etc. The developed ANN model was then validated using the investigation data as discussed in later sections.

3.2 PRODUCTION OF POLANGA (*CALOPHYLLUM INOPHYLLUM*) BIODIESEL

Polanga (*Calophyllum inophyllum*) oil was extracted from good quality seeds using a screw press. The oil so obtained was pressure filtered and heated at 120°C for 20 minutes to remove moisture. The oil was then preserved in an airtight screw cap bottle. Figure 3.1 shows neat Polanga (*Calophyllum inophyllum*) oil and the seeds. The FFA of the oil was found to be 23.52%.

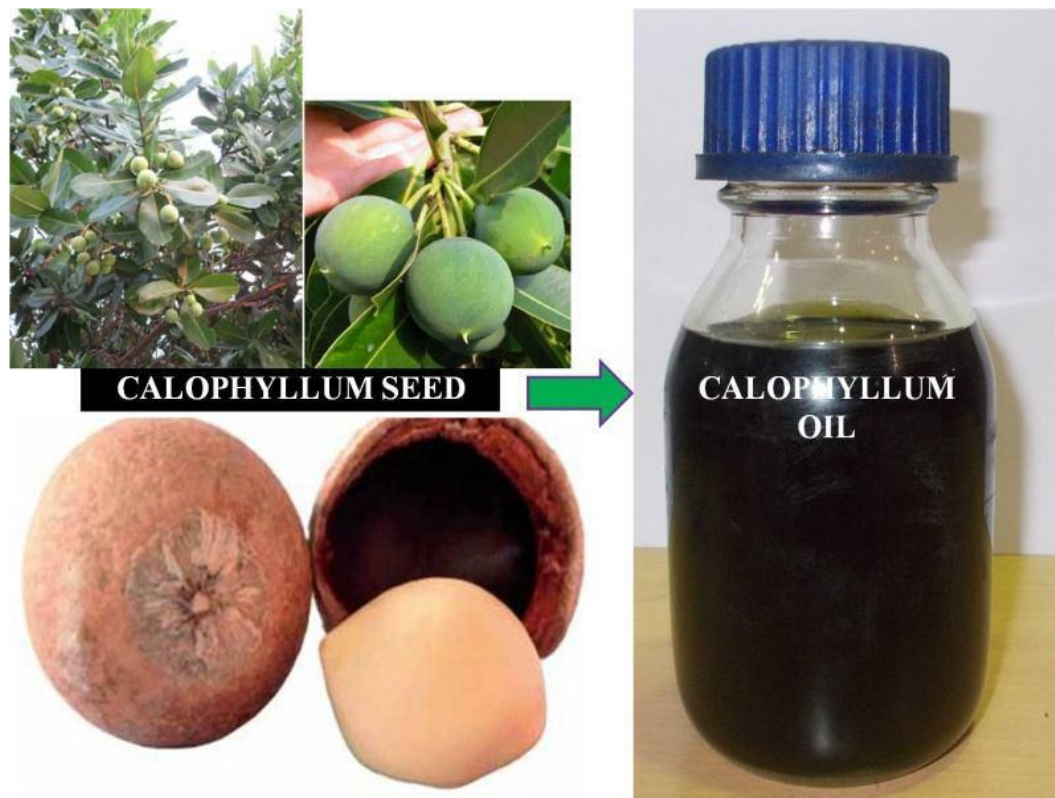


Fig.3.1: Polanga (*Calophyllum inophyllum*) seeds and oil

3.2.1 TRANSESTERIFICATION FOR PRODUCTION OF POLANGA BIODIESEL

Biodiesel is basically formed by the transesterification process from raw Polanga oil feedstock. Transesterification has been identified as the best way to manufacture biodiesel from non-edible raw oil in the company of an acid or base catalyst. Normally, sulfuric acid is considered as the suitable catalyst for this reaction, however a good range of acids may be considered for the same purpose. Oil feedstocks with more than 2% free fatty acid contents are generally transesterified in two stages. In the first stage the FFA reacts with the alcohol in the existence of an acid catalyst, when the FFA is reduced below 2%, then it is transesterified in the presence of alkaline catalyst. As mentioned in the previous section, the FFA of Polanga (*Calophyllum inophyllum*) oil was as high as 23.52%. Therefore, it has to

pass through a two stage transesterification process to produce biodiesel. Such type of reaction is generally very much time consuming and consumes large amounts of catalyst. Therefore, an optimization of process parameters like catalyst concentration, reaction time, etc. shall lead to commercially competitive production of biodiesel from Polanga oil.

3.2.2 BIODIESEL PRODUCTION OPTIMIZATION FROM POLANGA OIL

For the esterification stage, an optimal FFA of 4.74% was achieved for 1.5% catalyst (PTSA) concentration, 65°C reaction temperature and 60 minutes reaction time. Similarly, in the transesterification stage, 0.88% concentration of catalyst (KOH), 62.75°C reaction temperature and 90 minutes of reaction time produced the optimum yield of 96.48% at constant methanol to oil molar ratio of 1:6. Based on this result, bulk quantity of Polanga (*calophyllum inophyllum*) biodiesel was prepared in a large capacity biodiesel reactor. The reactor has a capacity of 1 liter. It's one of the notable features was its methanol recovery system which maintained the oil to methanol molar ratio precisely constant at 1:6 throughout the two stage transesterification process.

As mentioned above, the optimal FFA was 4.74% of the experimental design study. However, the literature indicated that it should be less than 2% of higher yield. Therefore, the esterification stage was carried out using the optimal parameters first to obtain 4.74% FFA in 60 minutes. After that, additional 20 minutes agitation provided the requisite less than 2% FFA. Subsequently, the oil was transesterified as per the optimum process parameters of 0.88% of KOH by original oil mass and nearly 63°C temperature for 90 minutes. The sample so obtained from the reactor was gravity separated for 12 hours to remove glycerol. However, the biodiesel sample so obtained contained impurities like methanol and KOH traces. For further purification the

sample was washed with slightly hot distilled water for several times to remove any traces of methanol or catalysts. The water washing was stopped when the washed water became colorless. Then the oil was heated at 120°C for 25 minutes to remove the moisture.

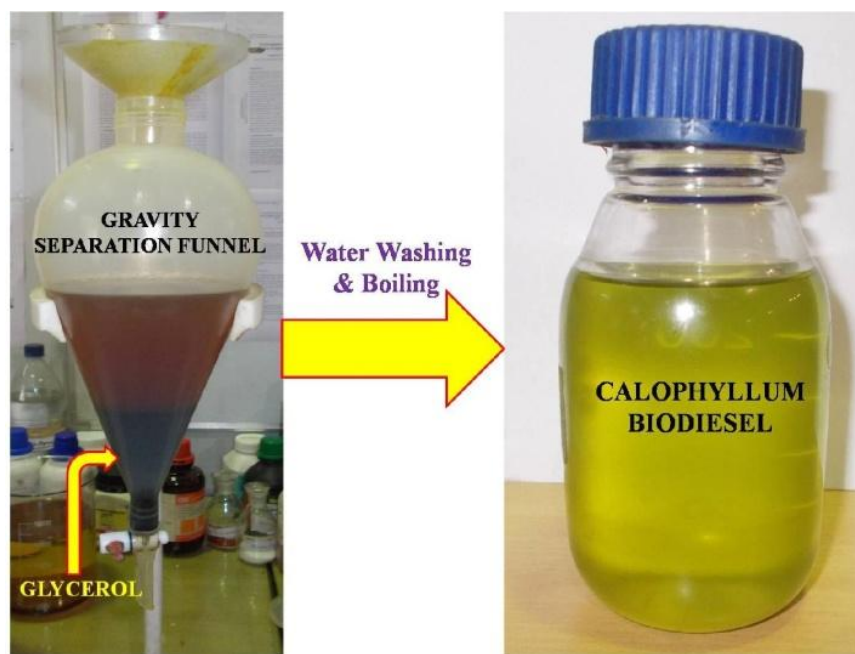


Fig. 3.2: Mineral Polanga (*Calophyllum inophyllum*) and Biodiesel

Finally the Polanga (*Calophyllum inophyllum*) biodiesel was obtained as a pale yellow color and more or less transparent fluid. The gravity separation funnel and the final biodiesel sample is shown in Figure 3.2.

The biodiesel so obtained was completely miscible with mineral diesel. To check the miscibility various proportions of biodiesel were added to mineral diesel and monitored for 15 days, no signs of separation were observed.

3.3 PHYSICO-CHEMICAL CHARACTERIZATION OF POLANGA BIODIESEL

Determination of various physico-chemical and fuel properties of Polanga (*Calophyllum Inophyllum*) biodiesel was essential for its standardization as well as for various calculations of engine trials. Moreover, the properties of blends of Polanga

(Calophyllum Inophyllum) biodiesel and diesel were also essential. Therefore, 4 test fuel samples of 500 cc each were prepared comprising of neat diesel. The blends were named as B10, B20, B30 and B40 with 10%, 20%, 30%, and 40% volume wise substitution of diesel by Polanga biodiesel respectively. Mineral diesel was named as the baseline. The properties of all these test fuel samples were evaluated in the laboratory as discussed below.

3.3.1 KINEMATIC VISCOSITY MEASUREMENT

The viscosity was measured using the Fungilab (Expert-L series) Viscometer. Polanga biodiesel (B100) exhibited kinematic viscosity of 5.55 cSt at 40°C temperature, which was lower than the ASTM 6751 limit of 6 cSt. Therefore, the viscosity of Polanga biodiesel B100 was within the ASTM standard limit. Further, all the Polanga biodiesel blends and diesel, within the entire experimental range of 30°C to 80°C temperature, exhibited viscosities within the prescribed limit of ASTM 6751. However, for lower blends viscosity variation with temperature was nominal. At 40°C diesel showed 2.91 cst of viscosity, whereas Polanga biodiesel B100 was having nearly twice the value. Therefore, atomization, vaporization and air-fuel mixing characteristics of Polanga biodiesel are supposed to be inferior as compared to mineral diesel.

3.3.2 DENSITY MEASUREMENT

Density is also a key property of fuel, with potential to directly influence the engine performance, emission and combustion behavior. Many important characteristics, such as cetane rating and heating value, are related to the density. It was measured using a Lemis made type DM300 density meter. In the current investigation, the density of Polanga biodiesel and its blends were determined at temperatures 15°C and 30-80°C with 10°C increases in every step. At 15°C, Polanga

biodiesel exhibited density of 0.944 g/cc as compared to 0.830 g/cc showed by the neat diesel. The density of Polanga biodiesel and its blends were less sensitive to temperature than viscosity. It may be observed that within the entire range of temperature variation, the change in density of Polanga biodiesel was merely 4.3%. Polanga biodiesel B100 and all its blends were well within the prescribed ISO12185 standard for density.

3.3.3 CALORIFIC VALUE MEASUREMENT

A bomb calorimeter was used to determine the calorific value of the test fuels. It may be observed that Polanga biodiesel B100 was having a calorific value of 36990.56 KJ/kg as compared to 43990.3 KJ/kg in the case of diesel. The calorific value with the fractional volume of Polanga biodiesel blends in the test fuel was 40095.2 KJ/kg, 39195.73 KJ/kg, 38395.3 KJ/kg and 37796.98 KJ/kg for B10, B20, B30 and B40 respectively.

3.3.4 OXIDATIVE STABILITY MEASUREMENT

As described earlier, the biodiesel Rancimat method was used for oxidation stability study. The EN14112 standard was followed with 10 L/h airflow and 110 °C bath temperature. The total induction time showed by the Polanga biodiesel B100 sample was 3.97 hours as against the standard of three hours. Therefore, the oxidation stability of Polanga biodiesel B100 was found to be within the limits of the European biodiesel standard. However, the stability of the oil was not excellent and just marginally over the prescribed limit. Therefore, addition of oxidation stability improvers to the Polanga biodiesel may be studied before commercial scale production or usage.

Various equipments used for determination of physico-chemical and fuel properties and the corresponding standards are given in Table 3.1.

Table 3.1: List of equipments and standards used for biodiesel property measurements

S. No	Property	Equipment	Manufacturer	ASTMD6751	Range
1	Kinematic viscosity	Petrotest Viscometer	Fungilab	D445	1-100 cSt
3	Oxidative stability	873 Rancimat	Metrohm	D675	3 hours
4	Density	Density meter	Lemis	D1298/ISO12185	0-3 g/cc
6	Calorific value	Bomb calorimeter	Rajdhani (India)	Not specified	Not specified

3.4 PREPARATION OF FUEL BLENDS FOR ENGINE TRIAL

As mentioned in the earlier sections, the National Biodiesel Mission envisaged 20% substitution of mineral diesel by biodiesel. The major reason of confining the biodiesel substitutions by 20% is the lack of feed stocks. Moreover, long term durability issues concerned with biodiesel usage in unmodified diesel engines are also one of the factors affecting the lower substitution targets of biodiesel. In this context, the present study considered only 10%, 20%, 30% and 40% blending of Polanga (*Calophyllum inophyllum*) biodiesel in diesel. Therefore, the test fuels for engine trial comprised of B10, B20, B30 and B40 along with the neat diesel. The test fuel samples were prepared by volume wise substitution of diesel in the blend and the subsequent accurate demonstration using a high RPM hand blender. Figure 3.3 shows various blends for the engine trial.

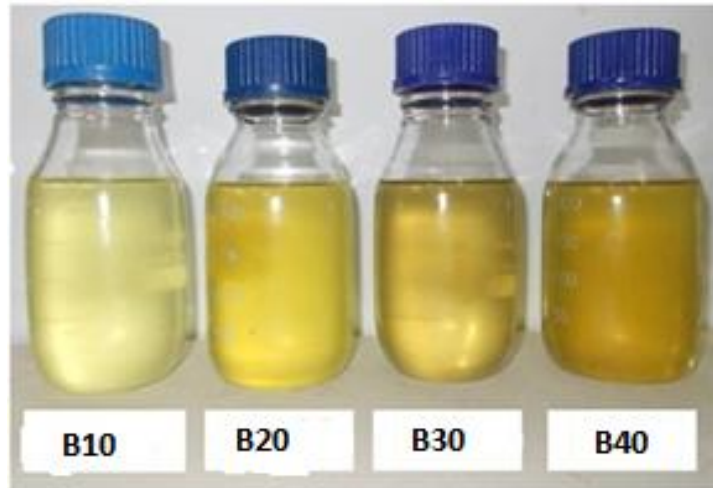


Fig.3.3: Various blends of Polanga biodiesel and diesel

3.5 SELECTION OF DIESEL ENGINE FOR EXPERIMENTAL TRIAL

As indicated earlier, single cylinder diesel engines play a vital role in Indian economy. Starting from small capacity single cylinder agricultural engines to heavy duty multi-cylinder railway locomotive and marine engines, they are widely used. However, in the present work a single cylinder, light duty diesel engine was chosen for experimental trials because of a number of reasons. Firstly, such types of engines are portable and hence can be used almost anywhere, even in the remotest parts of the country where the conventional energy modes are not accessible. Secondly, these engines are an integral part of the rural agrarian economy of India and thirdly, there are at least two million such engines that actively running across the country making it one of the largest sources of decentralized power.

3.5.1 DEVELOPMENT OF ENGINE TEST RIG

As discussed in the previous section in the present research work Kirloskar make single cylinder, 4-stroke and water cooled diesel engine was selected. Such types of small engines are generally used for agricultural activities and decentralized

power generation purposes across the India. Figure 3.4 shows the engine test setup used for research work located in UPES Dehradun (Uttarakhand) India.



Fig. 3.4: The Test Engine

Manual cranking is used to start diesel engine with operating a decompression lever. The centrifugal speed governor is used to control the constant speed of the engine. The engine cylinder material was cast iron and cast iron with a hardened high-phosphorus liner was fitted into the cylinder. Splash type wet sump lubrication method was used in this diesel engine. To operate exhaust and inlet valves an overhead camshaft is used which is driven by the crankshaft. The complete specification of the diesel engine is provided in Table 3.2.

Table 3.2 Engine specification

Make	Kirloskar
No. of cylinder	1
Strokes	4
Rated Power	3.5 kW@1500rpm
Stroke length	110mm
Cylinder diameter	80mm
Compression ratio	16.5:1
Connecting rod length	234mm
Orifice diameter	20mm
Dynamometer arm length	185mm
Valve Opening (Inlet)	4.5°bTDC
Valve Closing (Inlet)	35.5°aBDC
Valve Opening (Exhaust)	35.5°bBDC
Valve Closing (Exhaust)	4.5°aTDC
Fuel injection timing	23°bTDC

The specification of the fuel injector is shown in Table 3.3 and the injector with the spray cone is shown in Figure 3.5.

Table.3.3: Injector specification

Type	Bosch
No. of injector holes	3
Nozzle diameter	0.148 mm
Spray orientation angle	55°CA
Injection duration	18°CA
Full load diesel injection per cycle	32.8 mg



Fig. 3.5: Three hole injector and the spray cone

For the provision of loading, an eddy current dynamometer of 7.5kW rating was coupled to the engine shaft. A high precision strain gauge type load cell was attached to the dynamometer to accurately transmit the engine loading. A magnetic pickup type RPM sensor was fastened at the end of the dynamometer to measure RPM of the engine. The eddy current type dynamometer, the magnetic pickup type RPM sensor and the strain gauge type load cell are shown in Figure 3.6.



Fig. 3.6: The eddy current type Dynamometer

3.5.2 IN-CYLINDER PRESSURE

A quartz (piezoelectric) Kistler make transducer was used to determine the engine cylinder combustion gas pressure, mounted on the cylinder head. The signals from charging amplifier were fed to the data acquisition system where the engine control module converted the signals into digital data. The in-cylinder pressure data in terms of pressure crank angle history was obtained from the Legion Brothers database. The maximum resolution of the pressure sensor was 1°CA. The cylinder

pressure signal was passed through an amplifier to give outputs of 0-10volts for the calibrated pressure range of 0-100 bar.

3.5.3 TEMPERATURE MEASUREMENT

For exhaust gas temperature measurement, Chrome-Alumel K-Type thermocouples with stainless steel wire were implanted close to the engine exhaust manifold. The small micro-voltage outputs from these thermocouples were processed by the Express V5.76 software to give values in degrees centigrade for data logging and engine monitoring purposes. For cooling water temperature measurement, Chrome-Alumel K-Type thermocouples with stainless steel wire were implanted close to the engine water inlet and outlet manifold which gives the temperature of the water also obtained from the Legion Brothers database.

3.5.4 EMISSION MEASUREMENT

AVL make (AVL DiGas 444) Exhaust gas analyzer was used for evaluating the exhaust emissions CO, CO₂, UHC and NO_x from the diesel engine. AVL Gurgaon makes model 437C smoke meter was used for smoke opacity emission measurement from the diesel engine. Emissions of exhaust recorded were: CO carbon monoxide in % vol, UHC emission in ppm and NO_x in ppm by using AVL DiGas 444 gas analyzer. Smoke opacity present in the exhaust calculated in % by using an AVL 437C smoke meter. The specifications have been given is given Table 3.4.

Table 3.4: Exhaust gas analyzer and Smoke Meter technical specifications

AVL DiGas 444 Exhaust gas analyzer		
Measurement principle	CO, UHC, CO ₂	Infrared measurement
	O ₂	Electrochemical Measurement
	NO _x	Electrochemical Measurement
Operating temperature	+5 to +45°C	Keeping measurement Accuracy
	+1 to +50°C	Ready for measurement
	+5 to +35°C	With integral NO sensor (Peaks of: +40°C)
Power drawn	150 VA	
Dimensions	432 x 230 x 470 mm	(w x h x l)
Weight	16 Kg	
AVL 437C smoke meter		
Heating Time	Approx. 20 min	
Light source	Halogen bulb 12 V / 5W	
Detector	Selenium photocell dia. 45 mm	

The exhaust gas analyzer and the smoke meter were connected to the diesel engine exhaust manifold by means of probes. Figure 3.7 shows the photographic view

of the AVL 437C make smoke meter and the AVL DiGas 444 make exhaust gas analyzer respectively.



Fig.3.7: Smoke meter and Exhaust gas analyzer

For the measurement of gaseous emissions from the exhaust, a gas test bench AVL make (AVL DiGas 444) Exhaust gas analyzer was used for evaluating the exhaust emissions CO, CO₂, UHC and NO_x from the test diesel engine shown in Figure 3.7. The Exhaust gas analyzer and smoke directly connected to the exhaust pipe of diesel engine and it has been maintained 190°C wall temperature to avoid the sticking of hydrocarbons into the exhaust pipe line. The engine exhaust line is made longer from the engine exhaust port to the unit where the gas analyzer and a smoke meter has been located. In order to minimize the misalignment of the measured emission gas concentration, due to the difference between the sampling, transport time and the analyzer's response time, 20 seconds duration was used as per manufacturer specification.

3.5.5 DATA ACQUISITION SYSTEM

Centralized data acquisition system Engine test Express V5.76 was developed by Legion Brothers, which was Labview based software package. The entire signals gathered from the engine test rig required to be changed from analogue to a digital form. This task has been completed by using an analogue to digital converter (ADC) edge linking the computer and the transducers. For this work 16 channels and 500MHz bandwidth analogue to digital converter (ADC) was used. Figure 3.8 shows the data acquisition system used for this work at UPES Dehradun Engine testing lab.



Fig.3.8: The Data Acquisition System

The data acquisition system was working on 37 kHz and the sampling time used was normally 60 seconds. This time duration was selected to ensure that the data is representative. The CED 1401 power ADC is able to record waveform data, digital (event) data and marker information. It can also generate waveform and digital

outputs simultaneously for real-time, experimental system using its own clock memory, processor and underneath the control of the crowd computer.

3.5.5.1 ENGINE TEST EXPRESS V5.76

Engine test Express V5.76 software is a fully assimilated Windows 2000-XP based engine test software system developed and designed by the Legion Brothers Company. Express V5.76 software maintains straight digital control high speed proportional integral derivative control loops, supports User-Definable Control suitable for multifaceted non-linear conditions. The digital proportional integral derivative (PID) controller system is supplied with hardware and software device driver developed by CP Engineering, to make the real-time atmosphere underneath for Windows 2000-XP. Through the Engine test Express V5.76, the engine BTE, BSFC, EGT and peak cylinder pressure etc, were measured in this study.

3.5.6 ENGINE TEST CYCLES

Both steady and transient processes were designed to assess the exhaust emission and performance characteristics of the diesel engine which was run using Polanga biodiesel blends as a test fuel. The engine RPM and load were the two parameters to be controlled in the test. The transient processes were programmed using the Express V5.76 software.

3.6 TESTING PROCEDURES AND THE DETAILS OF THE MEASURED PARAMETERS

The experimental investigations have been carried out using the test rig explained in this section. The experiments have been carried out for a wide range of Polanga biodiesel blends. The types of tests carried out in this investigation are listed below:

1. Steady state test at the constant full load at 1500 RPM engine speed using B10, B20, B30 and B40 Polanga biodiesel blends at different fuel injection timing between 15° bTDC to 31° bTDC at an interval of 4° .
2. Steady state test of the constant full load at 1500 RPM engine speed using B10, B20, B30 and B40 Polanga biodiesel blends at a different fuel injection pressure between 160 bar to 240 bar at an interval of 20 bars.

Using these test cycles for different Polanga biodiesels blends, the CI engine's performance and emission parameters has been measured using the apparatus described above. These parameters have been selected due to their importance of engine design and performance and emission evaluation. During the testing process, after each test run the fuel lines were drained prior to filling them with the next Polanga fuel blend. The engine was operated using newly filled fuel for 10 minutes without collecting data. This was done to ensure that all previous fuel in flow meter, fuel filter and fuel pipes had been removed. A computer-based data acquisition system was used to collect the parameters of interest of research purpose.

The final experimental setup consisted of the CI engine, water cooling arrangement for the engine, the fuel supply and measurement system, air supply and measurement system, load variation and its measurement system, RPM measurement sensor, cylinder inside pressure measurement unit, emission measurement equipments, digital data acquisition system and a computer. Figure 3.9 shows the engine test rig layout comprising of individual components and their inter-connectivity.

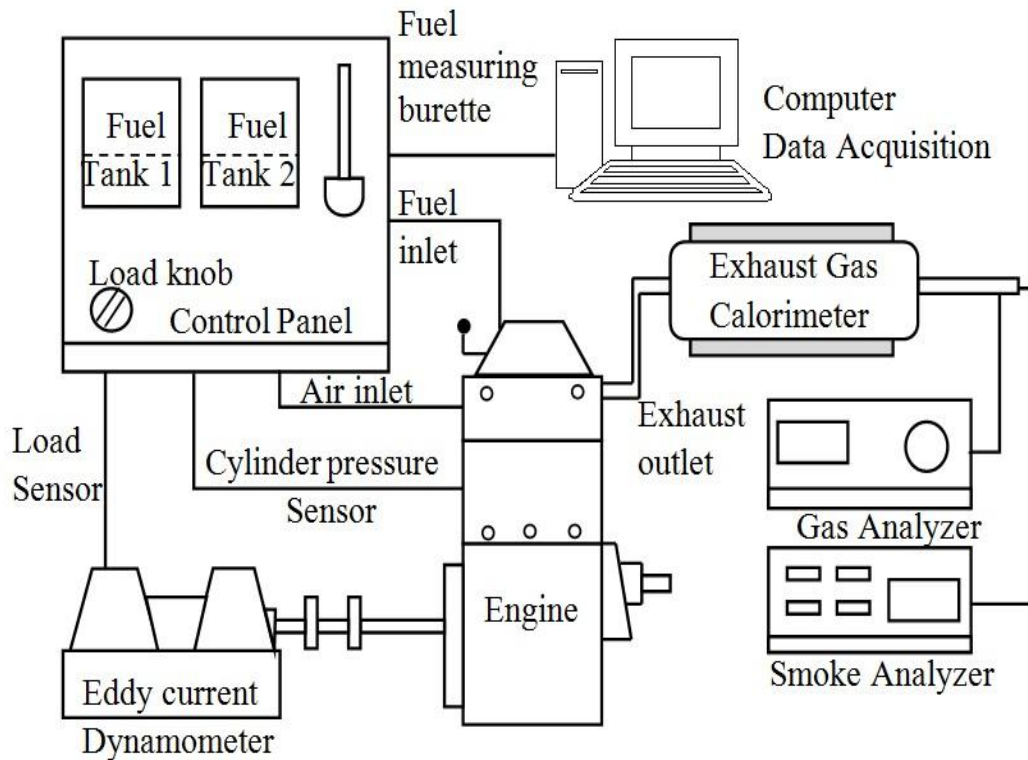


Fig.3.9: Layout of engine test rig

3.7 SELECTION OF ENGINE TEST PARAMETERS

The selections of appropriate test parameters are a vital part of engine research. The objective of the present research investigation is to determine the exhaust emission and performance of the single cylinder diesel engine operated on Polanga biodiesel blends followed by a comparison with the baseline data of conventional diesel fuel. The engine test was done as specified by IS: 10000. The main parameters desired from the engine were selected judiciously. Various engine test parameters are classified as the observed parameters and the calculated parameters. Observed parameters are enlisted below.

1. Engine load.
2. Brake thermal efficiency.
3. Fuel consumption rate.
4. In-cylinder pressure.

5. Emissions of CO, CO₂, NO_x, HC.
6. Exhaust temperature.
7. Smoke opacity.

Once the parameters were selected, the essential instruments required for sensing these parameters were installed at the appropriate points as described in the layout diagram, Figure 3.9, in the experimental set-up.

3.7.1 MEASUREMENT OF OPERATING PARAMETERS OF THE TEST ENGINE

In order to obtain precise and repeatable diesel engine trial data of engine performance and exhaust emission characteristics. The combustion pressure, EGT, RPM, engine load, BTE, BSFC, were the main parameters measured. The signal from the outlined instruments required some form of signal conditioning prior to being connected to the data acquisition system. It was, therefore, necessary to use amplification in order to increase the resolution of low level signals and to distinguish them from background noise. In order to achieve the highest clarity, the signals needed to be amplified so that the maximum voltage range of the conditioned signals was equal to the maximum input range of the analogue-to digital converter (ADC). This was used for transformation of the acquired data from analogue to digital form, enabling a computer to read, save and process the collected data.

3.7.2 MEASUREMENT METHODS

As already elaborated, the key components of the engine test rig setup are, fuel consumption measuring unit, fuel flow rate measuring unit, eddy current dynamometer for loading arrangement, temperature sensor, in-cylinder pressure sensor and emissions measurement equipments. While carrying out the experiment, the engine was always started and allowed to run for 30 minutes to warm up. For

baseline diesel data, the observations were taken only after the prescribed 30 minutes were complete. For Polanga biodiesel blends the fuel line was swapped, after the warm up period with neat diesel, allowing the Polanga biodiesel to connect to the engine for taking observations. The diesel engine shaft load was varied using the eddy current dynamometer. The gaseous exhaust emissions pollutant of diesel engine was measured by using the AVL gas analyzer and an AVL smoke meter. The emission data was collected manually from the gas analyzer and smoke meter.

3.7.3 ACCURACIES AND UNCERTAINTIES OF THE EXPERIMENTAL RESULT

Table 3.5 shows the accuracies and uncertainties associated with various measurements. It may be observed that all of the measurements exhibited higher accuracy. The repeatability of all measurements were checked throughout the experimental trial and found sufficiently close. It may be noted that the various measured like viscosity, density, calorific value, oxidative stability, chromatography, etc. in the property characterization was not subjected to the data accuracy. It was so because equipments like chromatography and oxidative stability were at high precision and are regularly calibrated equipments. Therefore, the % uncertainties in these equipments were very low. For viscosity, density, calorific value and cold flow, plugging point the % uncertainty was less than 0.1%. The repeatability of these equipments were checked and found highly satisfactory.

Table 3.5: Accuracies and uncertainties associated with various measurements

Instrument	Range of Instrument	Accuracy achieved	% uncertainty
Gas Analyser (AVL DiGAS 444)			
CO	0-10% Vol	<0.6% Vol: $\pm 0.03\%$ vol >0.6% Vol: $\pm 1\%$	± 0.3
UHC	0-20,000 ppm Vol	<200 ppm vol: ± 1 ppm vol >200 ppm % Vol: $\pm 1\%$	± 0.2
CO ₂	0-20% vol	<0.6% Vol: $\pm 0.03\%$ vol >0.6% Vol: $\pm 1\%$	0.1% vol
NO _x	0-5000 ppm Vol	<500 ppm vol: ± 5 ppm vol >500 ppm % Vol: $\pm 1\%$	± 0.2
AVL 437C smoke meter			
Smoke opacity	0-100%	$\pm 1\%$	± 1
Exhaust gas temperature	0-1250 ⁰ C	$\pm 1^0$ C	± 0.2
Burette for fuel measurement	-----	± 1 cc	± 1
Pressure transducer	0-100 bar	± 0.01 bar	± 0.1

3.7.4 CALIBRATION OF INSTRUMENTS

The measuring sensors and instruments which have been used were calibrated through the data acquisition system before the test was conducted. To achieve this, readings were taken by the data acquisition as the input signals were swept through

their operating ranges, in order to calculate the gain and offset values for each individual signal. The Kistler in-cylinder pressure transducer was calibrated by applying a known pressure to the sensor and measuring the voltage from the charge amplifier. As the Kistler pressure transducer only generated a signal with a change in pressure, the cylinder pressure was referenced to the atmospheric pressure during the exhaust stroke, with the resulting offset being applied automatically in the data acquisition software. The pressure measurements were taken through the data acquisition system and the appropriate gain and offset values for each transducer calculated. All emissions measurement equipments were calibrated daily prior to any experimental work according to the emission measurement procedures.

3.7.5 PROCEDURE TO ENSURE ACCURACY OF MEASUREMENT

It may be observed that all of the measurements exhibited higher accuracy. The repeatability of all measurements were checked throughout the experimental trial and found sufficiently close. It may be noted that the various measurands like viscosity, density, calorific value, oxidative stability, chromatography, etc. in the property characterization were not subjected to the data accuracy. It was so because equipments like chromatography and oxidative stability where high precision and regularly calibrated equipments. During engine testing the measured parameters generally show some dispersion of the mean values. This is quantified in terms of measurement error which is the variation between measurements of the same quantity of the same test. To quantify measurement error, the same test needs to be repeated several times. One of the common parameters used to quantify this error is the standard deviation (SD). SD is a measurement of variability. To estimate the repeatability of measurement and the accuracy of the procedure the tests were repeated three times and the mean values have been obtained for the detailed analyses.

The parameters that were investigated include BSFC, BTE, Pmax and exhaust emission during operating conditions. The SD of the data obtained on emissions and in-cylinder pressure was calculated by using the 36 segments during the steady state operations as well. As the parameters of the transient conditions varied from one segment to the other, the SD of in-cylinder pressure and emissions was determined from the three sets of tests conducted at same operating conditions.

3.8 ARTIFICIAL NEURAL NETWORKS (ANN) MODEL

An ANN is an in sequence processing concept that is encouraged by a human genetic nervous system. It's a simply numerical model of the artificial neuron, the consequences of synapses are signified by correlation of weights that transform the outcome of the coupled input signals, and the nonlinear characteristics displayed by artificial neurons are characterized by an ANN network transfer function. The artificial neuron impulse is then calculated as the weighted sum of the network inputs. The learning ability of an artificial neuron is attained by regulating the weights in harmony with the type of learning algorithm selected. The schematic arrangement of a feed forward ANN network is given in Figure 3.10.

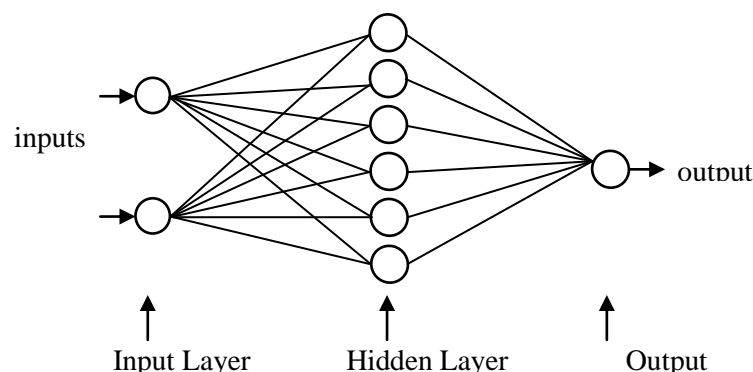


Fig.3.10 Representation of feed forward network for single hidden layer

The network summation function used for the present study is specified by Eq. (3.1).

$$NT_i = \sum_{j=1}^n w_{ij}x_j + w_{bi} \quad (3.1)$$

For the training and development of the ANN network model for exhaust emission and performance prediction of engine flow chart is given in Figure 3.11.

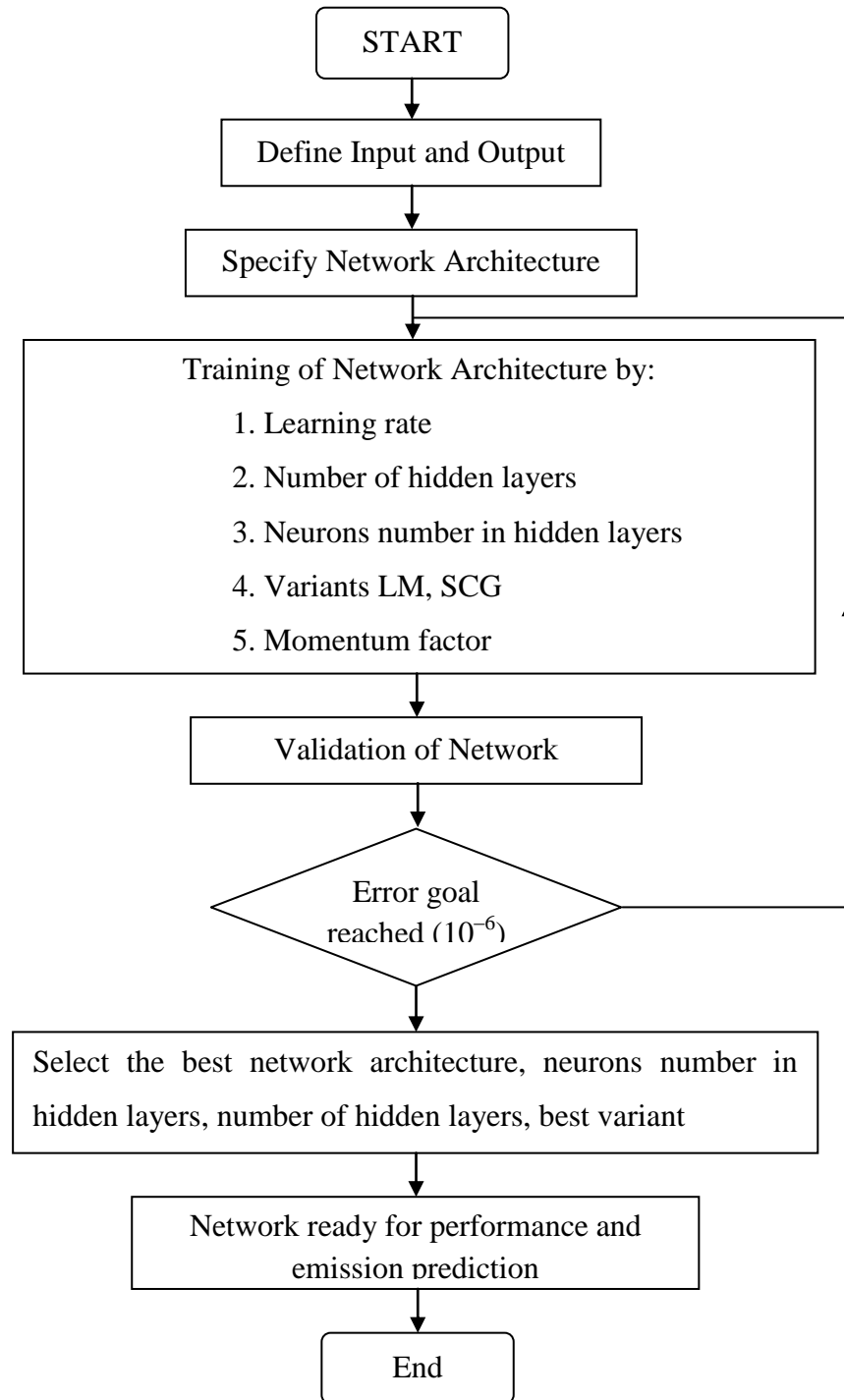


Fig. 3.11 Flow chart for the training of ANN network model

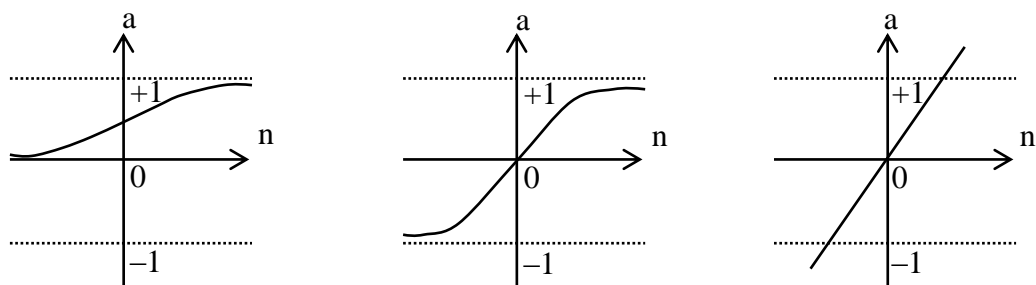
The activation function provides a curvilinear relation between the input and output layers. It also determines the output of the cell by processing the net input to the cell. The selection of an appropriate activation function significantly affects network performance. Commonly used activation functions are the threshold function, step activation function, sigmoid function, and hyperbolic tangent function. The type of activation function depends on the type of neural network to be designed. A sigmoid function is widely used for the transfer function. The Logistic transfer function of the ANN model in this study is given in Eq. (3.2).

$$f(NT_i) = \frac{1}{1 + e^{-NT_i}} \quad (3.2)$$

The hyperbolic tangent function is given by Eq. (3.3).

$$\tanh(NT_i) = \frac{e^{NT_i} - e^{-NT_i}}{e^{NT_i} + e^{-NT_i}} \quad (3.3)$$

The transfer functions used in the present work are shown in Figure 3.12. For pattern recognition sigmoid output neurons have been used and for function fitting linear output neurons basically used.



(a) Log-sigmoid

(b) Tan-sigmoid

(c) Pure linear

Fig. 3.12 Different transfer functions

The basically three transfer functions explained here for commonly used for multilayer ANN networks, but different types of transfer functions can also be used if required.

The significant advantages of artificial neural networks are learning ability and the use of different learning algorithms. The most important factor which determines its success in practice, after the selection of ANN architecture, is the learning algorithm. In order to obtain the output values closest to the numerical values, the best learning algorithm and the number of optimum neurons in the hidden layer must be determined.

A most sought-after algorithm is the back-propagation algorithm, which has different variants. Back-propagation algorithm is a revising the ANN network weights and biases in the way that performance function reduces quickly. The attuned biases and weights of mth layer at iteration k are calculated by Eqs. (3.4) and (3.5).

$$w_{i,j}^m(k+1) = w_{i,j}^m(k) - \alpha \frac{\partial F}{\partial w_{i,j}^m} \quad (3.4)$$

$$b_i^m(k+1) = b_i^m(k) - \alpha \frac{\partial F}{\partial b_i^m} \quad (3.5)$$

Where α is the learning rate and w_{ij} represents the weights of connections between neurons i and j. The value of α should be small adequate for accurate approximation. Gradient in Eqs. (3.4) and (3.5) can be calculated by means of chain law of differentiation.

Various network training options are available in the back-propagation algorithm, for example BP with variable learning rate, Levenberg Marquardt (LM), SCG, Quasi-Newton etc. Back-propagation training algorithms such as conjugate gradient, quasi-Newton, and Levenberg-Marquardt (LM) use standard numerical optimization techniques. ANN with back-propagation algorithm learns by changing the weights

which are stored as knowledge. The algorithm uses the second-order derivatives of the cost function so that a better convergence behavior can be obtained. Back-propagation through gradient descent with momentum and gradient descent are extremely time-consuming for realistic problems while Quasi-Newton, Levenberg Marquardt, conjugate gradient are quick learning algorithms.

To train ANN networks various network training functions can be used to obtain the precise goal output. As everyone's input is functional to the ANN network and output of the network is evaluated after then this output value is compared with the authentic objective value and also same time error is computed. This error will be reduced by adjusting the ANN network biases and weights. The objective is to minimize the mean square error.

The algorithm has least mean square error obtained when organized ANN network training is carried out, where the network learning rule is offered with a set of examples of needed network behavior:

$$\{\mathbf{p}_1, \mathbf{t}_1\}, \{\mathbf{p}_2, \mathbf{t}_2\}, \dots, \{\mathbf{p}_Q, \mathbf{t}_Q\}$$

Here \mathbf{t}_Q is the corresponding target output and \mathbf{p}_Q is an input to the network. As each input is useful to the ANN network because this ANN network output is judged by the goal. The inaccuracy is computed as the disparity between the goal output and the ANN network output. The least mean square algorithm regulates the weights and biases of the linear ANN network so that reduce the MSE. For the linear network, the mean square error is a quadratic function. Particularly, the features of ANN input vectors determine whether a unique solution exists for this Eq. (3.6) is used.

$$\text{MSE} = \frac{1}{Q} \sum_{k=1}^Q (t(k) - a(k))^2 \quad (3.6)$$

Where $a(k)$, $t(k)$ are the network value and actual value respectively and Q is the epoch number. Once the mean square error dropped below a preset value or the highest epochs digit, the network training ends. Then this ANN trained network may be utilized for replicating the outputs for the given inputs.

The performance of the ANN network is also estimated by using MRE and it is defined by the mean ratio between the error and the investigational values which is given by Eq. (3.7).

$$\text{MRE} = 1/N \left(\sum_{i=1}^N 100 \left(\frac{a_i - p_i}{a_i} \right) \right) \quad (3.7)$$

Where N is the data number present in the trial data set, a_i is the investigational value and p_i is the forecasted value of ANN network. MRE demonstrates how large error occurs by ANN network with respect to the actual value and is given by in term of percentage. The lesser value of mean square error indicates that there is a better relationship between investigational and forecasted values.

To get the best prediction by the network, several architectures are evaluated and trained using the experimental data. The back-propagation algorithm is utilized in the training of all ANN models. In the training stage, to obtain the output precisely, the number of neurons in the hidden layer is increased step by step (i.e. 5 to 20). For this purpose, BFGS (Quasi-Newton back propagation), LM (Levenberge Marquardt learning algorithm) and SCG (scaled conjugate gradient learning algorithm) learning algorithms are used in the building of the network structure.

The Back propagation algorithm is decomposed by giving four steps:

- i) Computation by Feed-forward method
- ii) Back propagation to the output layer
- iii) Back propagation to the hidden layer

iv) Weight updates of the network

The algorithm is ended when the error function value becomes satisfactorily small.

3.8.1 ANN BACK PROPAGATION ALGORITHM

Following steps are used in back propagation algorithm

1. Apply the inputs to the ANN network and find the output this initial network output could be no matter which, as the opening weights are random numbers.

2. Compute the error for output neuron (ON). The error is:

$$\text{Error}_{\text{ON}} = \text{Output}_{\text{ON}} (1 - \text{Output}_{\text{ON}}) (\text{Target}_{\text{ON}} - \text{Output}_{\text{ON}})$$

The “*Output (1-Output)*” expression is essential in the equation for the reason that of the Sigmoid Function-if it is just using a threshold neuron it would be (*Target-Output*).

3. Modify the weight. Let W_{AB}^+ be the new weight and W_{AB} be the initial weight, relation between W_{AB}^+ and W_{AB} is given by following a formula

$$W_{AB}^+ = W_{AB} + (\text{Error}_{\text{ON}} \times \text{Output}_{\text{HN}})$$

This is the output of the connecting hidden neuron not an output neuron. In this way update all the weights for the output layer.

4. Compute the errors for the network neurons present in the hidden layer. The result of output layer can't be calculated openly, so these are *Back Propagated* from the output layer as the name indicated of the algorithm. This activity is carried out by collecting the errors from the output neurons and successively sends back to get the hidden layer.

5. After getting the error for the network hidden layer, artificial neurons at this time proceed to stage 3 to modify the network hidden layer weights.

6. By reiterating this method network is trained for any number of layers.

7. Calculation of the total error is computed by summing up every one of the errors for each neuron entity and then for every pattern.

3.8.2 NORMALIZATION PROCESS FOR INPUT AND OUTPUT DATA

From back propagation ANN network modelling process, ranging of inputs and outputs data significantly affects the presentation of ANN network. For logistic sigmoid transfer function, we can use values between 0 and 1. Before training and testing ANN network inputs and outputs sets of data are normalized. In ANN network, after normalization data set values can be lying between -1 and 1 or 0 and 1 .

$$nv_i = \left(\frac{v_{min} - v_i}{v_{min} - v_{max}} \right) \quad (3.8)$$

$$nv_i = 2 \left(\frac{v_{min} - v_i}{v_{min} - v_{max}} \right) - 1 \quad (3.9)$$

According to the literature survey, basically two mathematical methods are used for normalization the data which are given by (Eqs. (3.8) and (3.9)). In the present work, normalization values of input and output was between 0.1 and 0.9 and calculated by using Eq. (3.9).

3.8.3 TRAINING PROCESS DESIGN

The ANN network training process designed using Levenberg Marquardt (LM) algorithm is given as follows:

1. With the randomly generated preliminary weights, calculate the error (e_k).
2. Adjusting the weights by using Eq. (3.10).

$$w_{k+1} = w_k - (J_k^T J_k + \mu I)^{-1} J_k e_k \quad (3.10)$$

w_k is the present weight, w_{k+1} is the next weight, e_k is the training error, J_k is the Jacobian matrix, μ is the combination coefficient and I is the Identity matrix.

As per the network update law, if the net error goes to smaller amount which, means it is lower than the previous one, it means that the estimate on total error function is running and the total μ could be adjusted smaller to lessen the influence of the gradient descent path. If the network error finds positive, means it's more than the previous error, it proves that it is essential to chase the gradient more to look for a appropriate curvature for quadratic estimate.

3. Apply the fresh weights, estimate the overall error.

4. If the overall error is boosted after the result of the modernized, then withdraw the step (such as retune the weight vector to the valuable value) and amplify combination coefficient by 9 or by some erstwhile factors. Then again go to step 2 and try to reduce error again.

5. If the total present error is lessened after a result of the weight update, then recognize the step (such as consider new weight vector as the present one) and reduced, the combination coefficient by a factor of 10 or by the same factor as discussed in step 4.

6. Follow step 2 with the new fresh network weights until the present total network error reached lesser than the needed value. This whole method is discussed by flowchart given in Figure 3.13.

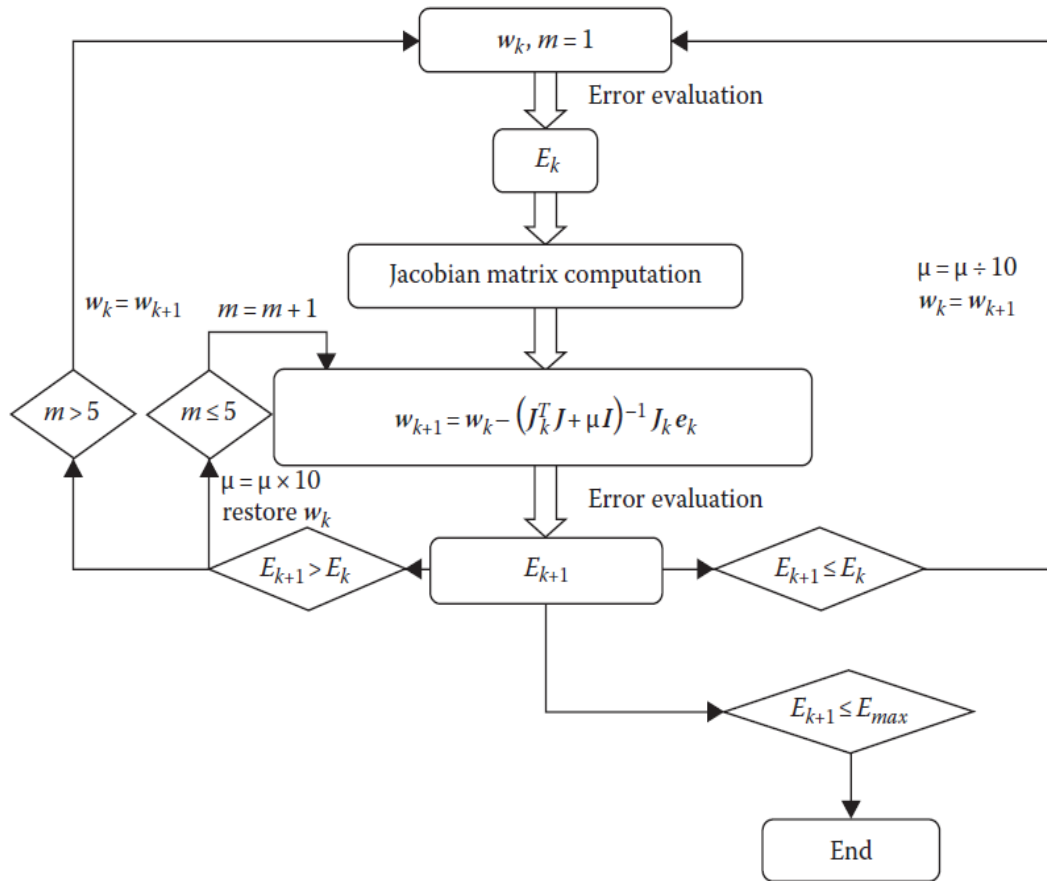


Fig. 3.13 Levenberg–Marquardt algorithm block diagram for training

: E_{k+1} is the present total error, and E_k is the last total error.

3.8.4 POST-TRAINING ANALYSIS

The accuracy of an ANN trained network can be given by the errors obtained on the validation, test and training sets, but it is frequently helpful to examine the response of the ANN network in detail. One method is to execute a regression analysis, among the corresponding targets and the network response. A computer code is deliberate to execute this analysis. Figure 3.14 demonstrates the graphical network output provided by the code.

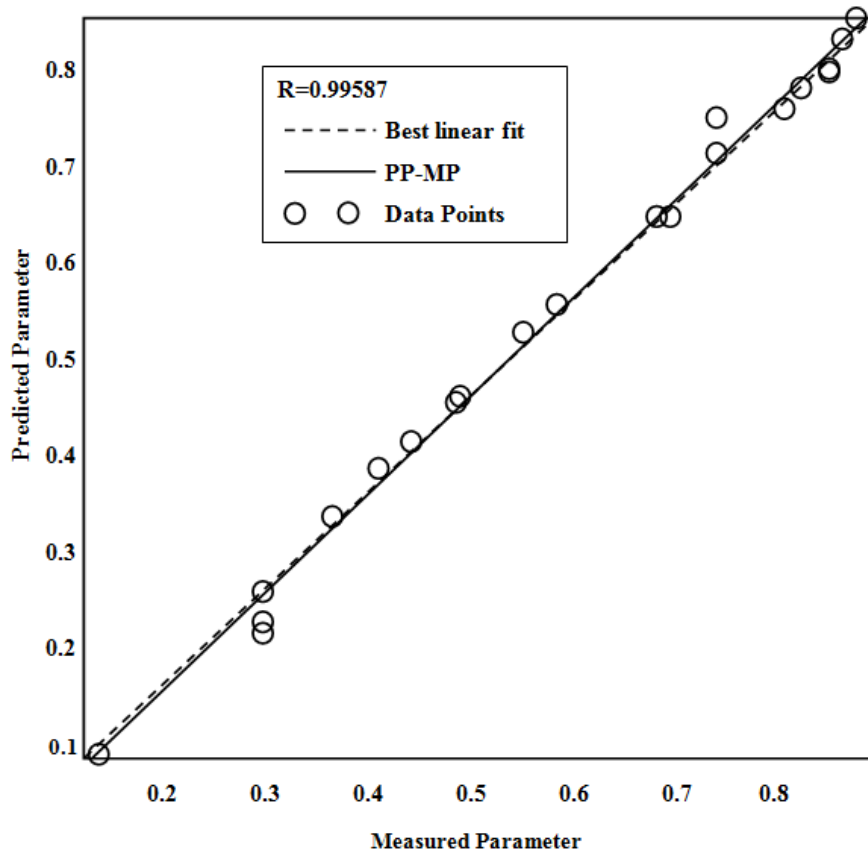


Figure 3.14 Predicted and experimental results for testing sets of parameters

The ANN network output and the consequent targets are compared and three parameters are generated. These corresponding to the slope and the y-intercept of the best linear regression to ANN network outputs. If an ideal fit (network outputs are exactly equal to the targets) is achieved the slope would be 1. The third variable returned by the code is the correlation coefficient (R-value) between the targets and outputs. It is an evaluation of how well the disparity in the network output is explained by the goals. If the obtained number is one, then this can be called a perfect association between targets and network outputs. The ANN network outputs are plotted against the targets as open circles. The finest linear fit is indicated by a dashed line. The ideal fit (output equal to the targets) is shown by the solid line.

3.8.5 ANN MODEL FOR VARIABLE INJECTION TIMING

Stable diesel engine trial experimental data are used for ANN modeling. In this study, 100 experimental data sets are prepared for the training and testing data for the ANN. The ratio for training and testing data is selected as 80%:20%, i.e. 20 and 80 sets of the experimental data are randomly selected for the testing data and training data, respectively. In the back propagation model, the scaling of inputs and outputs dramatically affects the performance of an ANN. As mentioned above, the logistic sigmoid transfer function is used in this study. One of the characteristics of this function is that only a value between 0 and 1 can be produced. The input and output data sets are normalized between 0.1 and 0.9 before the training and testing process to obtain the optimal predictions. Linear function suited best for the output layer. This arrangement of functions in function approximation problems or modeling is common and yields better results. However, many other networks with several functions and topologies are examined. The training and testing performance (MSE) are chosen to be 0.00001 for all ANNs. The smaller ANNs had the priority to be selected as the complexity and size of the network is also important. Finally, a regression analysis between the network response and the corresponding targets is performed to investigate the network response in more detail.

Percentage blends of biodiesel present in test fuel, percentage load and fuel injection timing are used as the input parameters for ANN network. Engine load is most important parameters affecting engine exhaust emissions and engine performance. In this study single cylinder diesel engine was initially run from zero load to full load with the increment of 20% load. Percentage blends of Polanga biodiesel are one more input to the ANN network. Engine tests were conducted on Polanga biodiesel blend percentages of B10, B20, B30 and B40. Finally third most

important network input was fuel injection timing which is varied from 15°bTDC to 31°bTDC at an interval of 4°. In present research work these ANN network input parameters wrap the whole problem. Brake specific fuel consumption (BSFC), Brake thermal efficiency (BTE), peak cylinder pressure and EGT are the engine performance output parameters and CO, CO₂, UHC emissions, NO_x and smoke are basically an engine exhaust emission output parameters used for the ANN modelling. Schematic representation of an ANN modelling is shown in Figure 3.15. To make sure that all network inputs provide an equivalent involvement in the ANN network modelling; the inputs are converted and scaled into a widespread normalizing range.

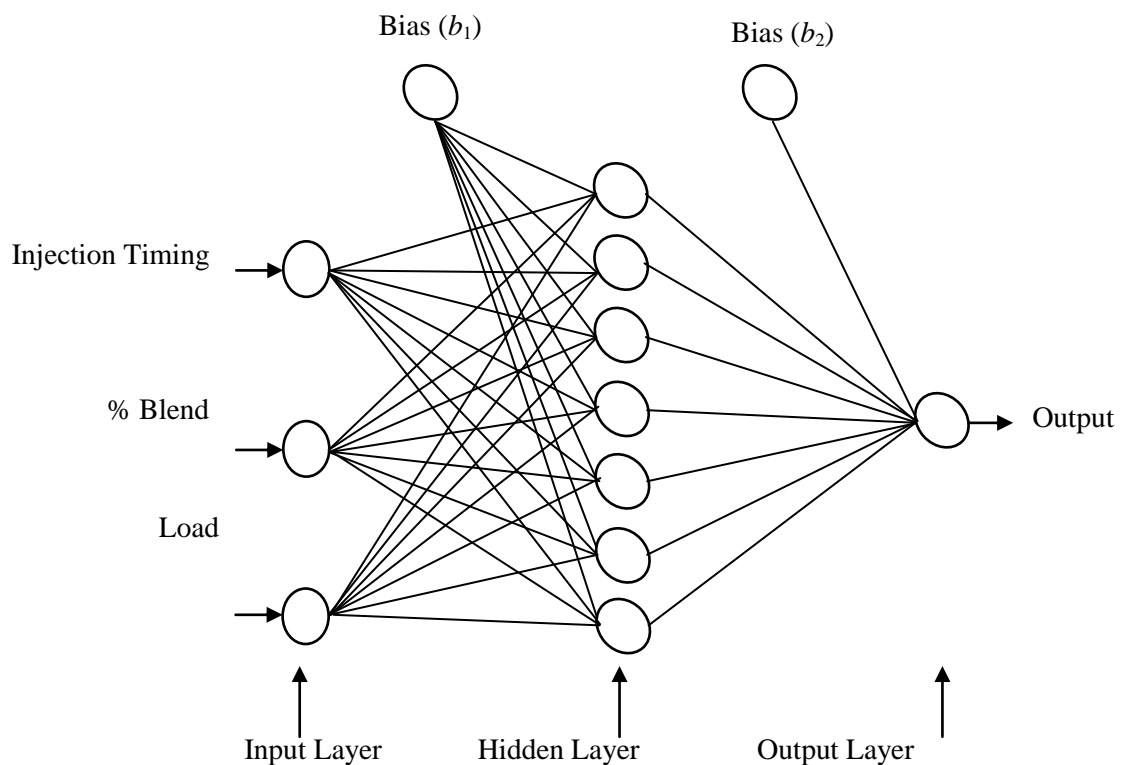


Fig. 3.15 Schematic representation of ANN model for variable injection timing

ANN network having only one hidden layer is tested by the activation function tan sigmoid as well as log sigmoid. The primarily ANN network is trained by choosing a random number of neurons in the network hidden layer. After then the number of neurons is either raised or reduced so that the mean square error attained its minimum value. The value of neurons at which the mean square error is least, that neuron number is selected as the best possible number of neurons present in the hidden layer of ANN network.

The detailed network architecture containing three input variables, one hidden layer contains tan-sigmoid as a transfer function and one output layer having linear function is shown in Figure 3.16.

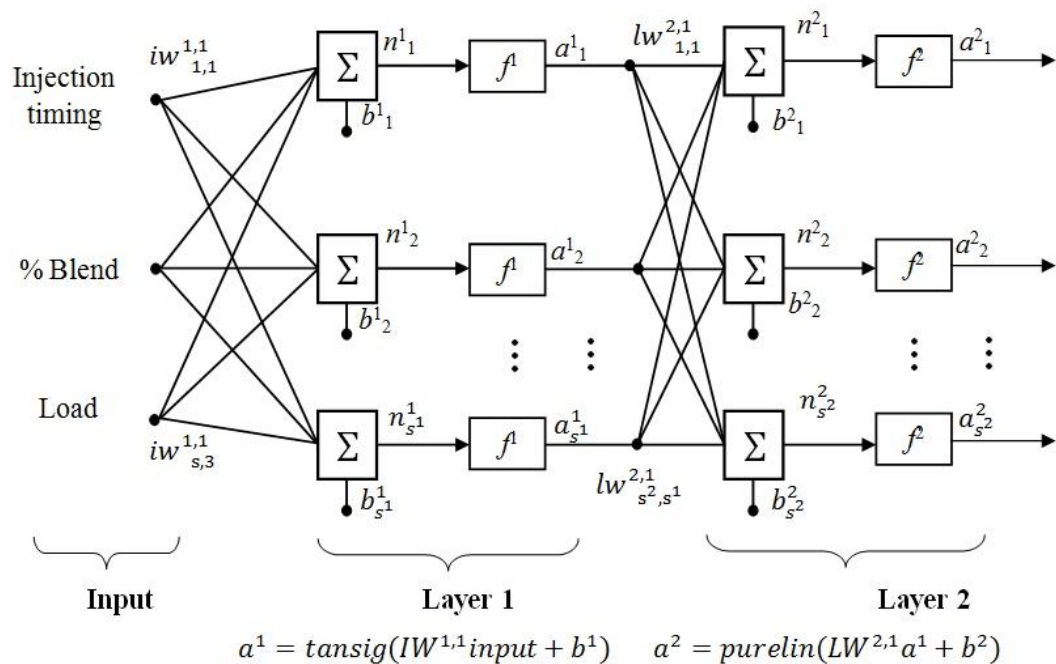


Fig. 3.16 Network architecture for variable injection timing

As shown in Figure 3.16, each layer of network has a weight matrix W , an output vector a , and a bias vector b . To differentiate between the output vectors, weight matrices, etc. For each of these layers, the number of the layer is attached as a

superscript to the variable attention. The network shown above has 3 inputs, S^1 neurons present in the first layer, S^2 neurons present in the subsequent layer, etc. The different layers may have a dissimilar amount of neurons.

The outputs of every middle layer act as an inputs to the next layer. This layer 2 can be treated as a single layer network having S^1 inputs, S^2 artificial neurons, and an $S^2 \times S^1$ weight matrix W^2 . On the other side the input to network layer 2 is a^1 ; the network output is a^2 . Hence all the matrices and vectors of layer 2 have been recognized; now it can be considered as a single-layer ANN network. This method can be used for any layer of the ANN network.

3.8.6 ANN MODEL FOR VARIABLE INJECTION PRESSURE

The performance test of the engine included fuel consumption and rating test. In order to carry out the fuel consumption test, initially the engine was started and warmed up on zero loads. After that the engine was gradually loaded up to 100 percent load to stabilize its operation. The experiment with each selected fuel type was replicated three times and the average value of different performance and emission parameters measured was taken for analysis. In the present investigation, biodiesel derived from Polanga oil was used as the test fuel. Four biodiesel blends of Polanga were used viz., B10, B20, B30, B40. The injection pressure of the engine was kept at 180 bars (as set by the manufacturer) and the fuel was altered to biodiesel. The performance, emissions and combustion characteristics of diesel engine were recorded with a constant speed of 1500 RPM. Similar procedures were repeated for other biodiesel blends at the same injection pressure. To visualize the effect of injection pressure, the entire procedure was repeated for injection pressure of 160 bar, 200 bar, 220 bar and 240 bar.

In this study, 20 experimental data sets are prepared for the training and testing data for the ANN. The ratio for training and testing data is selected as 70%:30%, i.e. 14 and 6 sets of the experimental data are randomly selected for the data training and testing data, respectively. A neural network toolbox of MATLAB 2010a is used for ANN modelling.

Schematic representation of the model is shown in Figure 3.17. Percentage load, blend percentage of Polanga biodiesel and fuel injection pressure are used as the input parameters for ANN modelling. BSFC, BTE, P_{max} and EGT are the diesel engine performance output parameters and CO, CO₂, UHC emissions, NO_x and smoke are the output engine exhaust emission parameters for the ANN modelling.

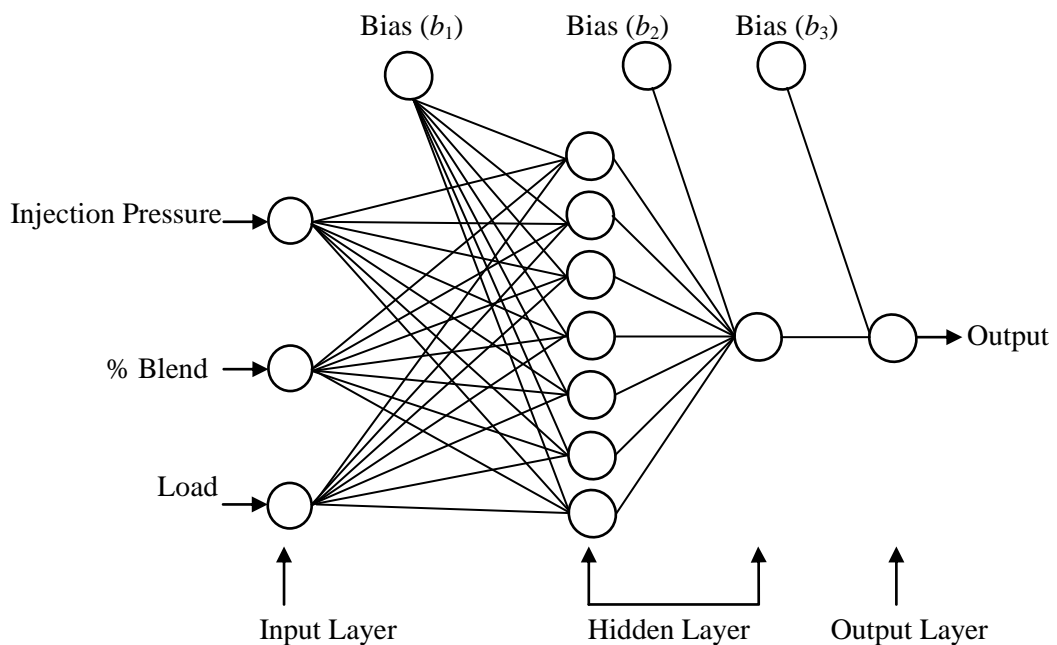


Fig. 3.17 Schematic representation of ANN model for variable injection pressure

The detailed network architecture containing three input variables, two hidden layers with log-sigmoid as a transfer function and one output layer having linear function is shown in Figure 3.18.

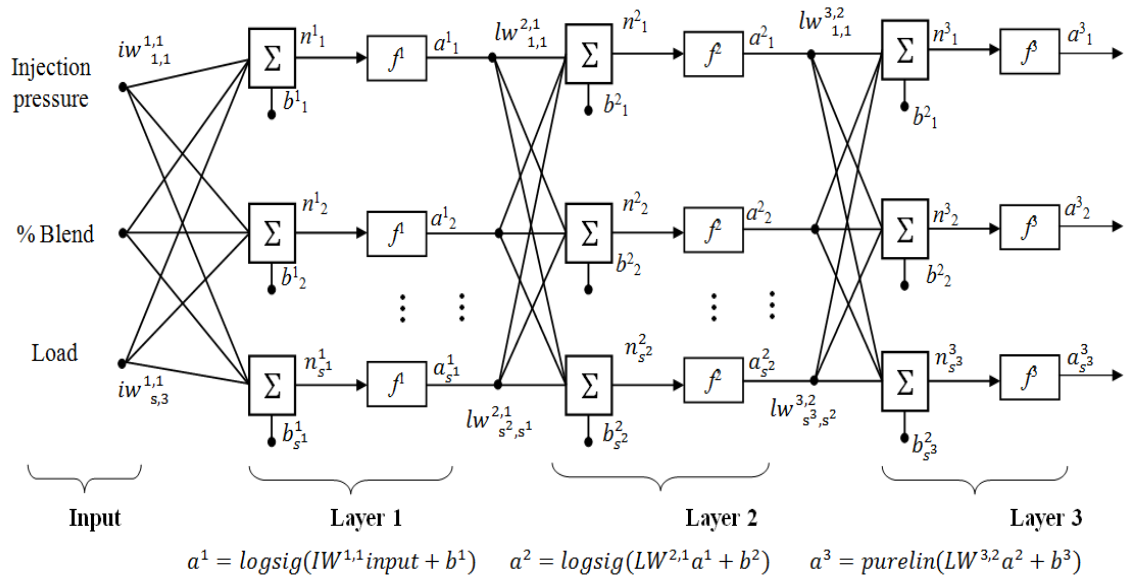


Fig. 3.18 Network architecture for variable injection pressure

3.9 OPTIMIZATION OF ENGINE PARAMETERS

The experimental study conducted using single cylinder diesel engine provides a huge number of experimental results. But, it is impracticable to select the input parameters such as fuel injection timing; fuel injection pressure and percentage blends of Polanga biodiesel for obtaining best possible engine performance and engine exhaust emission parameters. Hence, objective is to find the best grouping of the engine input parameters under different preset priorities, an appropriate computational study is required. The fixed priority is a mixture of weightages in share of engine performance and engine exhaust emissions, for example 50-50, 80-20, 20-80, etc. Equilibrium can be strikingly as to what could be the appropriate combination of best possible input parameters which will result in maximizing the engine performance while minimizing the exhaust emission ingredients. For this purpose genetic algorithm method is one of the appropriate tools available which can be used for the optimization process. Genetic algorithms are optimization algorithms and computerized search supported on the mechanics of natural genetics and natural

selection. Genetic algorithms are fundamentally different from others conventional optimization techniques. On the other side, since GAs needs only function values at different discrete points, an isolated or irregular function can be handled without any additional cost. This permits GAs to be applied to a broad variety of engineering problems. An additional plus point is that the GA operators developed the resemblance in string-structures to make an efficient research.

CHAPTER 4

RESULTS AND DISCUSSION

4.1 INTRODUCTION

This section presents the results obtained by conducting the experiments for performance and the emission parameters evaluation. Before performing different sets of experiments, physico-chemical characterization of Polanga biodiesel and its blends is performed and the results thus obtained are discussed in section 4.2. The input parameters selected in the present work are injection timing and injection pressure along with the percentage blends of Polanga biodiesel. The results are discussed simultaneously in section 4.3 for variable fuel injection timing and variable fuel injection pressure. The results of the numerical simulation and model validation by artificial neural networks using MATLAB are discussed in section 4.4 for both variable fuel injection timing and variable fuel injection pressure parameters. In section 4.5 validation of ANN model is carried out with experimental data. After that Multi-objective Optimization of Engine parameters is carried out in section 4.6.

4.2 PHYSICO-CHEMICAL PROPERTIES OF POLANGA BIODIESEL AND ITS BLENDS

Various equipments used for determination of physico-chemical and fuel properties and they are provided in Table 4.1.

Table 4.1: List of equipment

S. No	Property	Equipment
-------	----------	-----------

1	Kinematic viscosity	Petrotest Viscometer
2	Oxidative stability	873 Rancimat
3	Density	Density meter
4	Calorific value	Bomb calorimeter

The various physico-chemical properties of Polanga biodiesel blends was carried out is given in Table 4.2

Table 4.2: Properties of Polanga biodiesel and its blends

Fuel	Calorific value (KJ/kg)	Viscosity (cSt) at 15 °C	Density (gm/cc)	Flash point (°C)	Cloud point (°C)	Pour point (°C)
Diesel	43990.3	2.93	0.831	74	6.5	-4.3
10%B	40095.2	3.3	0.849	84	7.3	-2.9
20%B	39195.73	3.31	0.849	89	8.0	-1.1
30%B	38395.3	3.33	0.857	95	8.3	1.9
40%B	37796.98	3.8	0.867	100	8.9	3.2
100%B	36990.56	6.9	0.944	155	14.1	4.7

The comparative assessment of various physico-chemical properties of Polanga biodiesel was also carried out with Jatropha methyl ester and the comparison is shown in Table 4.3.

Table 4.3: Comparison between Polanga and Jatropha properties

S. No.	Property	Polanga	Jatropha
1	Viscosity at 40°C (cst)	5.5	4.94
2	Viscosity at 80°C (cst)	4.1	1.85
3	Density at 40°C (g/cc)	0.9138	0.8642
4	Density at 15°C (g/cc)	0.9411	0.8991
5	Calorific value (KJ/kg)	36990.56	38738.25

On the basis of above data provided in the Table 4.2 and 4.3, it may be concluded that Polanga biodiesel was well within the limits of international biodiesel standards. Its various critical physico-chemical characteristics closely matched with the methyl ester of *Jatropha curcas* recognized by Government of India as best oilseed for biodiesel production.

4.3 RESULTS OF ENGINE TRIALS WITH VARYING INJECTION TIMING AND PRESSURE

4.3.1 BRAKE THERMAL EFFICIENCY (BTE)

Fig. 4.1 shows the deviation of the brake thermal efficiency for various tests blends of Polanga biodiesel with fuel injection timings at a full load condition of CI engine. As it can be seen from Figure 4.1, among all the Polanga biodiesel blends B30 shows maximum values of brake thermal efficiency 33.51 % on 27°bTDC. It is also observed that BTE of Polanga blends increases with advancing injection timing.

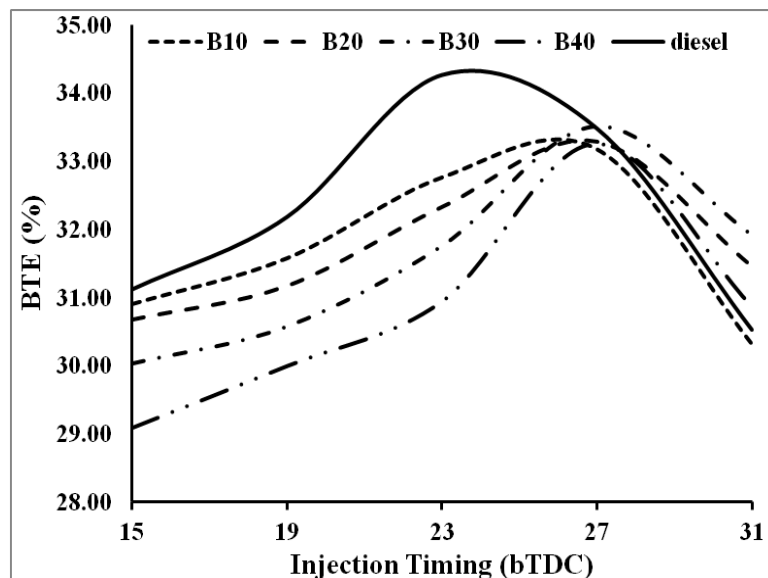


Fig. 4.1: Variation of BTE with Injection timing

Fig. 4.2 illustrates the deviation of the BTE for diverse tests blends of Polanga biodiesel with fuel injection pressure. For a higher percentage of Polanga blends B30 and B40, BTE increases with fuel injection pressure.

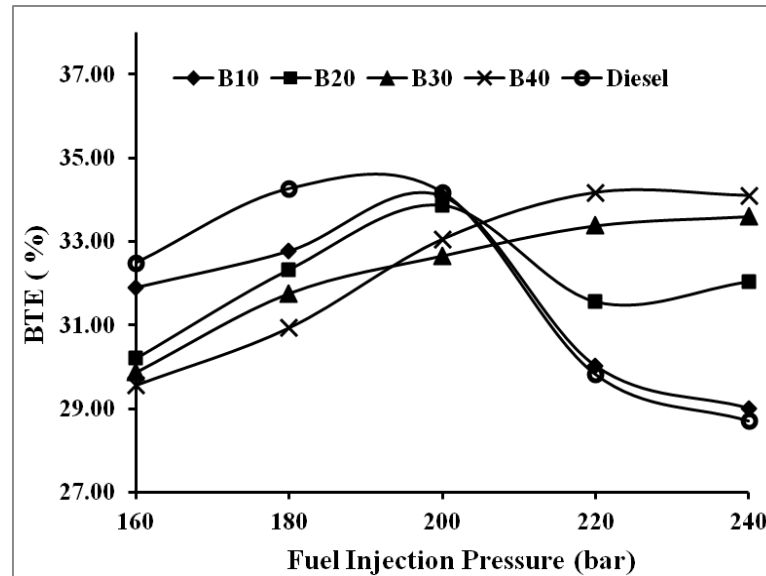


Fig. 4.2: Variation of BTE with injection pressure

The maximum value of BTE was 34.17% for B40 Polanga blend at 220 bar injection pressure, this is due to very fine fuel spray produced at a high injection pressure hence improved atomization of fuel occur. Further, at elevated injection pressure the brake thermal efficiency tends to decline, this could be due to that the size of fuel particles reduces and very fine biodiesel fuel spray will be injected, due to this diffusion of biodiesel, fuels spray less and momentum of biodiesel droplets will be reduced. For B10 and B20 test fuel highest value of BTE is 34.08% and 33.87% at 200 bar fuel injection pressure.

4.3.2 BRAKE SPECIFIC FUEL CONSUMPTION (BSFC)

Figure 4.3 shows that the minimum BSFC for B20, B30 and B40 the blends is 0.23Kg/Kw.hr., 0.226 Kg/Kw.hr. and 0.236 Kg/Kw.hr. correspondingly, at the timing of fuel injection 27°bTDC. BSFC is minimum for B10 and diesel is 0.224 Kg/Kw.hr.

and 0.221 Kg/Kw.hr. at 23°bTDC.

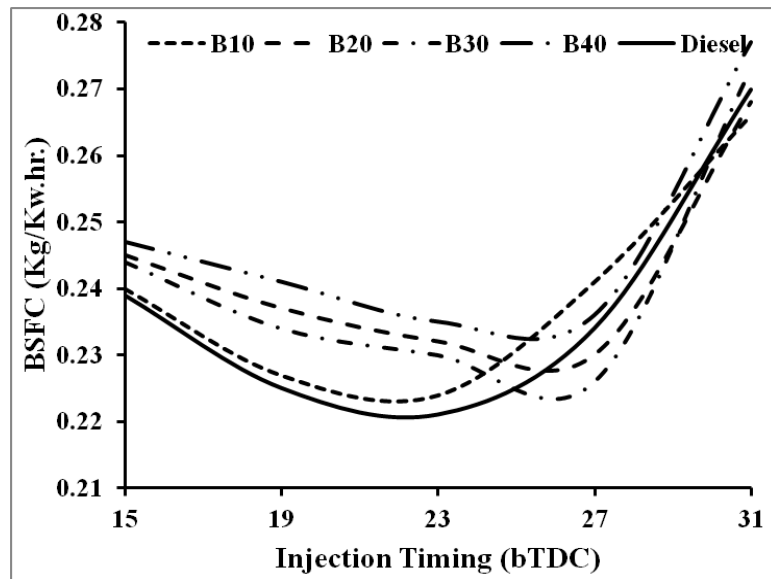


Fig. 4.3: Variation of BSFC with Injection timing

Figure 4.4 shows BSFC results for various Polanga biodiesel blends trial fuels with changed fuel injection pressures at full load condition. A decrease in fuel injection pressure enhanced the BSFC values for all the blends.

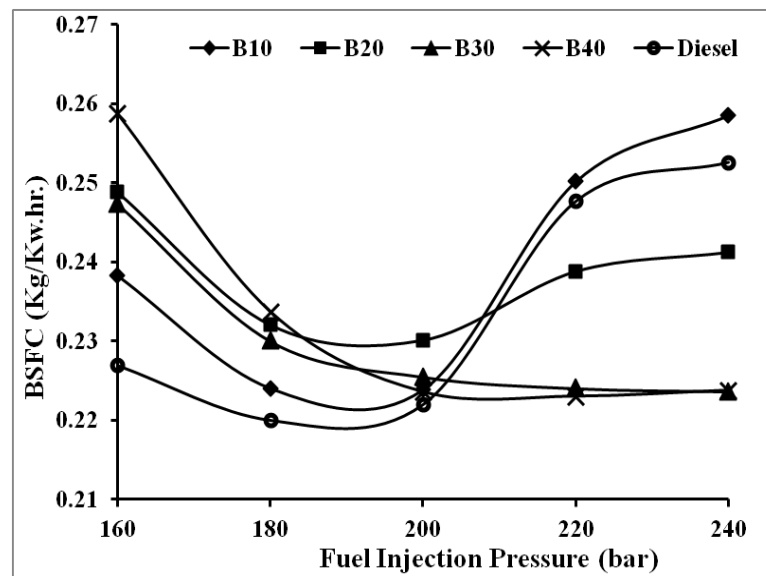


Fig. 4.4: Variation of BSFC with Injection pressure

The reason is that due to falling injection pressure, particle diameter will expand and ignition delay time will enhance. This condition causes an extended in the brake

specific fuel consumption. On the other side, rising fuel injection pressure from the original pressure decreases the BSFC values for B20, B30 and B40 due to better combustion of test fuels. For blends B10 an increase in injection pressure increases the BSFC values due to a shorter ignition delay period. Minimum BSFC for B10 is 0.226 Kg/Kw.hr. at 180 and 200 bar and enhancing in fuel injection pressure from 200 to 240 bars, the BSFC is increased by 0.036 Kg/Kw.hr.

4.3.3 PEAK CYLINDER PRESSURE (Pmax)

Figure 4.5 compares the peak engine cylinder pressure for Polanga biodiesel blends at different fuel injection timings at full engine load. Among all the tested fuel injection timings 31°bTDC have the highest cylinder gas pressure values for all Polanga biodiesel blends.

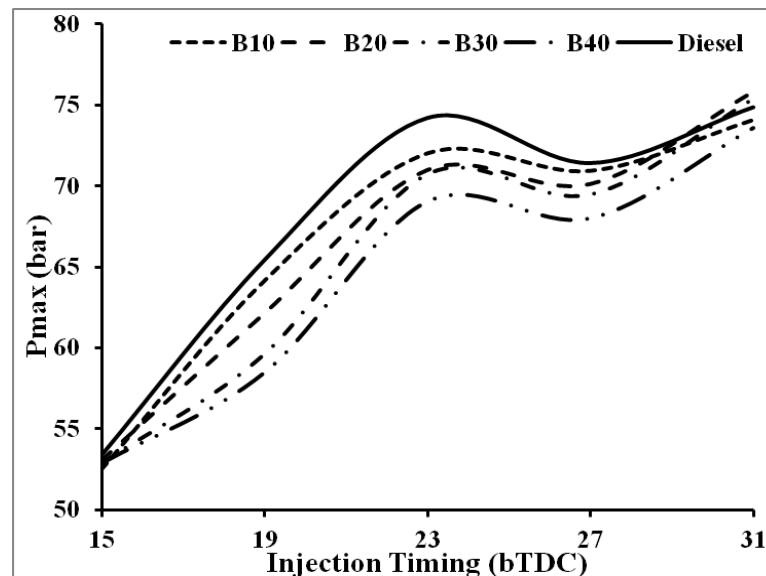


Fig. 4.5: Variation of Pmax with Injection timing

While advancing the fuel injection timing of engine from 23°bTDC to 31°bTDC, the maximum engine cylinder pressure attends closer to top dead center of the engine due an earlier crank angle fuel injection.

Figure 4.6 compares the peak engine cylinder gas pressure of Polanga biodiesel blends for diverse fuel injection pressure at full load. Among all the tested Polanga biodiesel blends B10, at injection pressure 220 bars have the highest cylinder gas pressure value 72.9 bar. It may be due to increasing the injection pressure from 180 bars to 220 bars, fine fuel spray fashioned during high fuel injection pressure and hence improved atomization of fuel take place.

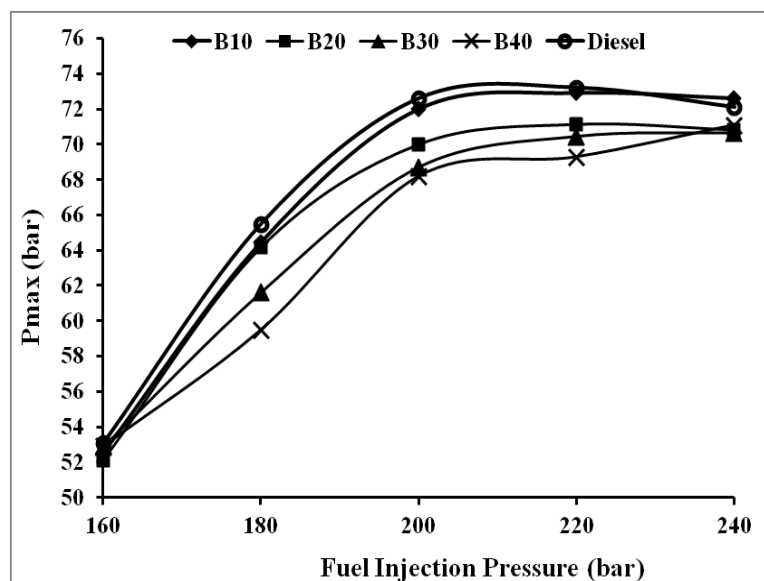


Fig. 4.6: Variation of Pmax with Injection pressure

Further the Pmax tends to decrease at 240 bar fuel injection pressure, this may be due to that at elevated fuel injection pressure the size of test fuel droplets decreases and very high fine fuel spray will be injected, because of this, penetration of fuel spray reduces and momentum of fuel droplets will be reduced.

4.3.4 EXHAUST GAS TEMPERATURE

The variation of exhaust gas temperature (EGT) with the injection timing at full load for biodiesel blends is shown in Figure 4.7. The EGT decreases for all fuels

by advancing injection timing for all Polanga biodiesel blend. EGT increased with the increasing blending of biodiesel percentage in the test's fuel. This is due to oxygen percentage increases with the increase in Polanga biodiesel blending. Of all the Polanga biodiesel blends, B10 found lesser values of EGT at all the fuel injection timings. As confirmed in the graph, the maximum EGT was acquired as 299°C with the B40 at 15°bTDC Injection timing. For Polanga biodiesel blend B10 minimum EGT was 252°C found at 31°bTDC. In case of diesel, minimum EGT was found 248°C at 31°bTDC. At original fuel injection timing set by manufacturer EGT of diesel fuel is 256°C at 23°bTDC, which is less than all Polanga biodiesel test fuels.

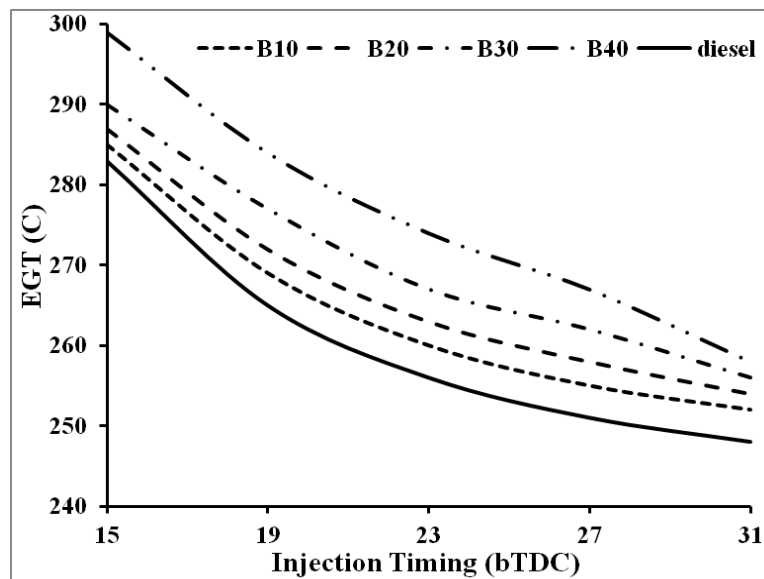


Fig. 4.7: Variation of EGT with Injection timing

The variation of EGT with the fuel injection pressure at constant full load for Polanga biodiesel blends is given in Figure 4.8. In general, EGT increase with load, at elevated injection pressure the EGT is higher due to the increased combustion duration, increased heat loss, etc.

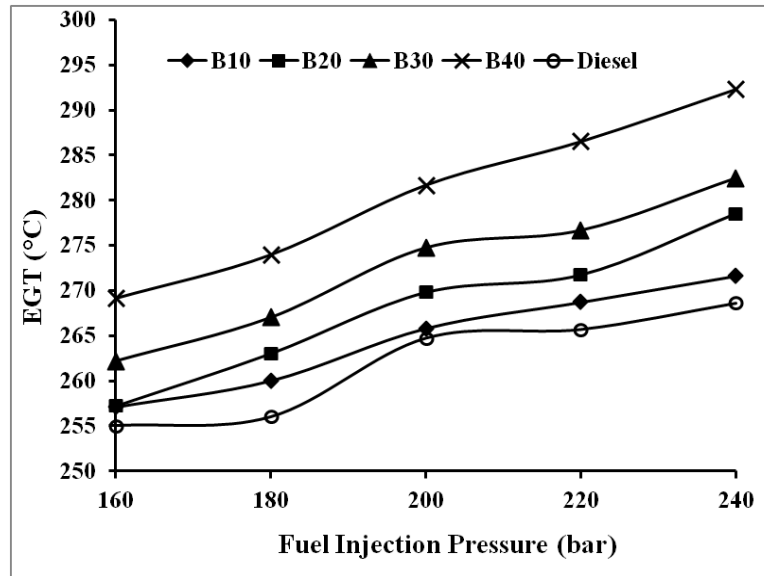


Fig. 4.8: Variation of EGT with injection pressure

4.3.5 CARBON MONOXIDE

Fig. 4.9 shows results CO emissions for dissimilar Polanga biodiesel blends and diesel test fuels with different timings fuel injection at full load. While the timing of fuel injection is advanced, CO emission level of all the test fuels was reduced. For all the test Polanga biodiesel blends B40, shows minimum value CO emission 0.06 %vol at 31°bTDC. By advancing the fuel injection timing 8° CA (23° to 31°bTDC), CO emission is reduced by 24.39% for B40 Polanga biodiesel. B40 shows least CO emissions at retarding timing of fuel injection. In case of diesel CO, emissions was 0.13%vol at 23°bTDC set by the manufacturer, which is 52% more than we get by using B40 Polanga biodiesel at 31°bTDC injection timing.

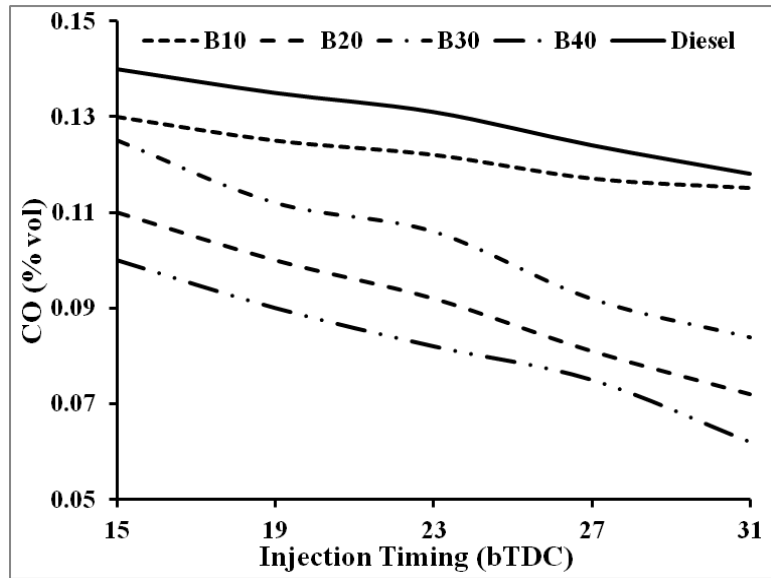


Fig. 4.9: Variation of CO with Injection timings

It is revealed from Figure 4.10 that CO emission reduced by the more biodiesel proportion. Also at an elevated injection pressure, the carbon monoxide emissions narrowed. It may be noted that emissions of CO get reduced with sharp rate for B40 at elevated fuel injection. However, a steep reduction in CO emission was observed 0.1 to 0.04% by vol for B40 test fuel when fuel injection pressure raises 160bar to 240bar.

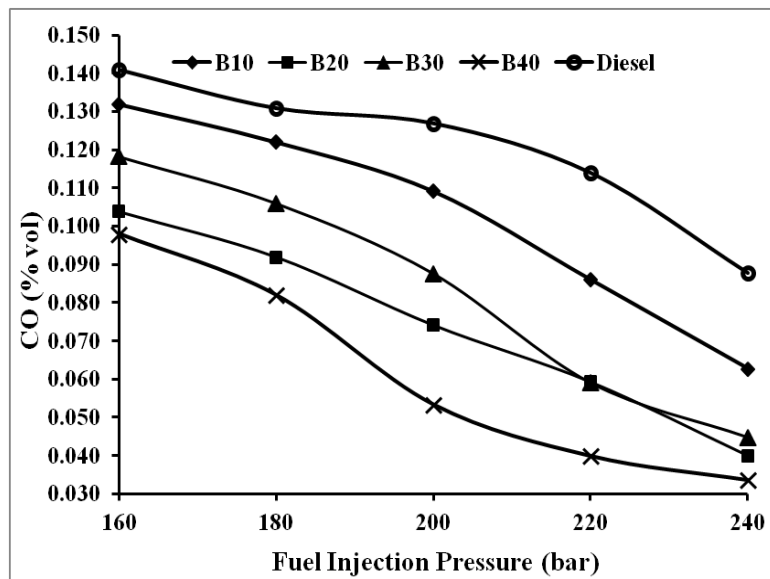


Fig. 4.10: Variation of CO with Injection pressure

4.3.6 UN-BURNT HYDROCARBON EMISSION (UHC)

Figure 4.11 shows the outputs of UHC with the fuel injection timings for all the test fuels of Polanga biodiesel blends and diesel at full load condition. By increasing fuel injection timing from 23° to 31°bTDC, reduction of UHC was found in all the Polanga biodiesel blends at peak load condition.

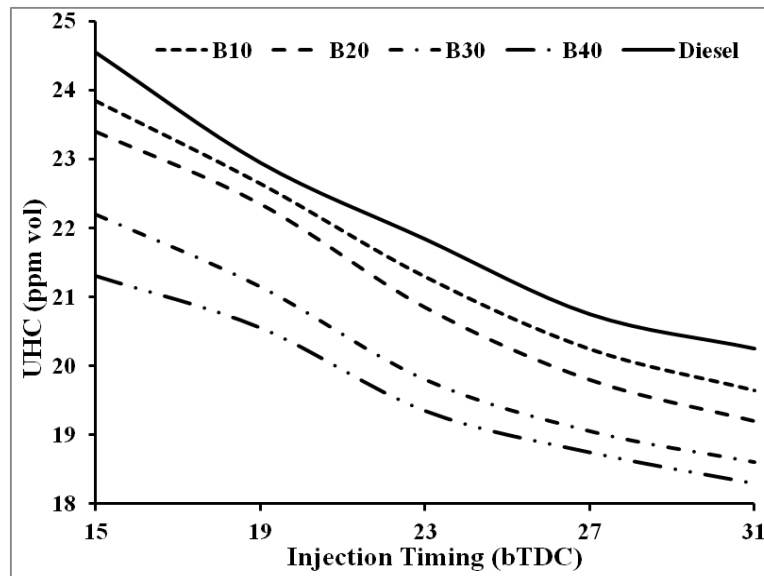


Fig. 4.11: Variation of UHC with Injection timings

B40 shows the lowest emissions of UHC for all the timing of fuel injections of the engine. The minimum value of UHC is 18 ppm for B40 at 31°bTDC, which is 5.4% less than diesel when the engine operated at 23°bTDC manufacturer design specification. Figure 4.12 gives UHC emission results for different Polanga biodiesel blends with fuel injection pressure at full load. A rise in fuel injection pressure develops better fuel air mixing in the combustion chamber resulting in less UHC emissions. Lowest UHC of 15 ppm was observed at 240 bar, which is 5 ppm lower than that of UHC emission at 160 bars for the same biodiesel blend B40. The reduction in UHC emission using Polanga biodiesel is generally due to the better vaporization and proper atomization.

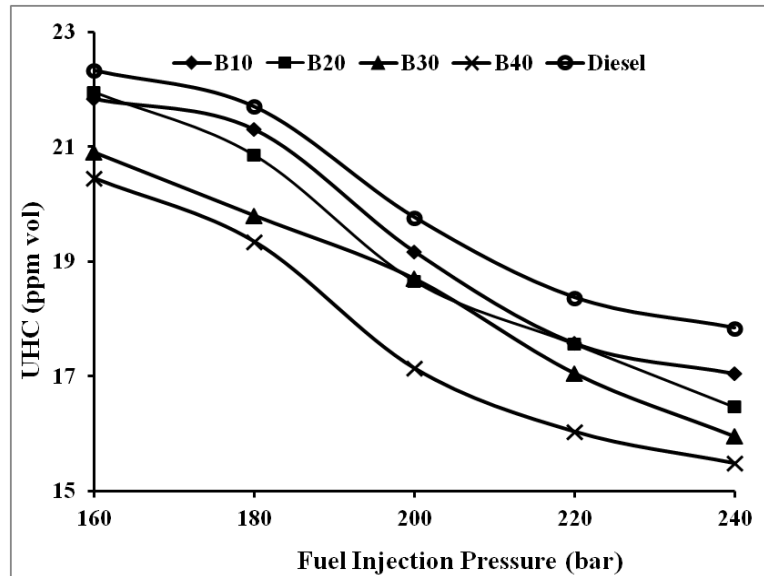


Fig. 4.12: Variation of UHC with Injection pressure

4.3.7 OXIDES OF NITROGEN EMISSIONS (NO_x)

Figure 4.13 shows NO_x emissions of blends of Polanga biodiesel and diesel on full load at different timing of fuel injections. It may be noticed that emissions of NO_x rise with engine load for biodiesel test fuels. This may be attributed to the fact that the increase as the engine loading leads to increase in-cylinder pressure and EGT.

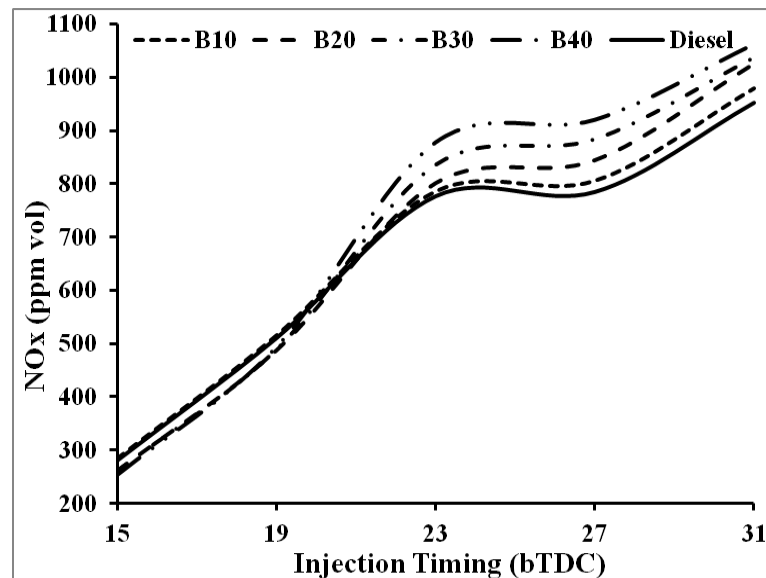


Fig. 4.13: Variation of NO_x with Injection timing

This is notice that at retarded timings of fuel injection less emissions of NO_x generation. Advancement of injection by 4°bTDC step, raise in NO_x for all Polanga biodiesel blend at full load. Sharp rise in NO_x emissions was found when fuel injection timing is advanced by 4°bTDC for all the test fuels. Polanga biodiesel blend B40 shows highest value of NO_x emissions 1062 ppm vol at 31°bTDC. As compared to diesel, Polanga biodiesel blends shows the high value of NO_x at 23°bTDC.

Figure 4.14 gives NO_x values for various Polanga biodiesel blends with diverse fuel injection pressures at full load condition. As seen from the figure, at elevated fuel injection pressure, NO_x emissions are higher. At an elevated fuel injection pressure smaller test fuel particle diameter caused to vaporize quickly.

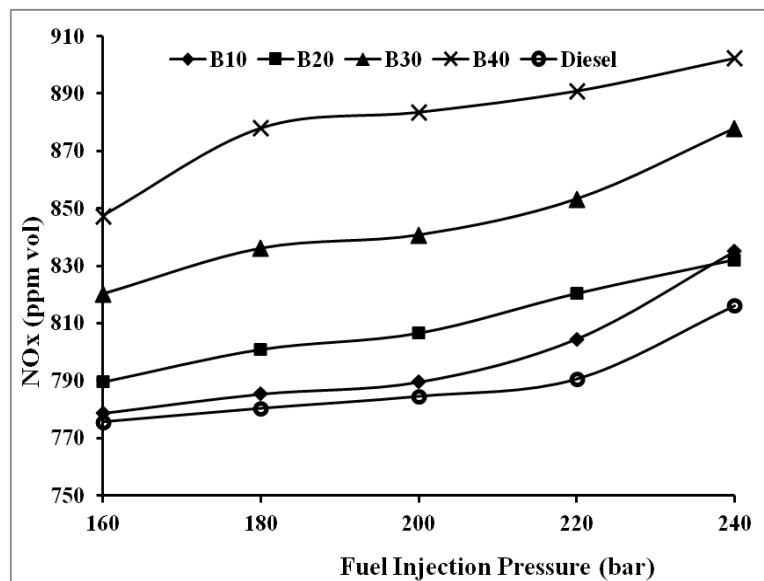


Fig. 4.14: Variation of NO_x with Injection pressure

However, the fuel particle cannot go through deep into the engine combustion chamber. So, at an elevated fuel injection pressure firstly produces quicker fuel combustion rates, resulting in a higher EGT as discussed previously section as an end result, NO_x start to increase at elevated fuel injection pressure. Maximum NO_x emissions was recorded to be 835, 832, 878 and 902 ppm vol for B10, B20, B30 and

B40 respectively at 240 bar of fuel injection pressure.

4.3.8 SMOKE OPACITY

Formation of smoke occurs due to deficiency of air. Figure 4.15 demonstrates the deviation of Smoke opacity with different fuel injection timings for Polanga biodiesel blends and diesel. It may be observed that Polanga biodiesel blends show reduced emissions of smoke at full loads.

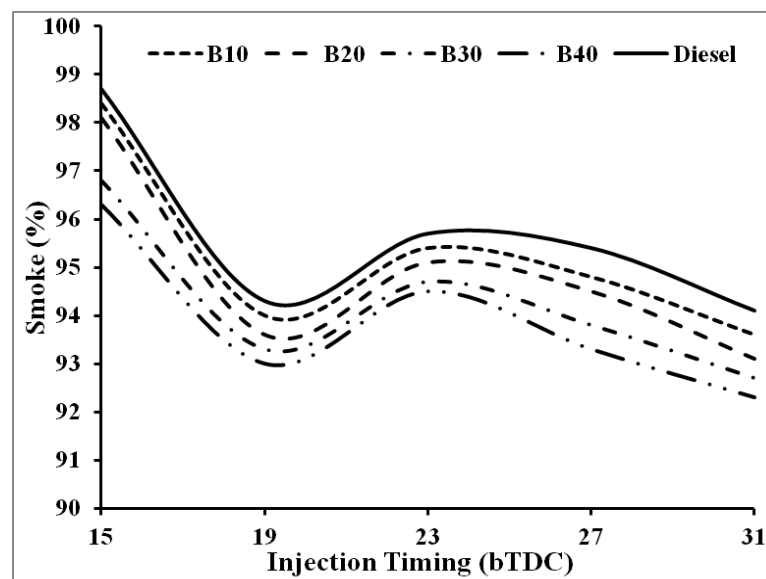


Fig. 4.15: Variation of smoke opacity with fuel Injection timing

At full load B10, B20, B30 and B40 showed smoke opacities of 95.4%, 95.1%, 94.7% and 94.5% as compared to 95.7% exhibited by diesel at 23^obTDC on full load condition. By advancing the timing of fuel injection, engine smoke opacity is lowered due to the better combustion and proper time is available for utilization of oxygen present in blends of Polanga biodiesel. Smoke opacity boost with the reduction of air-fuel fraction. Engine trial results point out that Smoke opacity emissions was reduced with the increasing percentage of blending biodiesel. The minimum value of smoke

emission is 92.3 % at 31^obTDC for B40 Polanga biodiesel blend, which is 3.24% less than the diesel smoke opacity value obtained at the 23^obTDC set by the manufacturer.

As illustrated in Figure 4.16, the smoke opacity, drop with increase the percentage of Polanga biodiesel in trial fuels. This can be due to the rise in O₂ content and reduction in carbon percentage in Polanga blends. An amplifying in fuel injection pressure decreases the size of fuel particles.

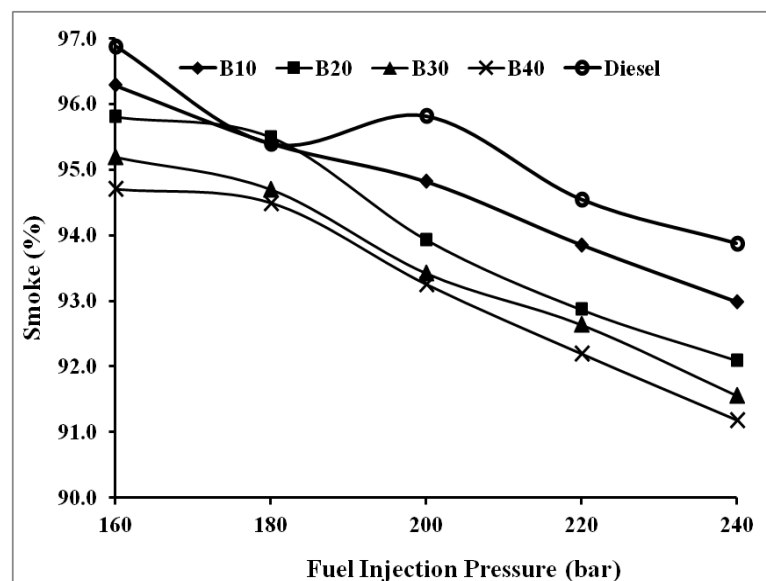


Fig. 4.16: Variation of smoke emission with Injection pressure

As seen in Figure 4.16, by increasing fuel injection pressure, smoke opacity reduced. B40 Polanga blend shows the less smoke opacity for all the fuel injection pressure. The opacity values are 94.7%, 94.5%, 93.3%, 92.5% and 92.2% at 160, 180, 200, 220 and 240 bar injection pressure respectively.

4.3.9 CARBON DIOXIDE (CO₂)

Figure 4.17 shows the variation in emission of carbon dioxide with injection timings at various blends of Polanga biodiesel with diesel and neat diesel. Carbon

dioxide in the exhaust gases is an indication of complete combustion. It was observed that CO₂ emissions increased with sharp rate when increased the percentage of biodiesel at advance fuel injection timing.

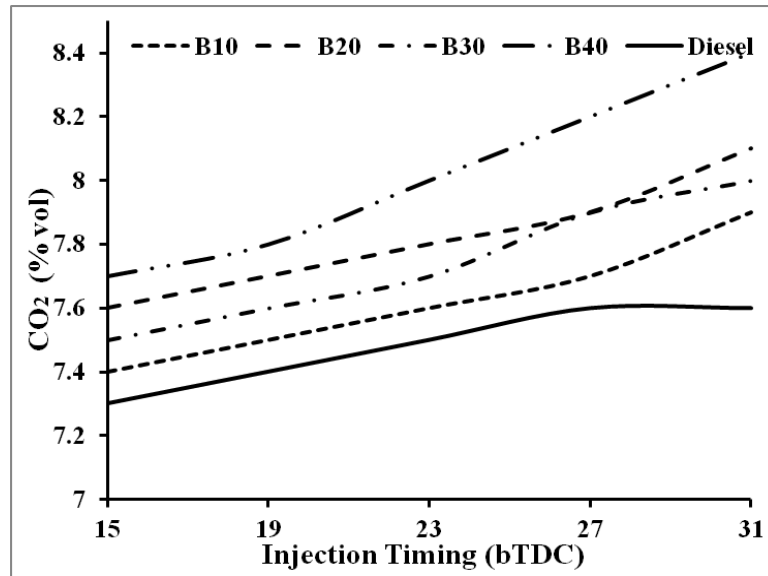


Fig. 4.17: Variation of CO₂ with Injection timings

For advanced fuel injection timings this emission was condensed due to the higher engine operating temperature and hence better chemical reaction takes place between a test fuel and oxygen. It may be observed that B40 exhibited higher CO₂ emissions as compared B10, B20, and B30 for all fuel injection timings in the present study. The maximum value of CO₂ emission was 8.41 % vol at 31°bTDC for B40 which is 12% more than CO₂ emissions obtained from the engine when run on diesel at manufacturer set injection timing 23°bTDC. CO₂ emission reduced when injection timing is reduced from 23°bTDC to 15°bTDC due to incomplete combustion of fuel and more ignition delay period for Polanga blends. From Figure 4.18, it is observed that percentage amount of biodiesel in test blends CO₂ emission increases.

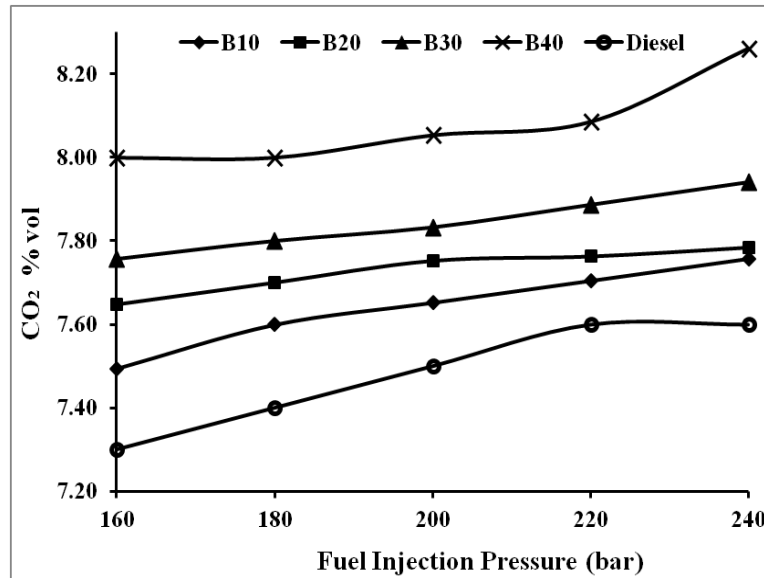


Fig. 4.18: Variation of CO₂ with Injection pressure

Higher values of CO₂ emission for B40 indicate complete combustion and higher heat release. CO₂ emission for diesel at 180 bar was 7.41% vol which is 8.1% less than B40 CO₂ emission at same injection pressure.

4.4 ANN MODELING OF ENGINE OPERATING PARAMETERS

As discussed earlier, the normalization values for inputs and outputs are obtained from equation Eq. (3.9) and the respective values are given in Appendix Table A4.1 and Table A4.2 for fuel injection timing and fuel injection pressure respectively. The network was primarily trained by picking some number of neurons in the hidden layer. After then neurons number, size were either enhanced or reduced so that Correlation coefficient (R) will be obtained nearby to unity. The number of neurons for which the Correlation coefficient (R) is nearly equivalent to unity is decided as the most favorable number of neurons in the hidden layer. Simultaneously network was also trained using different training functions as discussed in the previous chapter.

4.4.1 BRAKE THERMAL EFFICIENCY (BTE)

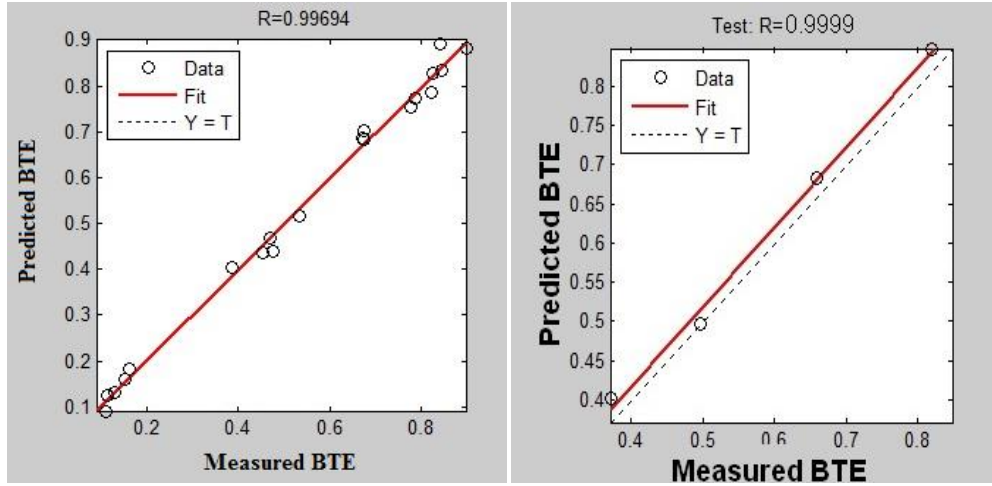
The network structures and statistical parameters of ANN models for different learning algorithms are given in Table 4.4. From the Table 4.4, it is clear that the best prediction results were obtained by the LM learning algorithm. The LM learning algorithm had the highest speed compared with other learning algorithms and it reached to optimal solutions with a small number of neurons in the hidden layer.

Table 4.4: Correlation coefficients for BTE using different learning algorithms

Parameter	Learning Algorithm	Activation function	Neurons (Numbers)	Correlation coefficient (R)	
				Training	Testing
IT	Trainlm	Sig/lin	5	0.99406	0.99004
	Trainlm	Sig/lin	6	0.99591	0.99081
	Trainlm	Sig/lin	15	0.99604	0.99694
	Trainlm	Sig/lin	20	0.99968	0.99651
	Trainlm	Tan/lin	10	0.9943	0.99067
	Trainscg	Sig/lin	5	0.9834	0.98096
	Trainscg	Sig/lin	6	0.98099	0.98137
	Trainscg	Sig/lin	10	0.98921	0.9853
	Traingdm	Sig/lin	10	0.8377	0.855
IP	Trainlm	Sig/ lin/lin	3/1	0.9986	0.9617
	Trainlm	Sig/lin/lin	4/1	0.9884	0.9999
	Trainlm	Sig/lin/lin	8/1	0.9999	0.9448

It is observed that best Correlation coefficient (R),with varying IT, Training (0.99604), Testing (0.99694) for BTE is obtained for learning algorithm trainlm, activation function Sig/lin and number of neurons 15. For varying IP, the best Correlation coefficient (R) Training 0.9884 Testing 0.9999 for BTE is obtained, when learning algorithm trainlm Activation function Sig/lin/lin and number of Neurons are 4/1.

The relation between predicted and experimental results for testing sets of BTE parameters is shown in Figure 4.19.



(a) For injection timing

(b) For injection pressure

Fig. 4.19: Predicted and experimental results for testing sets of BTE parameters

The brake thermal efficiency of the diesel engine for varying IT can be accurately calculated by Eq. No. (4.1).

$$BTE = \frac{1}{1 + e^{-(\sum_{i=1}^{15} w_{2i} F_i - 0.476)}} \quad (4.1)$$

where F_i ($i = 1, 2, 3, \dots, n$) can be calculated according to Eq. 3.2 in which E_i is the weighted sum of the inputs, and is calculated using

$$E_i = (w_{11} \times IT + w_{12} \times BD + w_{13} \times EL + b_1) i$$

The data flow was accomplished with the weights between the layers. The equation of the brake thermal efficiency diesel engine for varying IP is given by Equation (4.2).

$$BTE = \frac{1}{1 + e^{-(\sum_{i=1}^3 w_{2i} F_i + 27.144)}} \quad (4.2)$$

where F_i ($i = 1, 2, 3, \dots, n$) can be calculated according to Eq. 2.2 in which NT_i is the weighted sum of the inputs, and is calculated using $NT_i = (w_{11} \times IP + w_{12} \times BD + b_1) i$. The weight values appearing in Equation no 4.1 and 4.2 are given in the Table A 4.3 and table A4.4 respectively.

4.4.2 BRAKE SPECIFIC FUEL CONSUMPTION (BSFC)

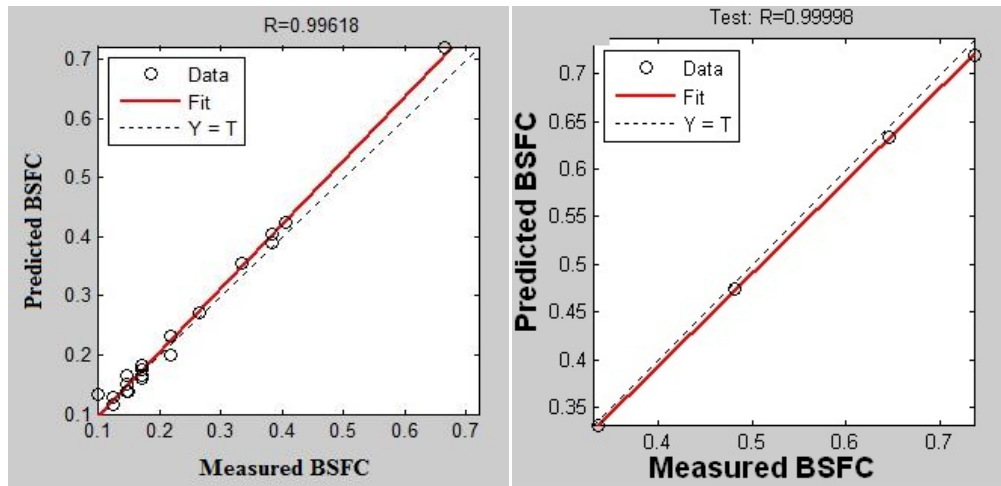
The initially ANN network was trained by choosing five numbers of neurons in the network hidden layer. After then number of neurons was increased for obtaining Correlation coefficient (R) close to unity. At the same time different learning algorithm also changed to obtain this goal. The network structures and statistical parameters of the ANN model for Brake specific fuel consumption (BSFC), different learning algorithms are given in Table 4.5.

Table 4.5: Correlation coefficients for BSFC using different learning algorithms

Parameter	Learning Algorithm	Activation function	Neurons (Numbers)	Correlation coefficient (R)	
				Training	Testing
IT	Trainlm	Sig/lin	5	0.99358	0.99471
	Trainlm	Sig/lin	6	0.99709	0.98604
	Trainlm	Sig/lin	10	0.99727	0.99168
	Trainlm	Sig/lin	15	0.99881	0.99618
	Trainlm	Sig/lin	20	0.99946	0.99359
	Trainscg	Sig/lin	5	0.97973	0.98542
	Trainscg	Sig/lin	6	0.98729	0.9905
	Trainscg	Sig/lin	10	0.99007	0.97519
	Traingdm	Sig/lin	10	0.75024	0.81653
	Trainscg	Sig/lin	6	0.96305	0.98925
	Trainscg	Sig/lin	10	0.98058	0.9458
	Traingdm	Sig/lin	10	0.92551	0.92046
IP	Trainlm	Sig/Sig/lin	10/10	0.9998	0.9988
	Trainlm	Sig/Sig/lin	5/5	0.9989	0.9994
	Trainlm	Sig/Sig/lin	7/5	0.9983	0.9956
	Trainlm	Sig/Sig/lin	5/2	0.99681	0.9953
	Trainlm	Sig/ lin/lin	5/5	0.999	0.9964
	Trainlm	Sig/lin/lin	5/1	0.9999	0.9959
	Trainlm	Sig/lin/lin	8/1	0.99992	0.99998
	Trainlm	Tan/lin/lin	8/1	0.998	0.995
	Trainlm	Tan/lin/lin	12/1	0.999	0.996

From Table 4.5 it is observed that best Correlation coefficient (R) for Training (0.99881) and Testing (0.99618) for BSFC is obtained for learning algorithm trainlm, activation function Sig/lin and number of Neurons 15. For varying IP, best

Correlation coefficient (R) Training (0.99992) and Testing (0.99998) for BSFC is obtained, when learning algorithm trainlm Activation function Sig/lin/lin and number of Neurons is 8/1. The relation between predicted and experimental results for testing sets of BSFC parameters is shown in Figure 4.20.



(a) For injection timing

(b) For injection pressure

Fig. 4.20: Predicted and experimental results for testing sets of BSFC parameters

The brake specific fuel consumption for this diesel engine when operate with Polanga biodiesel blends can be accurately calculated by Eq. (4.3)

$$BSFC = \frac{1}{1 + e^{-(\sum_{i=1}^{15} w_{2i} F_i + 0.83931)}} \quad (4.3)$$

The information run was completed with the weights between the layers. For varying IP, BSFC is calculated by equation (4.4).

$$BSFC = \frac{1}{1 + e^{-(\sum_{i=1}^8 w_{2i} F_i + 0.34313)}} \quad (4.4)$$

The weight values appearing in Equation no 4.3 and 4.4 are given in the Table A4.5 and A4.6 respectively.

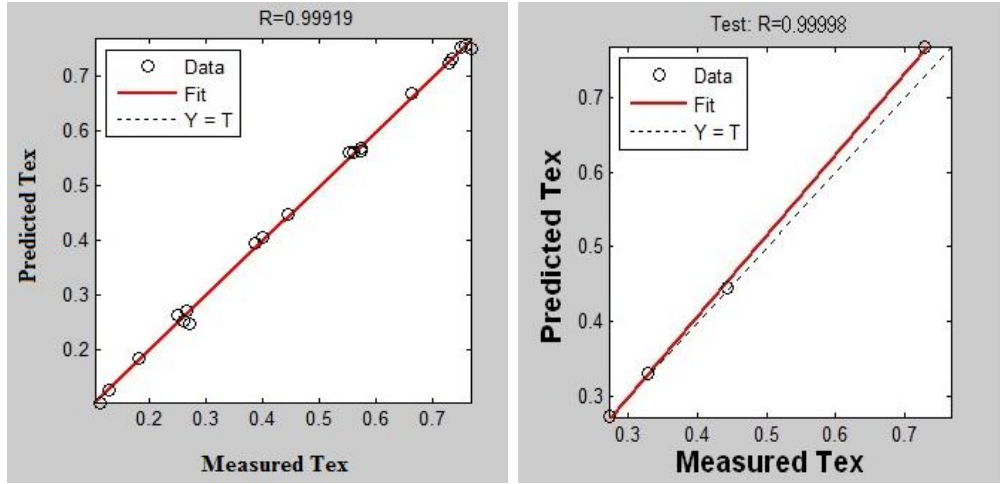
4.4.3 EXHAUST GAS TEMPERATURE (EGT)

The network structures and statistical parameters of the ANN model for Exhaust Gas Temperature (EGT), different learning algorithms are given in Table 4.6.

Table 4.6: Correlation coefficients for EGT using different learning algorithms

Parameter	Learning Algorithm	Activation function	Neurons (Numbers)	Correlation coefficient	
				Training	Testing
IT	Trainlm	Sig/lin	5	0.99819	0.99646
	Trainlm	Sig/lin	6	0.99898	0.99618
	Trainlm	Sig/lin	10	0.99931	0.99849
	Trainlm	Sig/lin	15	0.99967	0.99919
	Trainscg	Sig/lin	5	0.99397	0.99597
	Trainscg	Sig/lin	6	0.99321	0.99427
	Trainscg	Sig/lin	10	0.98791	0.99083
IP	Trainlm	Sig/lin/lin	2/1	0.9968	0.99996
	Trainlm	Sig/lin/lin	4/1	0.9999	0.9982
	Trainlm	Sig/lin/lin	6/1	0.9996	0.99998

From Table 4.6, it is observed that the best Correlation coefficient (R) Training (0.99967) and Testing (0.99919) for Tex is obtained, for learning algorithm trainlm, Activation function Sig/lin and number of neurons 15. For varying pressure best Correlation coefficient (R) Training (0.9996) and Testing (0.99998) for EGT is obtained, when learning algorithm trainlm Activation function Sig/lin/lin and number of Neurons is 6/1. The relation between Predicted and experimental values for testing sets of EGT is shown in Figure 4.21.



(a) For injection timing

(b) For injection pressure

Fig. 4.21: Predicted and experimental results for testing sets of EGT parameters

For varying IT, Exhaust Gas Temperature can be accurately calculated by Eq. (4.5).

$$EGT = \frac{1}{1 + e^{-(\sum_{i=1}^{15} w_{2i} F_i + 0.83009)}} \quad (4.5)$$

For varying IP, Exhaust Gas Temperature can be accurately calculated by Eq. (4.6).

$$EGT = \frac{1}{1 + e^{-(\sum_{i=1}^6 w_{2i} F_i + 0.35893)}} \quad (4.6)$$

The weight values appearing in Equation no 4.5 and 4.6 are given in the Table A4.7 and Appendix 4.8.

4.4.4 PEAK CYLINDER PRESSURE (Pmax)

The network structures and various statistical parameters of the ANN model for Peak Engine cylinder pressure (Pmax), different learning algorithms are given away in Table 4.7.

From Table 4.7, it is observed that for injection timing, the best Correlation coefficient (R) Training (0.99988) and Testing (0.99587) is obtained, when learning algorithm trainlm Activation function Sig/lin and number of Neurons is 20.

Table 4.7: Correlation coefficients for Pmax using different learning algorithms

Parameter	Learning Algorithm	Activation function	Neurons (Numbers)	Correlation coefficient (R)	
				Training	Testing
IT	Trainlm	Sig/lin	5	0.99424	0.99404
	Trainlm	Sig/lin	6	0.9947	0.99633
	Trainlm	Sig/lin	10	0.99264	0.99384
	Trainlm	Sig/lin	20	0.99988	0.99587
	Trainscg	Sig/lin	5	0.97638	0.96727
	Trainscg	Sig/lin	6	0.98404	0.97345
	Trainscg	Sig/lin	10	0.97305	0.98589
IP	Trainlm	Sig/Sig/lin	10/10	0.9998	0.9988
	Trainlm	Sig/Sig/lin	5/5	0.9989	0.9994
	Trainlm	Sig/Sig/lin	7/5	0.9983	0.9956
	Trainlm	Sig/Sig/lin	5/2	0.99681	0.9953
	Trainlm	Sig/ lin/lin	5/5	0.999	0.9964
	Trainlm	Sig/lin/lin	5/1	0.99975	0.99587
	Trainlm	Sig/lin/lin	8/1	0.99992	0.99398

For varying pressure, best Correlation coefficient (R) Training (0.9999) and Testing (0.99587) is obtained, when learning algorithm trainlm Activation function Sig/lin/lin and number of Neurons is 5/1.

For varying fuel injection pressure , Pmax is calculated using Equation no. 4.7.

$$P_{max} = \frac{1}{1 + e^{-(\sum_{i=1}^{20} w_{2i}F_i + 0.22691)}} \quad (4.7)$$

For varying IP, Pmax is calculated by Equation no. 4.8.

$$P_{max} = \frac{1}{1 + e^{-(\sum_{i=1}^5 w_{2i}F_i + 12.3932)}} \quad (4.8)$$

The weight values appearing in Equation no 4.7 and Equation no 4.8 are given in the Appendix Table A4.9 and A4.10.

The relation between predicted and experimental outcome for testing sets of Pmax parameters given by ANN modeling is shown in Figure 4.22.

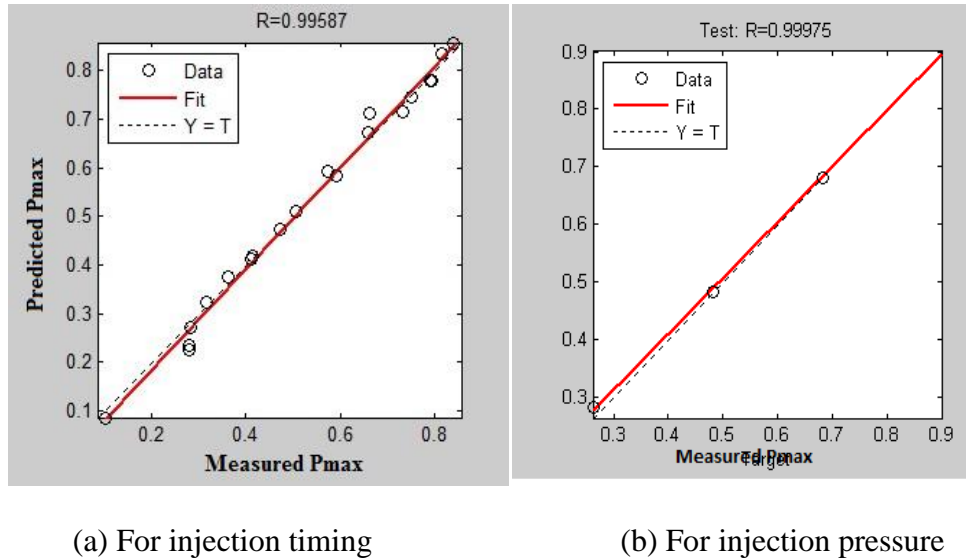


Fig. 4.22: Predicted and experimental results for testing sets of Pmax parameters

4.4.5. OXIDES OF NITROGEN (NO_x)

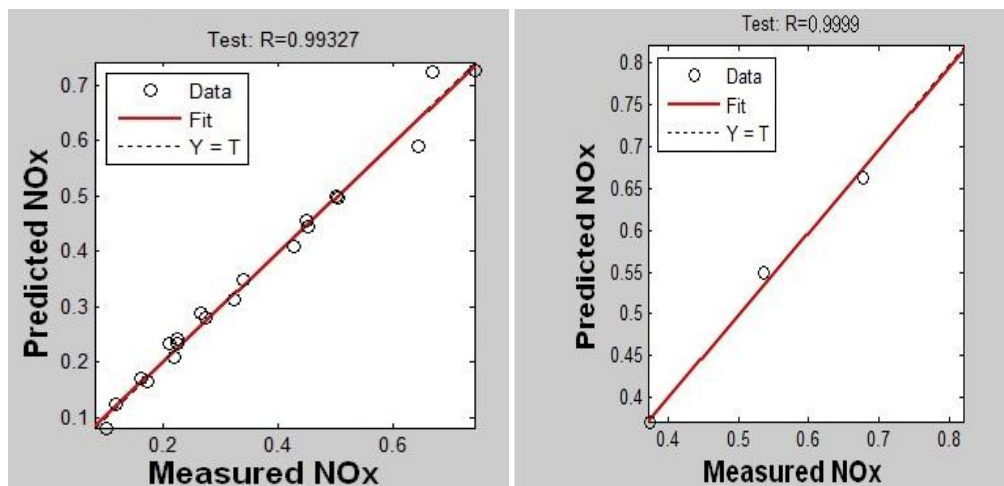
The network structures and various statistical parameters of the ANN model for Oxides of nitrogen (NO_x), different learning algorithms are given in Table 4.8.

For varying IT, the best Correlation coefficient (R) Training 0.99838 Testing 0.99327 for NO_x is obtained, when learning algorithm trainlm Activation function Sig/lin and number of Neurons is 10. For IP, it is observed that best Correlation coefficient (R) Training (0.9994) and Testing (0.9999) for NO_x is obtained, when learning algorithm trainlm Activation function Sig/lin/lin and number of Neurons is 4/1.

Table 4.8: Correlation coefficients for NOx using different learning algorithms

Parameter	Learning Algorithm	Activation function	Neurons (Numbers)	Correlation coefficient (R)	
				Training	Testing
IT	Trainlm	Sig/lin	5	0.99403	0.9852
	Trainlm	Sig/lin	6	0.99747	0.99329
	Trainlm	Sig/lin	10	0.99838	0.99327
	Trainlm	Sig/lin	15	0.99899	0.99659
	Trainlm	Sig/lin	20	0.99987	0.99873
	Trainlm	Tan/lin	10	0.9983	0.99396
	Trainscg	Sig/lin	5	0.98684	0.99406
	Trainscg	Sig/lin	6	0.98158	0.97792
	Trainscg	Sig/lin	10	0.98309	0.99188
	Traingdm	Sig/lin	10	0.93193	0.89309
IP	Trainlm	Sig/ lin/lin	2/1	0.9951	0.9977
	Trainlm	Sig/lin/lin	4/1	0.9994	0.9999
	Trainlm	Sig/lin/lin	6/1	0.9991	0.9984

The relation between Predicted and experimental trial end results for testing sets of NOx parameters give by ANN modeling is shown in Figure 4.23.



(a) For injection timing

(b) For injection pressure

Fig. 4.23: Predicted and experimental results for testing sets of NOx parameters

Equation (4.9) gives the expression for NOx for varying IT.

$$NOx = \frac{1}{1 + e^{-(\sum_{i=1}^{20} w_{2i} F_i - 0.49899)}} \quad (4.9)$$

For varying IP, expression for NOx is given by

$$NOx = \frac{1}{1 + e^{-(\sum_{i=1}^4 w_{2i} F_i + 0.55572)}} \quad (4.10)$$

The weight values appearing in Equation no 4.9 and 4.10 are given in the Table A4.11 and A4.12.

4.4.6 SMOKE

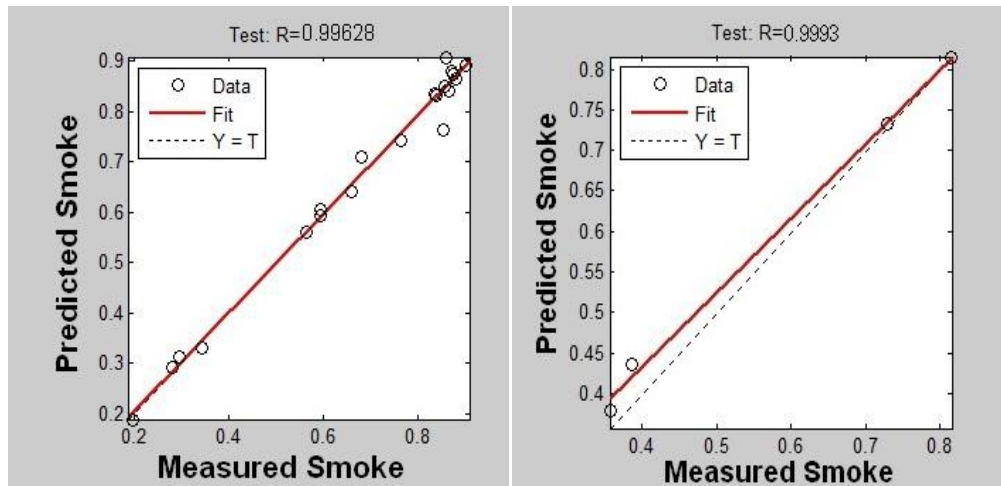
The network structures and various statistical parameters of the ANN model for Smoke different learning algorithms are given in Table 4.9.

Table 4.9 Correlation coefficients for smoke using different learning algorithms

Parameter	Learning Algorithm	Activation function	Neurons (Numbers)	Correlation coefficient (R)	
				Training	Testing
IT	Trainlm	Sig/lin	5	0.98721	0.94474
	Trainlm	Sig/lin	6	0.98339	0.98946
	Trainlm	Sig/lin	10	0.99401	0.98814
	Trainlm	Sig/lin	15	0.99941	0.99628
	Trainlm	Sig/lin	20	0.99979	0.9956
	Trainlm	Sig/lin	25	0.99969	0.98134
	Trainlm	Tan/lin	10	0.99868	0.99375
	Trainscg	Sig/lin	5	0.95591	0.96122
	Trainscg	Sig/lin	6	0.96305	0.98925
	Trainscg	Sig/lin	10	0.98058	0.9458
Trainngdm	Sig/lin	10	0.92551	0.92046	
IP	Trainlm	Sig/lin/lin	2/1	0.9975	0.9912
	Trainlm	Sig/lin/lin	4/1	0.9987	0.9993
	Trainlm	Sig/lin/lin	6/1	0.9989	0.9974

The best Correlation coefficient in case of IT, Training (0.99941) and Testing (0.99628) for smoke are obtained, when learning algorithm trainlm Activation

function Sig/lin and number of Neurons is 15. For varying IP, best Correlation coefficient (R) Training (0.9987) Testing (0.9993) for smoke is obtained, when learning algorithm trainlm Activation function Sig/lin/lin and number of Neurons is 4/1. The relation between Predicted and experimental results for testing sets of smoke parameters is shown in Figure 4.24.



(a) For injection timing

(b) For injection pressure

Fig. 4.24: Predicted and experimental results for testing sets of Smoke parameters

The expressions for smoke for varying IT and IP are given in equations 4.11 and 4.12 respectively.

$$Smoke = \frac{1}{1 + e^{-(\sum_{i=1}^{15} w_{2i} F_i + 2.6321)}} \quad (4.11)$$

$$Smoke = \frac{1}{1 + e^{-(\sum_{i=1}^4 w_{2i} F_i - 5.2244)}} \quad (4.12)$$

The weight values appearing in Equation no 4.11 and 4.12 are given in the Table A4.13 and Appendix 4.14 respectively.

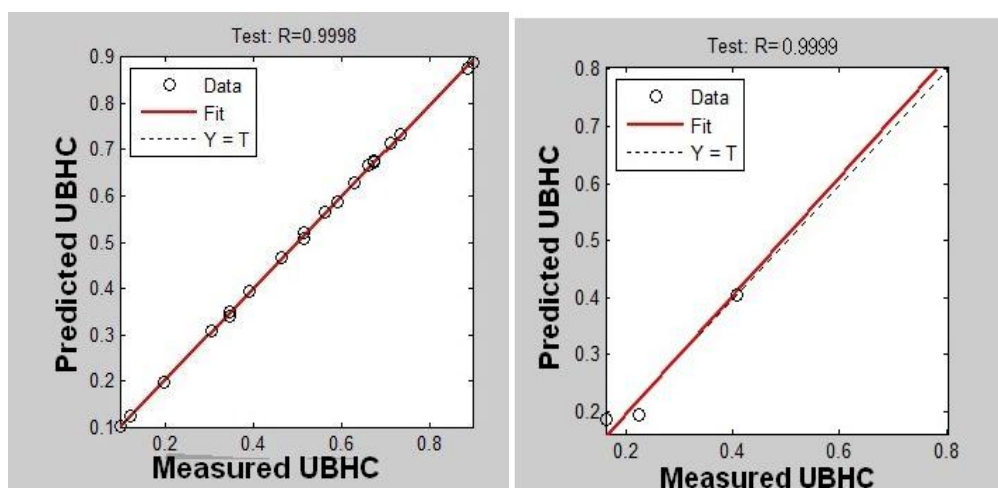
4.4.7 UNBURNED HYDRO CARBON (UHC)

The network structures and various statistical parameters of ANN model for Unburned Hydro Carbon (UHC) different learning algorithms are given in Table 4.10.

Table 4.10: Correlation coefficients for UHC using different learning algorithms

Parameter	Learning Algorithm	Activation function	Neurons (Numbers)	Correlation coefficient (R)	
				Training	Testing
IT	Trainlm	Sig/lin	5	0.97969	0.96352
	Trainlm	Sig/lin	10	0.99976	0.99905
	Trainlm	Sig/lin	11	0.99991	0.9998
IP	Trainlm	Sig/ lin/lin	1/1	0.9974	0.9983
	Trainlm	Sig/lin/lin	2/1	0.9976	0.9996
	Trainlm	Sig/lin/lin	4/1	0.9896	0.9999

For varying IT, it is observed that best Correlation coefficient (R) Training (0.99991) and Testing (0.9998) for unburned hydrocarbon (UHC) is obtained, when learning algorithm trainlm Activation function Sig/lin and number of Neurons is 11. For IP, best Correlation coefficient (R) Training (0.9896) and Testing (0.9999) for unburned hydrocarbon (UHC) is obtained, when learning algorithm trainlm Activation function Sig/lin/lin and number of Neurons is 4/1.



(a) For injection timing

(b) For injection pressure

Fig. 4.25: Predicted and experimental results for testing sets of UHC parameters

The relation between predicted and experimental results for testing sets of unburned hydrocarbon (UHC) parameters is shown in Figure 4.25. The expressions for UHC for varying IT and IP are given in equations 4.13 and 4.14 respectively.

$$UHC = \frac{1}{1 + e^{-\sum_{i=1}^{11} w_{2i} F_i + 2.1668}} \quad (4.13)$$

$$UHC = \frac{1}{1 + e^{-\sum_{i=1}^4 w_{2i} F_i - 1.40738}} \quad (4.14)$$

The weight values appearing in Equation (4.13) and (4.14) are given in the Table A4.15 and A4.16.

4.4.8 CARBON MONO OXIDE (CO)

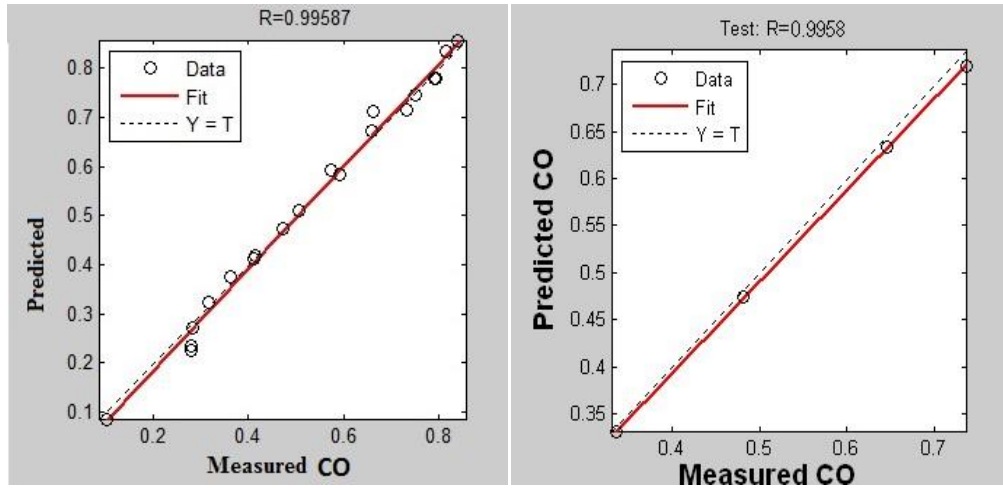
The network structures and various statistical parameters of the ANN model for CO with different learning algorithms are given in Table 4.11.

Table 4.11: Correlation coefficients for CO using different learning algorithms

Parameter	Learning Algorithm	Activation function	Neurons (Numbers)	Correlation coefficient (R)	
				Training	Testing
IT	Trainlm	Sig/lin	5	0.99403	0.9852
	Trainlm	Sig/lin	6	0.99747	0.99587
	Trainlm	Sig/lin	10	0.99838	0.99327
	Trainlm	Sig/lin	15	0.99899	0.99659
	Trainlm	Sig/lin	20	0.99987	0.99873
	Trainlm	Tan/lin	10	0.9983	0.99396
	Trainscg	Sig/lin	5	0.98684	0.99406
	Trainscg	Sig/lin	6	0.98158	0.97792
	Trainscg	Sig/lin	10	0.98309	0.99188
	Traingdm	Sig/lin	10	0.93193	0.89309
IP	Trainlm	Sig/ lin/lin	2/1	0.9951	0.9977
	Trainlm	Sig/lin/lin	4/1	0.9994	0.9999
	Trainlm	Sig/lin/lin	6/1	0.9984	0.9968

For varying IT, the best Correlation coefficient (R) Training 0.99747 Testing 0.99587 for CO is obtained, when learning algorithm trainlm Activation function

Sig/lin and number of Neurons is 6. For IP, it is observed that best Correlation coefficient (R) Training (0.9984) and Testing (0.9968) for CO is obtained, when learning algorithm trainlm Activation function Sig/lin/lin and number of Neurons is 6/1. The relation between Predicted and experimental trial end results for testing sets of CO parameters give by ANN modeling is shown in Figure 4.26.



(a) For injection timing

(b) For injection pressure

Fig. 4.26: Predicted and experimental results for testing sets of CO parameters

The expressions for CO for varying IT and IP are given in equations 4.15 and 4.16 respectively.

$$CO = \frac{1}{1 + e^{-(\sum_{i=1}^6 w_{2i} F_i - 0.5329)}} \quad (4.15)$$

$$CO = \frac{1}{1 + e^{-(\sum_{i=1}^6 w_{2i} F_i + 0.21331)}} \quad (4.16)$$

The weight values appearing in Equation (4.15) and (4.16) are given in the Table A4.17 and A4.18.

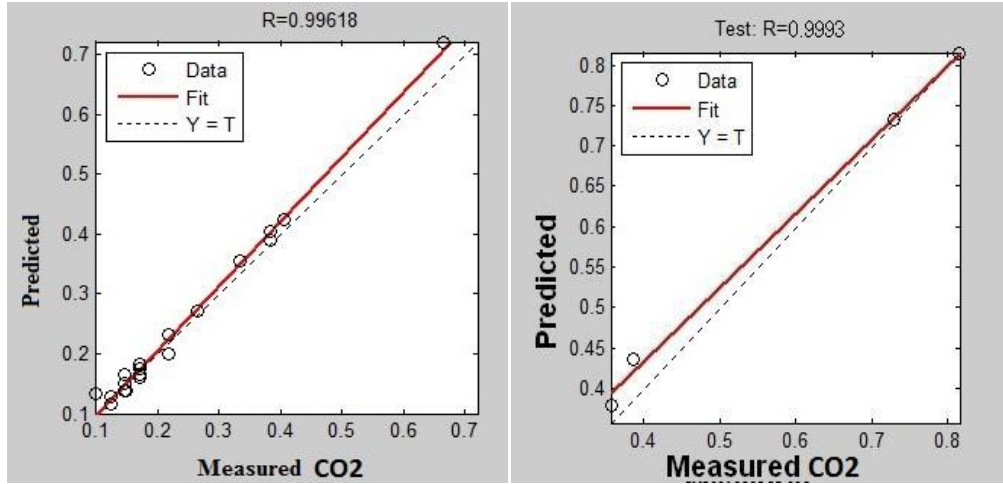
4.4.9 CARBON DIOXIDE (CO₂)

The network structures and various statistical parameters of the ANN model for CO₂ with different learning algorithms are given in Table 4.12.

Table 4.12: Correlation coefficients for CO₂ using different learning algorithms

Parameter	Learning Algorithm	Activation function	Neurons (Numbers)	Correlation coefficient (R)	
				Training	Testing
IT	Trainlm	Sig/lin	5	0.99424	0.9852
	Trainlm	Sig/lin	6	0.9947	0.99587
	Trainlm	Sig/lin	9	0.99264	0.99618
	Trainlm	Sig/lin	20	0.99988	0.99659
	Trainscg	Sig/lin	5	0.97638	0.99873
	Trainscg	Sig/lin	6	0.98404	0.99396
	Trainscg	Sig/lin	10	0.97305	0.99406
IP	Trainlm	Sig/Sig/lin	10/10	0.9998	0.97792
	Trainlm	Sig/Sig/lin	5/5	0.9989	0.99188
	Trainlm	Sig/Sig/lin	7/5	0.9983	0.89309
	Trainlm	Sig/Sig/lin	5/2	0.99681	0.9977
	Trainlm	Sig/ lin/lin	5/5	0.999	0.9999
	Trainlm	Sig/lin/lin	5/1	0.99975	0.9993

For varying IT, the best Correlation coefficient (R) Training 0.99264 Testing 0.99618 for CO is obtained, when learning algorithm trainlm Activation function Sig/lin and number of Neurons is 9. For IP, it is observed that best Correlation coefficient (R) Training (0.99975) and Testing (0.9993) for CO is obtained, when learning algorithm trainlm Activation function Sig/lin/lin and number of Neurons is 5/1. The relation between Predicted and experimental trial end results for testing sets of CO parameters give by ANN modeling is shown in Figure 4.26.



(a) For injection timing

(b) For injection pressure

Fig. 4.27: Predicted and experimental results for testing sets of CO₂ parameters

The expressions for CO₂ for varying IT and IP are given in equations 4.17 and 4.18 respectively.

$$CO_2 = \frac{1}{1 + e^{-(\sum_{i=1}^9 w_{2i} F_i - 0.3429)}} \quad (4.17)$$

$$CO_2 = \frac{1}{1 + e^{-(\sum_{i=1}^5 w_{2i} F_i + 0.5451)}} \quad (4.18)$$

The weight values appearing in Equation (4.17) and (4.18) are given in the Table A4.19 and A4.20.

4.5 VALIDATION OF ANN MODEL

The developed ANN model is validated using a different set of input conditions that were used in training and testing of models. The selected input variables are: injection timing of 17, 21, 25, 29°bTDC, 100% engine load, Polanga biodiesel blend B25 and injection pressure of 180 bar for the variable injection timing model. For variable injection pressure model the selected input variables are: injection timing of 23°bTDC, 100% engine load, Polanga biodiesel blend B25 and injection pressure of 170, 190, 210 and 230 bar. The results obtained through the developed models are compared with those obtained experimentally. The validation results are

shown below in Table 4.13. The experimental values appearing in Table 4.13 are given in the Table A4.21.

Table 4.13: Validation of ANN Model

Parameter	Input	ANN predicted value	Experimental value	% error
BTE (%)	17° bTDC	29.84	30.31	1.57
	21°bTDC	30.56	31.12	2.12
	25° bTDC	32.11	32.72	1.89
	29° bTDC	32.29	32.91	1.93
	170 bar	30.59	31.11	1.61
	190 bar	31.35	31.92	1.81
	210 bar	31.93	32.53	1.87
	230 bar	32.59	33.26	2.05
BSFC (Kg/Kw.hr)	17°bTDC	0.230	0.235	2.17
	21°bTDC	0.223	0.228	2.24
	25°bTDC	0.224	0.229	2.21
	29°bTDC	0.239	0.245	2.51
	170 bar	0.233	0.239	2.57
	190 bar	0.223	0.228	2.24
	210 bar	0.224	0.229	2.22
	230 bar	0.227	0.233	2.64
EGT (°C)	17°bTDC	275.43	283	2.74
	21°bTDC	262.16	269	2.61
	25°bTDC	256.41	263	2.57
	29°bTDC	251.59	258	2.55
	170 bar	256.39	266	3.75
	190 bar	261.96	270	3.08
	210 bar	265.71	273	2.75
	230 bar	268.58	270	0.52
CO (% vol)	17°bTDC	0.1083	0.11	1.56
	21°bTDC	0.0986	0.10	1.41
	25°bTDC	0.0881	0.09	2.15
	29°bTDC	0.0793	0.08	0.82
	170 bar	0.0977	0.10	2.35
	190 bar	0.0871	0.09	3.32
	210 bar	0.0671	0.07	4.32
	230 bar	0.0524	0.05	4.58
UHC (ppm)	17°bTDC	22.43	22	1.91
	21°bTDC	20.55	21	2.18
	25°bTDC	19.59	19	1.99
	29°bTDC	19.09	19	0.47
	170 bar	20.74	21	1.73
	190 bar	19.57	19	3.01

	210 bar	17.89	18	0.61
	230 bar	16.61	17	2.34
CO ₂ (% vol)	17°bTDC	7.37	7.51	1.89
	21°bTDC	7.48	7.61	1.73
	25°bTDC	7.52	7.72	3.05
	29°bTDC	7.64	7.88	3.14
	170 bar	7.59	7.72	1.61
	190 bar	7.50	7.78	3.73
	210 bar	7.47	7.8	4.41
	230 bar	7.62	7.85	3.01
NO _x (ppm vol)	17°bTDC	386.0	396	2.59
	21°bTDC	672.3	682	1.53
	25°bTDC	838.2	848	1.16
	29°bTDC	900.4	920	2.17
	170 bar	803.4	819	1.94
	190 bar	812.0	832	2.46
	210 bar	821.5	851	3.65
	230 bar	834.9	844	1.08

As can be seen from Table 4.13 the percentage error for all the parameters lies in the range of 0.47 to 4.58. Also the variation in error for all the parameters is negligible. The mean percentage error for performance parameters BTE, BSFC and EGT are 1.85, 2.35 and 2.57 % respectively. On the other side mean percentage error for Engine emission parameters UHC, NO_x, CO₂ and CO are 1.78, 2.57, 2.79 and 2.56 % respectively. The mean percentage error for variable fuel injection timing is 2.39% and for variable fuel injection pressure is 2.17%. The developed ANN model thus depicts the performance and emission parameters quite efficiently and hence can be a useful tool in assessment of Polanga based biodiesel single cylinder diesel engine.

4.6 MULTI-OBJECTIVE OPTIMIZATION OF ENGINE PARAMETERS

As discussed in section 3.9, optimization is the task of judgment one or more than one solution which communicate to minimizing (or maximizing) one or additional individual objectives which satisfy all given constraints. A solo-objective optimization process involves a particular objective function and generally results in a

lone solution. On the other side, a multi-objective optimization task considers numerous conflicting objectives all together. In this case, there is usually no unique one solution, but a set of options with altered trade-offs. From the existence of various finest solutions, generally only one of these solutions is to be elected. Thus, as compared to single objective optimization process multi-objective optimization process have two equally considerable tasks: an optimization assignment for finding an optimal set of solutions (concerning a computer based process) and the second task is decision making for selecting a particular single most favourable solution. IC engines are the lightest power generating units known and therefore are of the greatest applications in transportation. An engine is expected to give highest possible efficiency with the least possible emissions in order to meet the environmental standards. Generally, it is observed that the engine gives maximum efficiency and also maximum emissions at high loads. This creates a scenario wherein, to get maximum efficiency, we must compromise on emissions or to get minimum emissions we must compromise on efficiency. This is a case of optimization to strike an optimal combination of input parameters to achieve maximization of engine performance and minimization of emission constituents.

The results obtained in the experimental study conducted at different preset injection timings, different loads and different injection pressures show that as engine efficiency of the engine increases, the harmful emissions constituents also increase. Hence, it is difficult to get the accurate minimum possible values of harmful emissions and maximum possible value of thermal efficiency. Hence an optimization is performed to obtain optimum values of load, injection timing, injection pressure and blend which give minimum possible emissions and maximum possible thermal efficiency i.e. optimise engine performance and emission constituents. There are

several algorithms which can be used to solve an optimization problem. The usage of these algorithms depends on the type of the problem, environment and the results required in real life situation. For engine applications, use of genetic algorithm is considered one of the best ways to solve the problem because of its inherent uniqueness. The optimization using genetic algorithm in MATLAB software is carried out to optimize the chosen engine input parameters to achieve specified priorities. The genetic algorithm makes use of the correlations obtained by performing nonlinear regression analysis on the experimental data for all Polanga biodiesel and diesel blends at all loads, injection timings and injection pressures. Curve Expert software is used to obtain the correlations. The different correlations evaluated are,

$$\text{Square function: } y = a \times (x_1) + b \times (x_2) + c \times (x_3) + d \times (x_1)^2 + e \times (x_2)^2 + f \times (x_3)^2 + g \times (x_1) \times (x_2) + h \times (x_2) \times (x_3) + i \times (x_3) \times (x_1)$$

$$\text{Cubic function: } y = a + b \times (x_1) + c \times (x_2) + d \times (x_3) + e \times (x_4) + f \times (x_1)^2 + g \times (x_2)^2 + h \times (x_3)^2 + i \times (x_4)^2 + j \times (x_1) \times (x_2) + k \times (x_2) \times (x_3) + l \times (x_3) \times (x_4) + m \times (x_3) \times (x_4) + n \times (x_1)^3 + o \times (x_2)^3 + p \times (x_3)^3 + q \times (x_4)^3$$

$$\text{Exponential function: } y = e^{[a(x_1) + b(x_2) + c(x_3) + d]}$$

$$\text{Linear: } y = a \times (x_1) + b \times (x_2) + c \times (x_3) + d$$

Where, x_1 = Load, x_2 = IT, x_3 = IP, x_4 = Blend

The optimization process is carried out after fixing the upper and lower bounds for constraints, defining the fitness function and number of variables. The constraints are load, blend, injection timing and injection pressure. The optimization is carried out considering full load condition and hence, both upper and lower bounds for loads are 10kg (full load). The upper and lower bounds for the constraints are given in Table 4.14. The correlations obtained by nonlinear regression analysis of the experimental data are used as fitness functions and the number of variables are given as 4 viz. load,

injection timing, injection pressure, blend proportion and are varied during experimentation

Table 4.14: Upper and Lower Bounds for Constraints

Constraints	Lower bound	Upper bound
Load (full load)	10	10
Injection timing (bTDC)	15	31
Injection Pressure (bar)	160	240
Blend (%)	10	40

The Optimization is conducted considering three cases, namely

1. Engine performance
2. Engine emission constituents
3. Both engine performance and emission constituents together with equal weightages to each

The optimization of engine performance, emission constituents and both engine performance and emission constituents together, giving equal weightages to each are, respectively, explained in sections 4.6.1, 4.6.2 and 4.6.3.

4.6.1 PERFORMANCE PARAMETERS

The optimization of engine performance parameters is conducted by considering three important parameters viz. BTE, BSFC and EGT. BTE is always preferred to be maximum, BSFC and EGT to be minimum. Hence, this creates a multimodal scenario of optimization. The solution procedure for optimization of engine performance is as follows:

1. Three types of mathematical equations viz. Polynomials, exponentials and power functions are developed from the captured experimental data (Table A4.22) to form a

relation between the input (Load, IT, IP, Blend) and output (BTE, BSFC and EGT) parameters using the Curve expert software.

2. The mathematical equation with best fit is selected based on best value of coefficient of determination (R^2) for all parameters. Cubic polynomial is found to be the best fit on both criterion and for all output parameters. Table 4.15 shows the cubic polynomials for engine performance parameters, with their respective R^2 values.

3. The equations thus obtained are defined as a function in MATLAB. This function is called as the fitness function for optimization in MATLAB. The Genetic Algorithm tool box of MATLAB is used for defining and solving the problem. Figure 4.34 shows an optimization problem definition screen.

Table 4.15: Polynomials for Engine Performance Parameters

Parameter	Polynomial Equation	R^2
BTE	$=28.9+1.472*x_1+0.3579*x_2+0.1382*x_3+6.3584E-02*x_4+-$ $0.1225*x_1^2+8.507E-03*x_2^2+5.903E-03*x_3^2+7.6951E-$ $03*x_4^2+8.4605E-03*x_1*x_2+2.3905E-03*x_2*x_3+7.853E-03*x_3*x_4+-$ $3.4099E-02*x_4*x_1+-9.971E-03*x_1^3+-4.839E-04*x_2^3+-4.214E-$ $04*x_3^3+-1.31584E-04*x_4^3$	0.916
BSFC	$= 0.13482+-1.327209E-03*x_1+-2.8259E-03*x_2+7.5319E-04*x_3+-$ $1.522E-03*x_4+8.662E-04*x_1^2+-7.6268E-05*x_2^2+7.0018E-05*x_3^2+-$ $5.91516E-05*x_4^2+-4.6337E-04*x_1*x_2+1.845E-05*x_2*x_3+-5.188E-$ $05*x_3*x_4+3.56817E-04*x_4*x_1+1.1E-04*x_1^3+7.352E-06*x_2^3+-$ $1.3465E-06*x_3^3+9.862E-07*x_4^3$	0.81
EGT	$=211.9+0.981*x_1+-2.5148*x_2+1.3535*x_3+3.429E-02*x_4+0.375*x_1^2+-$ $6.2631E-02*x_2^2+-2.446E-02*x_3^2+-2.5416E-03*x_4^2+-3.767E-$ $02*x_1*x_2+2.8E-02*x_2*x_3+4.591E-03*x_3*x_4+1.6154E-$ $02*x_4*x_1+0.0477*x_1^3+1.922E-03*x_2^3+2.3116E-05*x_3^3+1.283E-$ $04*x_4^3$	0.96

4. Record the value of the optimum and the result after a few repeated trials to eliminate the effects of specific initialisation.

Figure 4.28 shows a display screen of the MATLAB program before optimization of engine performance is carried out. The problem definition screen is where the solver, the fitness function and bounds are defined. The options column on the left hand side is used to select pareto front display. After the optimization is done, the number of iterations are displayed in the current iteration box. The function values are also displayed, suitably.

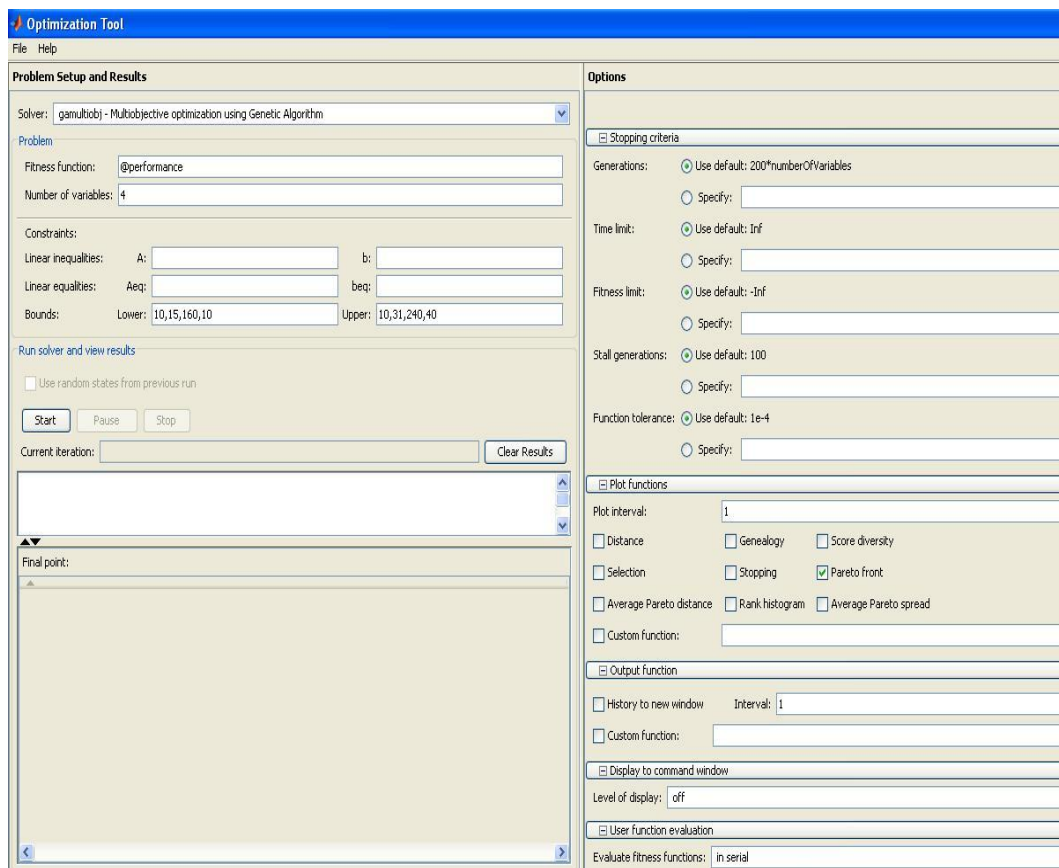


Fig. 4.28 Optimization tool problem definition screen

Figure 4.29 shows a display screen of the MATLAB program after optimization of engine performance is carried out. The problem definition screen is where the solver, the fitness function and bounds are defined. The optimization is carried out

considering full load condition and hence, both upper and lower bounds for load. The set bounds for the constraints are given in Table 4.14. The same are entered in the order of Load, IT, IP, Blend in the software.

The options column on the left hand side is used to select Pareto front display. After the optimization is done, the number of iterations is displayed in the current iteration box. The function values are also displayed, suitably.

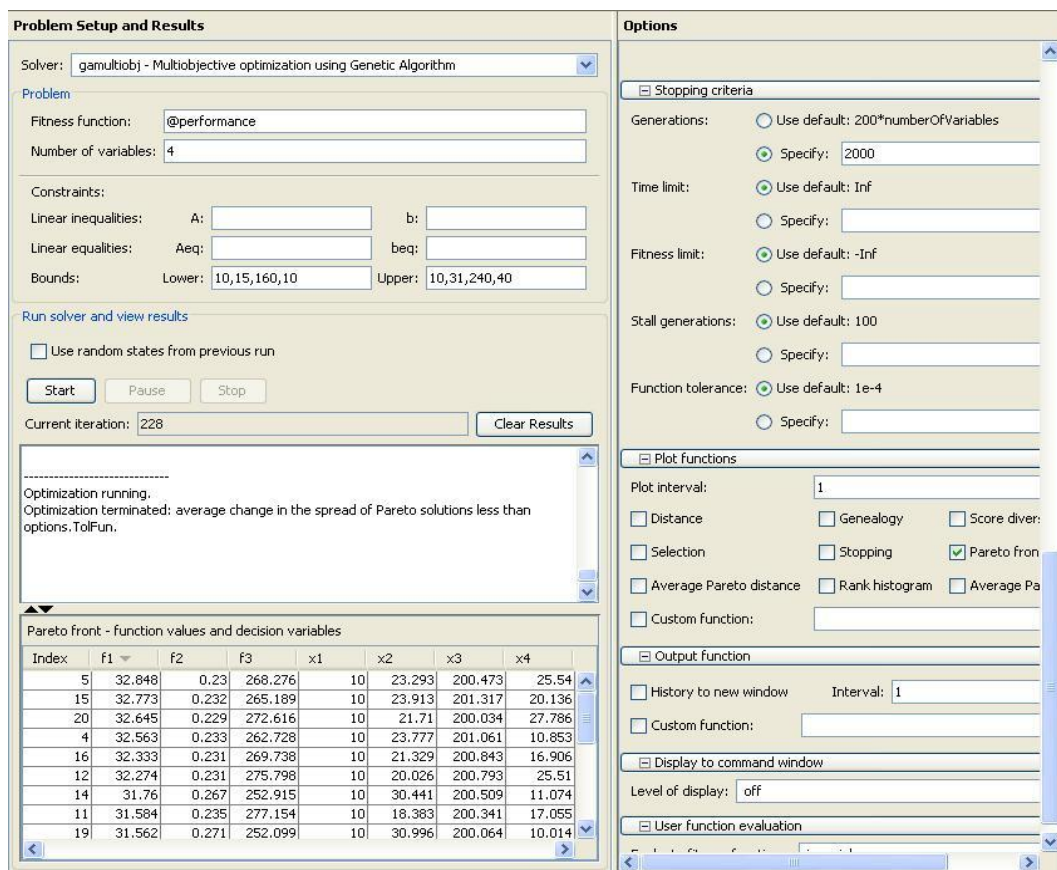


Fig. 4.29 MATLAB program showing optimization of engine performance

Figure 4.30 shows the Pareto front for optimization of thermal performance parameters to find maximum BTE with minimum BSFC and EGT for the diesel engine operating on different Polanga biodiesel and diesel blends at different ITs, IPs and full load. Pareto front shows the trade-off between the two objectives. The objectives are the functions which the software forms inherently based on the

maximising and minimising parameters given. Objective 1 is minimisation of BSFC and EGT and objective 2 is the maximisation of BTE. The pareto front is plotted in objective function space. It gives a set of points corresponding to different values of objective 1 and objective 2. Pareto front shows the trade-off between the two objectives. The objectives are the functions which the software forms inherently based on the maximising and minimising parameters given. The Pareto front is plotted in objective function space. It gives a set of points corresponding to different values of objective 1 and objective 2. The software uses Pareto front to strike a balance between objective 1 and objective 2 and picks up a point to suggest the optimum values of input parameters such as IT, IP and blend. The points appear to lie in the range 29.5 to 33 and 0.22 to 0.28 for objective 1 and objective 2 respectively. The values of objective 1 and objective 2 are used to determine the optimum input parameters by the software by following a set of complex calculations.

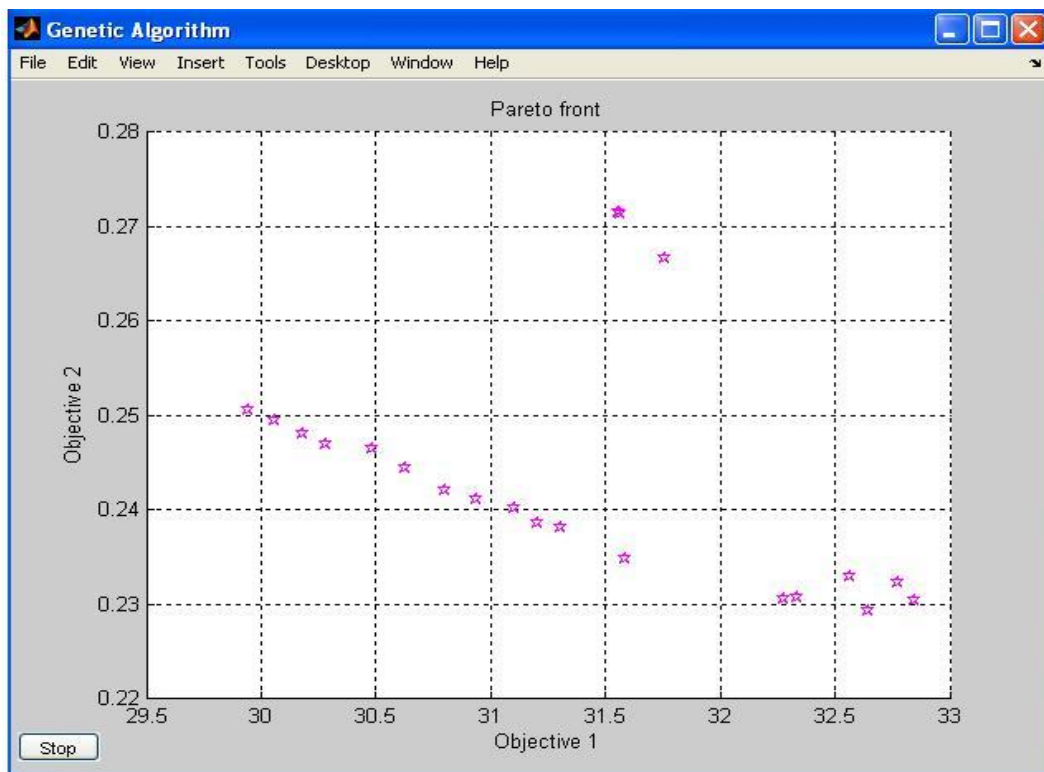


Fig. 4.30 Pareto front for optimization of performance parameters

The optimal set of solution for the present case is shown in Table 4.16

Table 4.16: Optimal set of solution for Engine Performance Parameters

S. No.	BTE (%)	BSFC (Kg/Kw.hr)	EGT (°C)	x₁ load(%)	x₂ I.T(°bTDC)	x₃ I.P(bars)	x₄ blend(%)
1	33.15	0.235	270.7	100	24.24	233.5	26.72
2	33.13	0.232	271.5	100	23.65	221.7	29.06
3	33.08	0.232	273.3	100	23.07	232.3	27.94
4	33.05	0.232	269.2	100	23.91	211.1	27.83
5	32.91	0.231	277.5	100	21.64	231.1	30.67

4.6.2 EMISSION CONSTITUENTS

The optimization of emission constituents is conducted by considering all the constituents of the exhaust gas measured in the experimental study. Among the emissions considered, oxygen is preferred to be maximum as it is not harmful to the environment and remaining emission constituents such as UHC, CO, NO_x, Smoke to be minimum. This creates a multimodal scenario as CO₂ is to be maximised at the expense of other constituents. The same steps adopted in solution procedure in section 4.6.1 of thermal performance are followed here also. The polynomials for emission constituents are given in Table 4.17 with their respective R² values. The experimental data is provided in appendix Table A4.23.

The polynomials for emission constituents are given in Table with their respective R² values.

Table 4.17: Polynomials for Engine Performance Parameters

Parameter	Polynomial Equation	R ²
NOx	$850.8+51*x1+43.05*x2+-0.925*x3+47.26*x4+-$ $17.859*x1^2+0.4353*x2^2+6.028E-03*x3^2+6.4626E-$ $03*x4^2+2.91321*x1*x2+4.51E-02*x2*x3+2.082E-03*x3*x4+-$ $4.6523*x4*x1+-0.46*x1^3+-3.35E-02*x2^3+-1.58E-05*x3^3+2.37E-$ $05*x4^3$	0.966
CO ₂	$9.787+0.22*x1+0.159*x2+3.6E-02*x3+-1.12E-02*x4+-$ $0.108*x1^2+4.48E-03*x2^2+7.12E-05*x3^2+-5.423E-04*x4^2+-$ $8.09E-03*x1*x2+-8.66E-04*x2*x3+-3.28E-05*x3*x4+4.17539E-$ $03*x4*x1+-9.33E-04*x1^3+-4.82E-05*x2^3+-2.92E-07*x3^3+8.49E-$ $06*x4^3$	0.87
HC	$=22.84+-0.45*x1+-0.64*x2+-4.34E-02*x3+-0.289*x4+0.1688*x1^2+-$ $2.5255E-03*x2^2+-1.352E-05*x3^2+-4.169E-04*x4^2+-1.41E-$ $02*x1*x2+4.479E-04*x2*x3+-6.101E-06*x3*x4+2.459E-$ $02*x4*x1+6.82329929599275E-03*x1^3+3.44E-04*x2^3+1.458E-$ $07*x3^3+5.378E-07*x4^3$	0.87
CO	$= 0.119+-8.608E-03*x1+-4.787E-03*x2+-1.906E-04*x3+2.54E-$ $05*x4+1.47E-03*x1^2+-8.6243E-05*x2^2+-1.07E-06*x3^2+1.1E-$ $05*x4^2+-1.379E-04*x1*x2+1.23E-05*x2*x3+-1.08E-06*x3*x4+-$ $1.55E-04*x4*x1+1.03E-04*x1^3+3.698E-06*x2^3+4.276E-$ $10*x3^3+7.383E-08*x4^3$	0.76

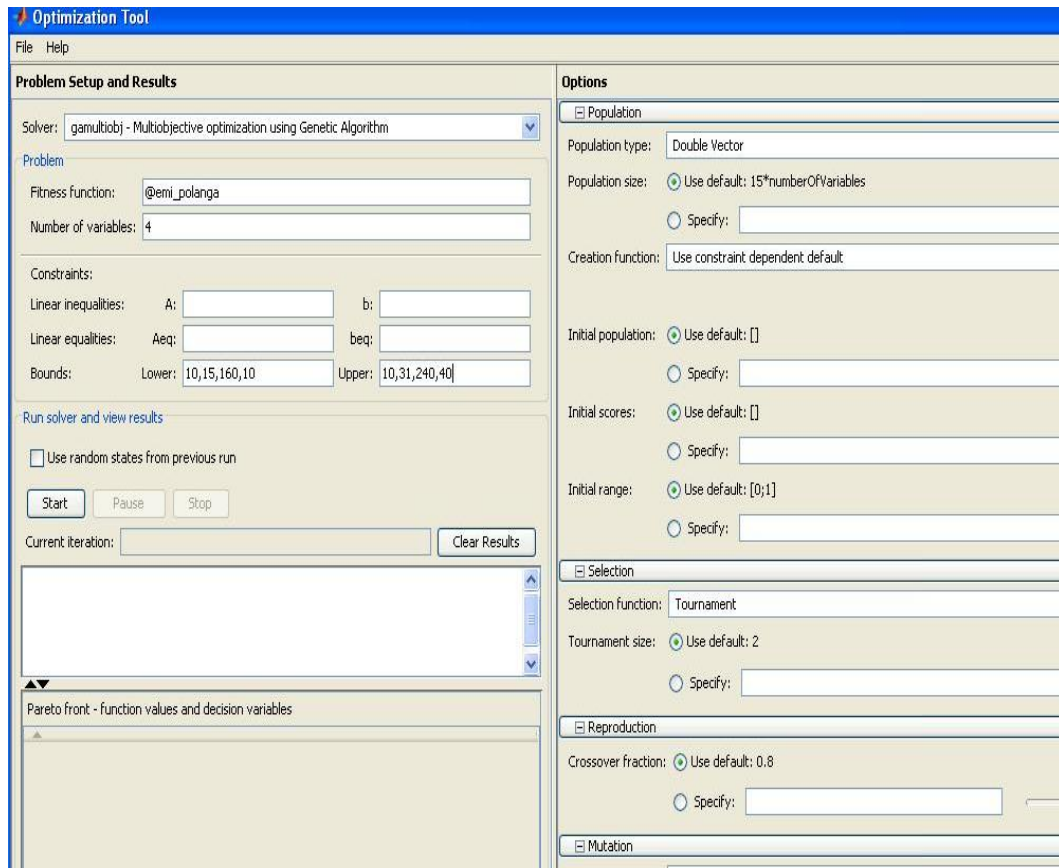


Fig. 4.31 Optimization tool problem definition screen

Figure 4.31 shows the screen indicating process of optimization of emission constituents. Figure 4.32 shows a display screen of the MATLAB program after optimization of engine emission parameters is carried out. The problem definition screen is where the solver, the fitness function and bounds are defined. The optimization is carried out considering full load condition and hence, both upper and lower bounds for load. The set bounds for the constraints are given in Table 4.14. The same are entered in the order of Load, IT, IP, Blend in the software.

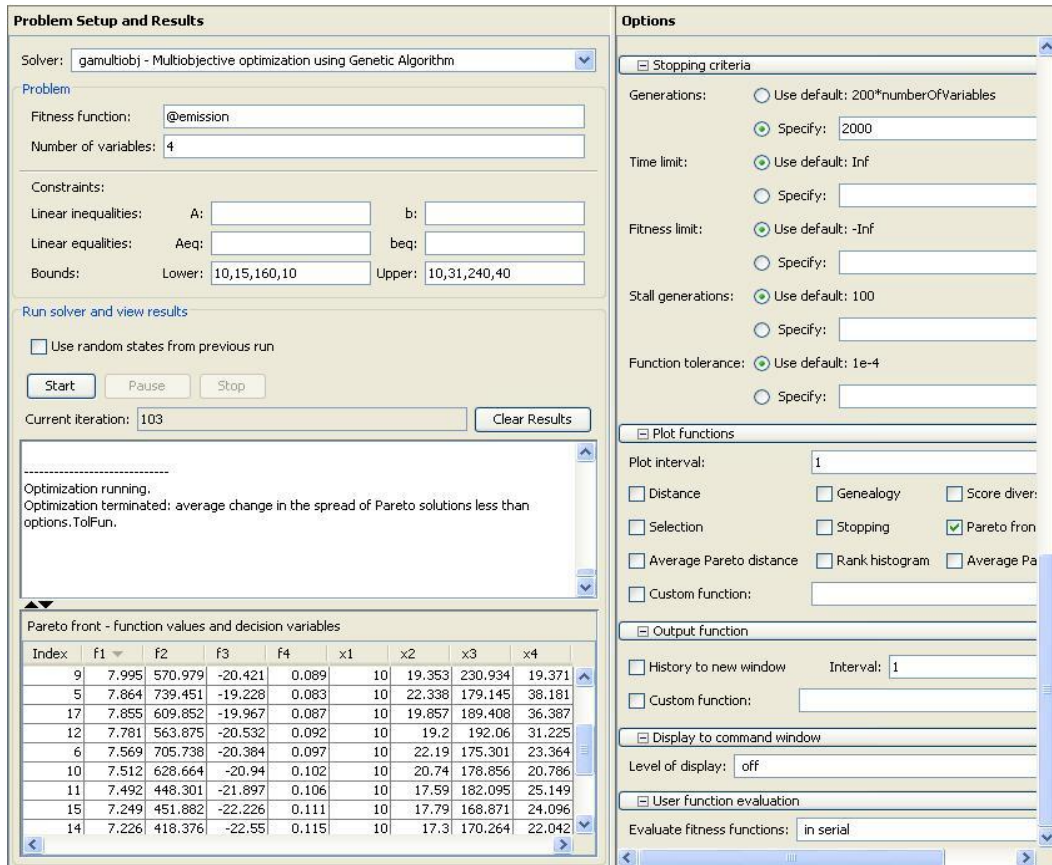


Fig. 4.32 MATLAB program showing optimization of engine emission

Figure 4.33 shows the Pareto front for optimization of emission constituents after the application of multi-objective optimization of emission constituents for maximisation of CO₂ emissions with minimisation of other emission constituents (HC, CO, NO_x, and smoke) for the diesel engine operating on different Polanga biodiesel and diesel blends at varying injection timings, injection pressures and full load. Objective 1 is maximisation of CO₂ and objective 2 is the minimisation of other emissions viz. UBHC, CO, NO_x and smoke. The Pareto front gives set of points corresponding to different values of objective 1 and objective 2. The point picked up by the software may lie between a value of 6.6 to 8.4 and 700 to 790 for objective 1 and objective 2 respectively.

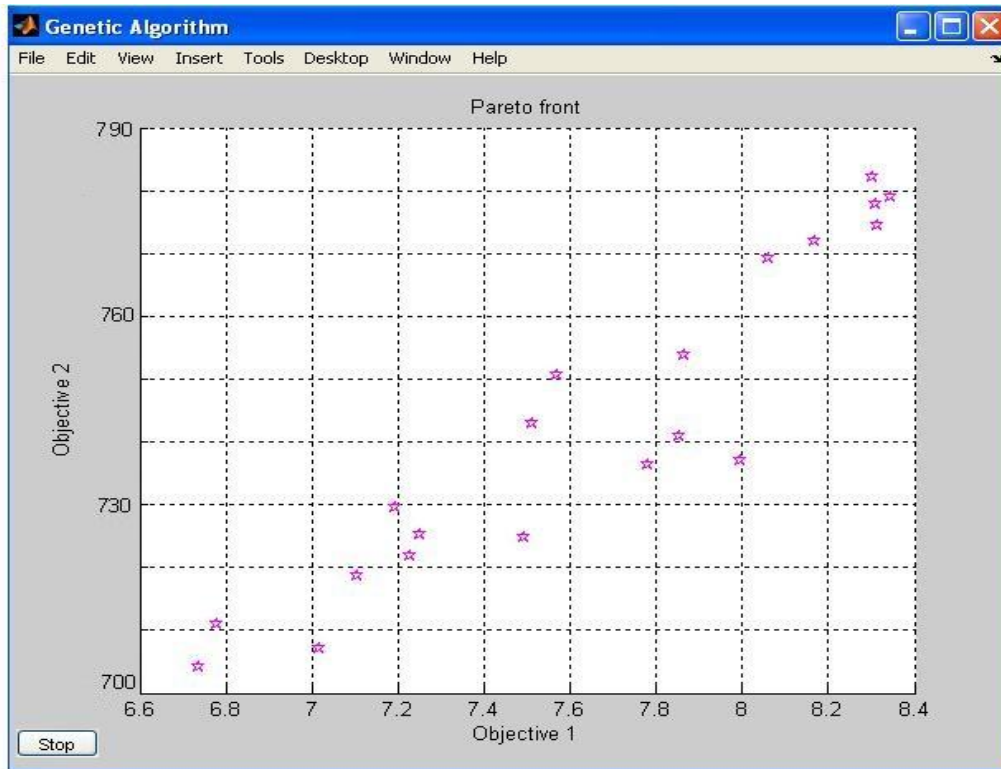


Fig. 4.33 Pareto front for optimization of emission constituents

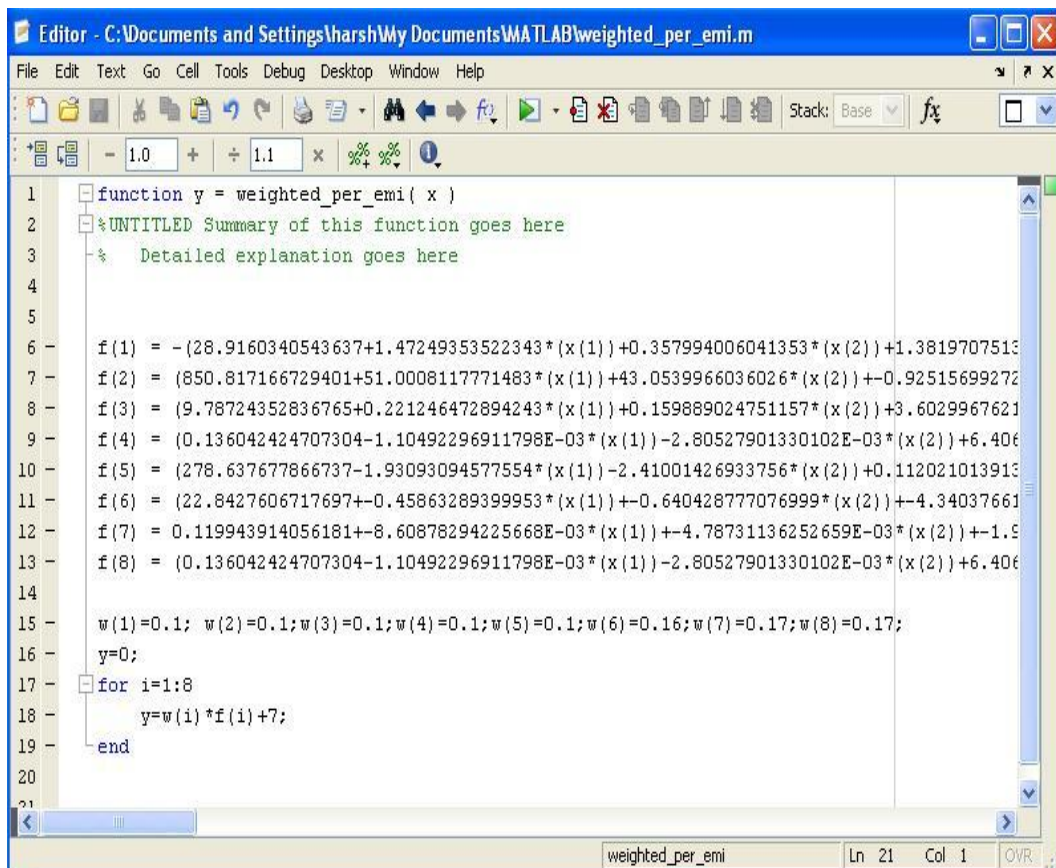
The optimal set of solution for the present case is shown in Table 4.18.

Table 4.18: Optimal set of solution for Engine Emission Parameters

S. No.	CO ₂ (% vol)	NOx ppm vol	HC ppm	CO (% vol)	x ₁ load(%)	x ₂ I.T(°bTDC)	x ₃ I.P(bars)	x ₄ blend(%)
1	7.99	570	20.4	0.089	100	19.35	230.9	19.37
2	7.86	739	19.2	0.082	100	22.33	179.1	38.18
3	7.85	609	19.9	0.087	100	19.85	189.4	36.38
4	7.78	563	20.5	0.092	100	19.19	192.06	31.22
5	7.56	705	20.3	0.096	100	22.18	175.31	23.36

4.6.3 THE MULTI-OBJECTIVE OPTIMIZATION ENGINE PERFORMANCE AND EMISSION CONSTITUENTS

The optimization of both engine performance and emission constituents is conducted by considering all the performance parameters and emission constituents considered in sections 4.6.1 and 4.6.2. The solution procedure is also the same as followed for engine performance optimization and emission constituents optimization. Weighted Multi-objective Optimization equations are developed for optimization as shown in MATLAB editor screen Figure 3.34.



```
1 function y = weighted_per_emi( x )
2 %UNTITLED Summary of this function goes here
3 % Detailed explanation goes here
4
5
6 f(1) = -(28.9160340543637+1.47249353522343*(x(1))+0.357994006041353*(x(2))+1.3819707513
7 f(2) = (850.817166729401+51.0008117771483*(x(1))+43.0539966036026*(x(2))+0.92515699272
8 f(3) = (9.78724352836765+0.221246472894243*(x(1))+0.159889024751157*(x(2))+3.6029967621
9 f(4) = (0.136042424707304-1.10492296911798E-03*(x(1))-2.80527901330102E-03*(x(2))+6.406
10 f(5) = (278.637677866737-1.93093094577554*(x(1))-2.41001426933756*(x(2))+0.112021013913
11 f(6) = (22.8427606717697+0.45863289399953*(x(1))+0.640428777076999*(x(2))+4.34037661
12 f(7) = 0.119943914056181+-8.60878294225668E-03*(x(1))+4.78731136252659E-03*(x(2))+1.9
13 f(8) = (0.136042424707304-1.10492296911798E-03*(x(1))-2.80527901330102E-03*(x(2))+6.406
14
15 w(1)=0.1; w(2)=0.1;w(3)=0.1;w(4)=0.1;w(5)=0.1;w(6)=0.16;w(7)=0.17;w(8)=0.17;
16 y=0;
17 for i=1:8
18     y=w(i)*f(i)+7;
19 end
20
21
```

Fig. 4.34 MATLAB editor

Figure 4.35 shows the Pareto front for optimization of both engine performance parameters and emission constituents giving equal weightages. Here,

objective 1 is maximisation of engine performance and objective 2 is the minimisation of exhaust emissions. The software uses a Pareto front to strike a balance between objective 1 and objective 2 and picks up a point to suggest the optimum values of input parameters such as IT, IP and blend. The point picked up by the software found to lie in a range of 0 to 5 and -4000 to -3000 for objective 1 and objective 2 respectively. The values of objective 1 and objective 2 are used to determine the optimum input parameters by the software by following a complex set of calculations.

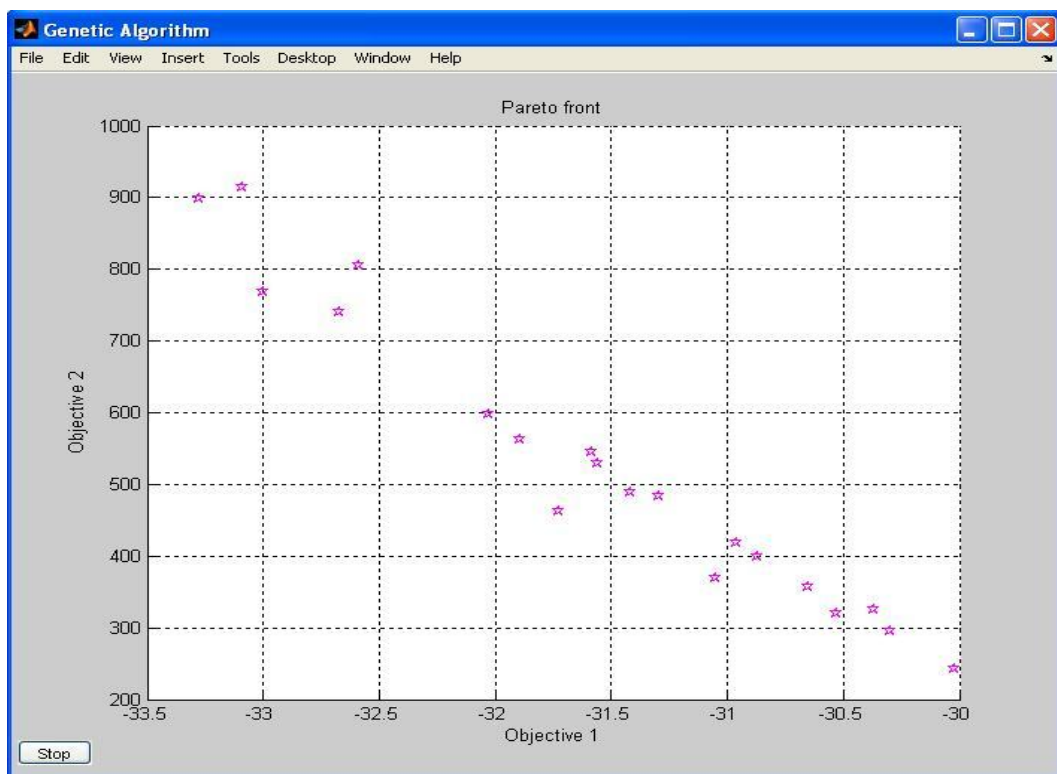


Fig. 4.35 Pareto front for optimization of both engine performance and emission

Here, objective 1 is maximisation of engine performance and objective 2 is the minimisation of exhaust emissions. The software uses a Pareto front to strike a balance between objective 1 and objective 2 and picks up a point to suggest the optimum values of input parameters. Figure 4.35 shows the Pareto front for optimization of both engine performance parameters and emission constituents giving

equal weightages. Here, objective 1 is maximisation of engine performance and objective 2 is the minimisation of exhaust emissions. The software uses a pareto front to strike a balance between objective1 and objective 2 and picks up a point to suggest the optimum values of input parameters such as IT, IP and blend. The point picked up by the software found to lie in a range of -30 to -33.5 and 200 to 1000 for objective 1 and objective 2 respectively. The values of objective 1 and objective 2 are used to determine the optimum input parameters by the software by following a complex set of calculations.

The multi-objective optimization carried out in the preceding section is conventional method. In such optimization equal preference is given to each individual parameter of both engine performance and exhaust emissions. But, usually, the purpose of an IC engine is to operate with maximum thermal efficiency and at considerably lesser emissions. Rarely there may be cases where emissions are of more importance than efficiency. Under all such cases, weighted optimization is to be carried out wherein suitable weights (preferences) are given to the engine performance parameters and emission constituents.

The weighted optimization is carried out using genetic algorithm solver and the procedure is similar to that for conventional optimization. The only difference is that weights are defined for all the equations of output parameters which are obtained by nonlinear regression analysis. Figure 3.34 shows the MATLAB editor which is used to define weights $w(1)$ to $w(8)$ for the equations $f(1)$ to $f(8)$. Table 4.19 gives a few combinations of the results of weighted optimization of engine performance and exhaust emissions.

Table 4.19: Optimal set of solution for different weightages Engine Parameters

S. No.	BTE (%)	NOx (ppm vol)	CO₂ (% vol)	x₁ load(%)	x₂ I.T(^obTDC)	x₃ I.P(bars)	x₄ blend(%)
1	33.27	899	8.17	100	25.32	235.1	31.35
2	33.09	913	8.10	100	26.10	225.5	24.99
3	33.00	767	8.08	100	22.65	229.2	26.89
4	32.67	740	7.84	100	22.56	194.1	25.24
5	32.58	806	7.74	100	24.33	182.1	21.22
6	32.02	598	7.63	100	20.00	184.2	26.42

It is seen that the weightage given to performance and exhaust emissions affect the values of ITs. The optimal solution when different weightages to performance and emission parameters is assigned is given by 25^obTDC fuel injection timing, 235 bar fuel injection pressure and B31 Polanga biodiesel blend.

CHAPTER 5

CONCLUSION

The experimental study is accomplished on a four stroke, single cylinder Kirloskar diesel engine using Polanga biodiesel and its blends with diesel. The thermal performance and emissions characteristics are evaluated by running the engine at different combinations of preset injection timings of 15, 19, 23, 27 and 31°bTDC and injection pressures of 160 bar, 180, 200, 220 bar and 240 bar and varying loads from no load to full load at a percentage increase of 20% in each step. The thermal performance parameters evaluated are BTE, BSFC and EGT while the emission constituents measured are CO, UHC, NO_x, CO₂ and Smoke. Further, for the optimization, genetic algorithm (GA) analysis is carried out selecting only BTE, BSFC and EGT as thermal performance parameters and CO, UHC, NO_x, CO₂ as emissions constituents. It should be noted that the two different studies conducted on thermal performance and emission constituents leads to prediction of each of them in isolation, although a unification of thermal performance and emission constituents is a possibility. However, it is difficult to strike an optimum combination of the possible maximum thermal performance and minimum emission constituents with respect to a combination of injection timing, injection pressure, bio-diesel blend when the engine operates at a preset load (at full load) using only the experimental data. Hence, a suitable technique of optimization is to be chosen to strike an optimum balance between the chosen four input parameters to predict the output parameters.

Thus, a computational study consisting of multi-objective optimization of thermal performance and emission characteristics using GA technique and modelling using ANN for the engine is carried out. The combination of optimization and modelling is intended to find the optimum combination of the three input parameters, viz, injection timing, injection pressure, load and blend and subsequently to predict the output parameters, viz. BTE, BSFC and EGT for thermal performance and CO, UHC, NO_x, CO₂ for emission constituents for the optimum combination of input parameters. The GA toolbox of MATLAB is used for the purpose of optimization. The ANN is modelled by using the selected results of the experimental study using MATLAB. The accuracy with which this neural network works is judged by comparing the outputs from the network with the experimental data. The output parameters can be determined from the optimized input parameters. Based on the experimental and computational studies, following are the important observations made and the conclusions drawn thereon.

1. A single cylinder, four stroke CI engine originally designed to operate on diesel as fuel may be operated on Polanga biodiesel blends without any system hardware modifications. Based on the experimental study, it can be concluded that with the increase in injection timing, the performance of diesel engine operated using a Polanga biodiesel blends approach to that operated using diesel oil. At higher injection timing and injection pressure, the thermal performance of Polanga biodiesel blend is closest to that of diesel oil compared to that operated at other injection timings. Higher injection pressure is preferable for Polanga biodiesel due to its higher viscosity.
2. The thermal performance evaluation, in isolation, indicates that the blend B20 operates closest to that of diesel oil whereas, the engine operated with any

higher injection timing, ranging from 27 to 31° bTDC, the emission constituents of CO, UHC, CO₂ and Smoke are the least and remains constant in the injection timing range of 27 to 31°bTDC. Both the above observations are made when the engine is operated with IP at 200 bar and at full load.

3. Polanga biodiesel blends give minimum harmful emissions as compared to all other blends. Further, at a higher injection timing of 31°bTDC and injection pressure of 240bar, the fairly reduced exhaust emissions are observed irrespective of the fuel blend used. Therefore, operating the diesel engine with Polanga biodiesel at a injection timings of 31°bTDC and injection pressure of 240 bar results in minimum emissions except NO_x emissions. If NO_x is also to be minimised, then the engine should be operated at the injection timing of 23°bTDC, which will result in a decrease in BTE of about 10% and an increase in BSFC of 11% which are not affordable just for the sake of reduced NO_x emissions.
4. ANN models have been developed to predict the performance and emission parameters. For training, different algorithms such as LM, GDM, SCG are tested. Multilayer feed forward network with back propagation training algorithm was found most suitable to predict the performance, emission and combustion features of a diesel engine at various injection timings and pressures. Logistic sigmoid, tangent sigmoid and linear transfer functions were used in the different network architectures. It was found that log sigmoid gives better results. The number of neurons in network layers is varied along with the layers. For performance model, two layer structure was sufficient to predict the results, whereas a three layer structure was found suitable for emission model.

5. The predicted R values were found to be very close to unity while the MSE error was less than 0.0004 for BSFC, BTE, EGT, CO, NO_x, CO₂ and UBHC and revealed that there was good correlation between the predicted and measured data. Analysis of the experimental data by the ANN revealed that there was good correlation between the predicted data resulted from the ANN and measured ones.
6. The percentage error for all the parameters lies in the range of 0.47 to 4.58%. The mean percentage error of Engine performance parameters BTE, BSFC and EGT are ± 1.85 , ± 2.35 and ± 2.57 %, respectively, also mean percentage error for Engine emission parameters UHC, NO_x, CO₂ and CO are ± 1.78 , ± 2.57 , ± 2.79 and ± 2.56 % respectively which is acceptable. The mean percentage error for variable injection timing is 2.39% and for variable injection pressure is 2.17%. The developed model thus reduces the experimental efforts and hence can serve as an effective tool for predicting the performance of the engine and emission characteristics under various operating conditions with different biodiesel blends.
7. From the large number of experimental data for thermal performance and emission constituents obtained for various input parameters such as load, injection timing, injection pressure and blends, picking up an optimum combination of the input parameters manually is not possible. The optimal solution for performance parameters is obtained by 24°bTDC, 233 bar fuel injection pressure and B27 biodiesel blend. For emission constituents, the optimal solution is obtained by 19°bTDC, 231 bar injection pressure and B19 biodiesel blend. The optimal solution when different weightages to

performance and emission parameters is assigned is given by 25°bTDC, 235 bar injection pressure and B31 biodiesel blend.

5.1 FUTURE SCOPE OF WORK

In the present work, ANN models have been developed for the performance and emission evaluation of the single cylinder CI engine using Polanga based biodiesel and its blends. The input parameters selected in the present work are; injection timing, injection pressure, and Polanga biodiesel blend. However, compression ratio of the engine may be an important parameter that influences the performance and emission evaluation. A study under varying compression ratio may be done to assess the performance and emission evaluation also multi-cylinder engine can be used for further investigation purpose. Further, an optimization of parameters viz., compression ratio, injection timing, injection pressure and Polanga biodiesel blend may be done.

REFERENCES

- [1]. A text book on “Energy its use and Environment” by Hinrichs and Kleinbach. Fifth edition, ISBN-13: 978-1-111-99083-1. Publisher – Cengage Learning Co. pp: 1-3.
- [2]. BPSR-2011.
- [3]. <http://maninair.in/gdp-growth-rate-india>. Data taken on 12.08.2014.
- [4]. Chauhan B.S, Kumar N, Jun Y.D, Lee K.B. Performance and emission study of preheated Jatropha oil on medium capacity diesel engine. Energy 35 (2010), pp: 2484-2492.
- [5]. <http://data.worldbank.org>. Data taken on 15.09.2014.
- [6]. International energy agency annual survey conducted in the financial year 2009-2010..http://www.iea.org/stats/pdf_graphs/INTPESPI.pdf
- [7]. Basic Statistics on Indian Petroleum & Natural Gas, 2009-10. Ministry of Petroleum & Natural Gas, Government of India, New Delhi, Economic Division.
- [8]. Basic Statistics on Indian Petroleum & Natural Gas, 2010-11. Ministry of Petroleum & Natural Gas, Government of India, New Delhi, Economic Division.
- [9]. Gill S.S, Tsolakis A, Dearn K.D, Fernandez R.J. Combustion characteristics and emissions of Fischer Tropsch diesel fuels in IC engines. Progress in Energy and Combustion Science 37 (2011), pp: 503-523.
- [10]. OECD Key environmental indicators 2008. OECD Environmental Directorate, Paris, France.
- [11]. Wang L, Yu H. Biodiesel from Siberian apricot (*Prunussibirica* L.) seed

- kernel oil. *Bioresource Technology* 112 (2012) 355–358.
- [12]. Agarwal A.K. Bio-fuels (alcohols and biodiesel) applications as fuels for internal combustion engines. *Prog Energy Combust* 2007;33:233-71.
- [13]. Chauhan B.S, Kumar N, Cho H.M. Performance and emission studies on an agriculture engine on neat *Jatropha* oil. *Journal of Mechanical Science and Technology* 24 (2) (2010), pp: 529-535.
- [14]. Chauhan B.S, Kumar N, Pal S.S, Jun Y.D. Experimental studies on fumigation of ethanol in a small capacity diesel engine. *Energy* 2011; 36:1030-8.
- [15]. Mishra R.D, Murthy M.S. Straight vegetable oils usage in a compression ignition engine—A review. *Renewable and Sustainable Energy Reviews* 14 (2010) 3005–3013.
- [16]. Achten W.M.J, Verchot L, Franken Y.J, Mathijs E, Singh V.P, Aerts R. *Jatropha* bio-diesel production and use. *Biomass Bioenergy* (2008). 32 1063–84
- [17]. Lin L, Ying D, Chaitep S, Vittayapadung S. Biodiesel production from crude rice bran oil and properties as fuel. *Applied Energy* 86 (2009) 681–688.
- [18]. Barnwal B. K, Sharma M. P. Prospects of biodiesel production from vegetable oils in India; *Renewable and Sustainable Energy Reviews* (2005), Vol.9, pp.363–378.
- [19]. <http://planningcommission.nic.in/plans/planrel/fiveyr/welcome.html>. Data taken on 27.06.2014.
- [20]. <http://mofpi.nic.in/ContentPage.aspx?CategoryId=687>. Data taken on 27.06.2013.

- [21]. <http://www.bioenergyconsult.com/tag/national-biodiesel-mission/>. Data taken on 21.08.2014.
- [22]. <http://www.jatrophabiodiesel.org/indianPrograms.php>. Data taken on 27.06.2013.
- [23]. http://mnre.gov.in/file-manager/UserFiles/biofuel_policy.pdf. Data taken on 27.06.2013.
- [24]. Friday J.B, Okano, D. Agro species profiles for Pacific Island - forestry.2006, ver. 2.1.
- [25]. Azam M.M, WarisA, Nahar N.M. Prospects and potential of fatty acid methyl esters of some non-traditional seed oils for use as biodiesel in India. *Biomass and Bio-energy* (2005);29(4):293–302.
- [26]. Pinzi S, Garcia I.L, Gimenez F.J.L, Castro M.D.L, Dorado G, Dorado M.P. The ideal vegetable oil-based biodiesel composition: a review of social, economic and technical implications. *Energy & Fuels* (2009); 23:2325–41.
- [27]. Kumar A, Sharma S. Potential non-edible oil resources as biodiesel feedstock: an Indian perspective. *Renewable and Sustainable Energy Reviews* (2011); 15(4):1791–800.
- [28]. Venkanna B.K, Venkataramana R.C. Biodiesel production and optimization from *Calophyllum Inophyllum* Linn oil (hone oil) — a three stage method. *Bio-resource Technology* (2009) ;100(21):5122–5.
- [29]. No S.Y. Inedible vegetable oils and their derivatives for alternative diesel fuels in CI engines: a review. *Renewable and Sustainable Energy Reviews* (2011) ;15(1):131–49.
- [30]. Atabani A.E, Silitonga A.S, Ong H.C, Mahlia T.M.I, Masjuki H.H, Badruddin I.A, Fayaz H. Non-edible vegetable oils: A critical evaluation of

- oil extraction, fattyacid compositions, biodiesel production, characteristics, engine performance and emissions production". Renewable and Sustainable Energy Reviews 18 (2013) 211–245.
- [31]. M.T. Hagan, H.B. Demuth, M. Beale, 1995, Neural Network Design, PWS Publishing Company, Boston.
- [32]. S. Haykin, Neural Networks, 1994, A comprehensive foundation, McMillian College Publishing Company, New York.
- [33]. I.A. Basheer, M. Hajmeer, 2000, Artificial neural networks: fundamentals, computing, design, J. Microbiol. Methods, 43, 3–31.
- [34]. Prieto, M. M., Montanes, E. and Menendez, O.. Power plant condenser performance forecasting using an on fully connected ANN. Energy 26, (2001) 65–79.
- [35]. Arcakliođlu, E., Erisen, A. and Yilmaz, R. Artificial neural network analysis of heat pumps using refrigerant mixtures. Energy Conversion and Management 45, (2004), 1917–1929.
- [36]. Hosoz, M. and Ertunc, H. M. Artificial neuralnetwork analysis of an automobile air conditioningsystem. Energy Conversion and Management 47, (2006), 1574–1587.
- [37]. Benjumea P, Agudelo J, Agudelo A. Basic properties of palm oil biodiesel–diesel blends. Fuel 87 (2008) 2069–2075.
- [38]. Sahoo P.K, Das L.M. Process optimization for biodiesel production from Jatropha, Karanja and Polanga oils. Fuel 88 (2009) 1588–1594.
- [39]. Chakraborty M, Baruah D.C, Konwer D. Investigation of terminalia (Terminalia belerica Robx.) seed oil as prospective biodiesel source for North-East India. Fuel Processing Technology 90 (2009) 1435–1441.

- [40]. Kaya C, Hamamci C, Baysal A, Akba O, Erdogan S, Saydut A. Methyl ester of peanut (*Arachis hypogea* L.) seed oil as a potential feedstock for biodiesel production. *Renewable Energy* 34 (2009) 1257–1260.
- [41]. Chen Y.H, Chen J.H, Chang C.Y, Chang C.C. Biodiesel production from tung (*Vernicia montana*) oil and its blending properties in different fatty acid compositions. *Bioresource Technology* 101 (2010) 9521–9526.
- [42]. Lee H.V, Yunus R, Juan J.C, Taufiq-Yap Y.H. Process optimization design for jatropha-based biodiesel production using response surface methodology. *Fuel Processing Technology* 92 (2011) 2420–2428.
- [43]. Omar W.N.N.W, Amin N.A.S. Optimization of heterogeneous biodiesel production from waste cooking palm oil via response surface methodology. *Biomass and bio-energy* 35(2011)1329-1338.
- [44]. Wu X, Leung D.Y.C. Optimization of biodiesel production from camelina oil using orthogonal experiment. *Applied Energy* 88 (2011) 3615–3624.
- [45]. Atadashi I.M, Aroua M.K, Abdul Aziz A.R, Sulaiman N.M.N. Production of biodiesel using high free fatty acid feedstocks. *Renewable and Sustainable Energy Reviews* 16 (2012) 3275– 3285.
- [46]. Wang R, Zhou W, Hanna M.A, Zhang Y.P, Bhadury P.S, Wang Y, Song B, Yang S. Biodiesel preparation, optimization, and fuel properties from non-edible feedstock, *Datura stramonium*. *Fuel* 91 (2012) 182–186.
- [47]. Ilham Z, Saka S. Optimization of supercritical dimethyl carbonates method for biodiesel production. *Fuel* 97 (2012) 670–677.
- [48]. Yücel Y. Optimization of biocatalytic biodiesel production from pomace oil using response surface methodology. *Fuel Processing Technology* 99 (2012) 97–102.

- [49]. Uzun B.B, Kılıç M, Özbay N, Pütün A.E, Pütün E. Biodiesel production from waste frying oils: Optimization of reaction parameters and determination of fuel properties. *Energy* 44 (2012) 347-351.
- [50]. Silitonga A.S, Ong H.C, Mahlia T.M.I, Masjuki H.H, Chong W.T. Characterization and production of *Ceiba pentandra* biodiesel and its blends. *Fuel* 108 (2013) 855–858.
- [51]. Chammoun N, Geller D.P, Das K.C. Fuel properties, performance testing and economic feasibility of *Raphanus sativus*(oilseed radish) biodiesel. *Industrial Crops and Products* 45 (2013) 155– 159.
- [52]. Atapour M, Kariminia H.R, Moslehabadi P.M. Optimization of biodiesel production by alkali-catalysed transesterification of used frying oil. *Process Safety and Environmental Protection* x x x (2 0 1 3) xxx–xxx. PSEP-338.
- [53]. Kılıç M, Uzun B.B, Pütün E,Pütün A.E. Optimization of biodiesel production from castor oil using factorial design. *Fuel Processing Technology* 111 (2013) 105–110.
- [54]. Yun H, Wang M, Feng W, Tan T. Process simulation and energy optimization of the enzyme-catalysed biodiesel production. *Energy* 54 (2013) 84-96.
- [55]. Hwai Chyuan Ong , H.H. Masjuki, T.M.I. Mahlia, A.S. Silitonga, W.T. Chong, K.Y. Leong. Optimization of biodiesel production and engine performance from high free fatty acid *Calophyllum inophyllum* oil in CI diesel engine. *Energy Conversion and Management* 81 (2014) 30–40.
- [56]. Rehman H, Phadatare A.G. Diesel engine emissions and performance from blends of karanja methyl ester and diesel. *Biomass and Bio-energy* 27 (2004) 393 – 397.

- [57]. Sahoo P.K, Das L.M, Babu M.K.G, Naik S.N. Biodiesel development from high acid value polanga seed oil and performance evaluation in a CI engine. *Fuel* 86 (2007) 448– 454.
- [58]. Raheman H, Ghadge S.V. Performance of compression ignition engine with mahua (*Madhuca indica*) biodiesel. *Fuel* 86 (2007) 2568–2573.
- [59]. Lapuerta M, Jose O.A, Ferná'ndez R. Effect of biodiesel fuels on diesel engine emissions. *Progress in Energy and Combustion Science* 34 (2008) 198–223.
- [60]. Nabi M.N, Hoque S.M.N, Akhter M.S. Karanja (*Pongamia Pinnata*) biodiesel production in Bangladesh, characterization of karanja biodiesel and its effect on diesel emissions. *Fuel Processing Technology* 90 (2009) 1080–1086.
- [61]. Sukumar Puan, R. Jegan, K. Balasubbramanian, G. Nagarajan. Effect of injection pressure on performance, emission and combustion characteristics of high linolenic linseed oil methyl ester in a DI diesel engine. *Renewable Energy* 34 (2009) 1227–1233.
- [62]. Cenk Sayin , Murat Ilhan, Mustafa Canakci, Metin Gumus. Effect of injection timing on the exhaust emissions of a diesel engine using diesel–methanol blends. *Renewable Energy* 34 (2009) 1261–1269.
- [63]. B. Baiju, M.K. Naik, L.M. Das. A comparative evaluation of compression ignition engine characteristics using methyl and ethyl esters of Karanja oil. *Renewable Energy* 34 (2009) 1616–1621.
- [64]. Bajpai S, Sahoo P.K, Das L.M. Feasibility of blending karanja vegetable oil in petro-diesel and utilization in a direct injection diesel engine. *Fuel* 88 (2009) 705–711.

- [65]. P.K. Sahoo, L.M. Das, M.K.G. Babu, P. Arora, V.P. Singh, N.R. Kumar, T.S. Varyani. Comparative evaluation of performance and emission characteristics of jatropha, karanja and polanga based biodiesel as fuel in a tractor engine. *Fuel* 88 (2009) 1698–1707.
- [66]. Canakci M, Ozsezen A.N. Arcaklioglu E. Erdil A. Prediction of performance and exhaust emissions of a diesel engine fuelled with biodiesel produced from waste frying palm oil. *Expert Systems with Applications* 36 (2009) 9268–9280.
- [67]. Godiganur S, Murthy C.H.S, Reddy R.P. 6BTA 5.9 G2-1 Cummins engine performance and emission tests using methyl ester mahua (*Madhuca indica*) oil/diesel blends. *Renewable Energy* 34 (2009) 2172–2177.
- [68]. Qi D.H. Chen H, Geng L.M. Bian Y.Z, Liu J, Ren X.C.H. Combustion and performance evaluation of a diesel engine fuelled with biodiesel produced from soybean crude oil. *Renewable Energy* 34 (2009) 2706–2713.
- [69]. Sahoo P.K, Das L.M. Combustion analysis of Jatropha, Karanja and Polanga based biodiesel as fuel in a diesel engine. *Fuel* 88 (2009) 994–999.
- [70]. Buyukkaya E. Effects of biodiesel on a DI diesel engine performance, emission and combustion characteristics. *Fuel* 89 (2010) 3099–3105.
- [71]. Qi D.H. Chen H, Geng L.M. Bian Y.Z. Experimental studies on the combustion characteristics and performance of a direct injection engine fuelled with biodiesel/diesel blends. *Energy Conversion and Management* 51 (2010) 2985–2992.
- [72]. G.R. Kannan, R. Anand. Experimental evaluation of DI diesel engine operating with diestrol at varying injection pressure and injection timing. *Fuel Processing Technology* 92 (2011) 2252–2263.

- [73]. Ganapathy T, Gakkhar R.P, Murugesan K. Influence of injection timing on performance, combustion and emission characteristics of Jatropha biodiesel engine. *Applied Energy* 88 (2011) 4376–4386.
- [74]. Muralidharan K, Vasudevan D, Sheeba K.N. Performance, emission and combustion characteristics of biodiesel fuelled variable compression ratio engine. *Energy* 36 (2011) 5385-5393.
- [75]. Cenk Sayin, Metin Gumus, Mustafa Canakci. Effect of fuel injection pressure on the injection, combustion and performance characteristics of a DI diesel engine fuelled with canola oil methyl esters-diesel fuel blends. *Biomass and Bioenergy* 46 (2012) 435-446.
- [76]. Chauhan B.S, Kumar N, Cho H.M. A study on the performance and emission of a diesel engine fuelled with Jatropha biodiesel oil and its blends. *Energy* 37 (2012) 616-622.
- [77]. Dhar A, Kevin R, Agarwal A.K. Production of biodiesel from high-FFA neem oil and its performance, emission and combustion characterization in a single cylinder DIC engine. *Fuel Processing Technology* 97 (2012) 118–129.
- [78]. Özener O, Yüksek L, Ergenç A.T, Özkan M. Effects of soybean biodiesel on a DI diesel engine performance, emission and combustion characteristics. *Fuel* xxx (2012) xxx–xxx.
- [79]. Selvam D.J.P, Vadivel K. Performance and emission analysis of DI diesel engine fuelled with methyl esters of beef tallow and diesel blends. *International Conference on Modelling Optimization and Computing- (ICMOC-2012)*. *Procedia Engineering* 38; (2012); 342 – 358.
- [80]. Ahmet Murcak, Can Haimođlu, Ismet Çevik, Murat Karabektas, Gökhan

- Ergen. Effects of ethanol–diesel blends to performance of a DI diesel engine for different injection timings. *Fuel* 109 (2013) 582–587.
- [81]. Sivalakshmi S, Balusamy T. Effect of biodiesel and its blends with diethyl ether on the combustion, performance and emissions from a diesel engine. *Fuel* 106 (2013) 106–110.
- [82]. Shehata M.S. Emissions, performance and cylinder pressure of diesel engine fuelled by biodiesel fuel. *Fuel* xxx(2013)xxx–xxx.
- [83]. Mofijur M, Masjuki H.H, Kalam M.A, Atabani A.E. Evaluation of biodiesel blending, engine performance and emissions characteristics of *Jatropha curcas* methyl ester: Malaysian perspective. *Energy* 55 (2013) 879-887.
- [84]. Chen L.Y, Chen Y.H, Hung Y.S, Chiang T.H, Tsai C.H. Fuel properties and combustion characteristics of *jatropha* oil biodiesel–diesel blends. *Journal of the Taiwan Institute of Chemical Engineers* 44 (2013) 214–220.
- [85]. Chauhan B.S, Kumar N, Cho H.M, Lim H.C. A study on the performance and emission of a diesel engine fuelled with *Karanja* biodiesel and its blends. *Energy* 56 (2013) 1-7.
- [86]. Liaquat A.M, Masjuki H.H, Kalam M.A, Fattah I.A.R, Hazrat M.A, Varman M, Mofijur M, Shahabuddin M. Effect of coconut biodiesel blended fuels on engine performance and emission characteristics. 5th BSME International Conference on Thermal Engineering. *Procedia Engineering* 56 (2013) 583 – 590.
- [87]. Ozer Can. Combustion characteristics, performance and exhaust emissions of a diesel engine fueled with a waste cooking oil biodiesel mixture. *Energy Conversion and Management* 87 (2014) 676–686.

- [88]. Gvidonas Labeckas, Stasys Slavinskas, Marius Maz̄eika. The effect of ethanol diesel biodiesel blends on combustion, performance and emissions of a direct injection diesel engine. *Energy Conversion and Management* 79 (2014) 698–720.
- [89]. I.M. Rizwanul Fattah, H.H. Masjuki, M.A. Kalam, M.A. Wakil, A.M. Ashraful, S.A. Shahir. Experimental investigation of performance and regulated emissions of a diesel engine with *Calophyllum inophyllum* biodiesel blends accompanied by oxidation inhibitors. *Energy Conversion and Management* 83 (2014) 232–240.
- [90]. S.M. Ashrafur Rahman, H.H. Masjuki, M.A. Kalam, A.Sanjid, M.J.Abedin. Assessment of emission and performance of compression ignition engine with varying injection timing. *Renewable and Sustainable Energy Reviews* 35 (2014) 221–230.
- [91]. Hwai Chyuan Ong, H.H. Masjuki, T.M.I. Mahlia, A.S. Silitonga, W.T. Chong, Talal Yusaf . Engine performance and emissions using *Jatropha curcas*, *Ceibapentandra* and *Calophyllum inophyllum* biodiesel in a CI diesel engine. *Energy* xxx (2014) 1-19.
- [92]. Erol Arcaklioglu, Ismet Celikten. A diesel engine performance and exhaust emission. *Applied Energy* 80 (2005) 11–22.
- [93]. Mustafa Canakci, Ahmet Erdil, Erol Arcakliog̃lu. Performance and exhaust emissions of a biodiesel engine . *Applied Energy* 83 (2006) 594–605.
- [94]. B. Ghobadian, , H. Rahimi, A.M. Nikbakht, G. Najafi, T.F. Yusaf. Diesel engine performance and exhaust emission analysis using waste cooking biodiesel fuel with an artificial neural network. *Renewable Energy* 34

(2009) 976–982.

- [95]. Mustafa Canakci, Ahmet Necati Ozsezen, Erol Arcaklioglu, Ahmet Erdil. Prediction of performance and exhaust emissions of a diesel engine fueled with biodiesel produced from waste frying palm oil. *Expert Systems with Applications* 36 (2009) 9268–9280.
- [96]. G. Najafi, B. Ghobadian, T. Tavakoli, D.R. Buttsworth, T.F. Yusaf, M. Faizollahnejad. Performance and exhaust emissions of a gasoline engine with ethanol blended gasoline fuels using artificial neural network. *Applied Energy* 86 (2009) 630–639.
- [97]. R.Manjunatha, P. Badari Narayana. Application of Artificial Neural Networks for Emission Modelling of Biodiesels for a C.I Engine under Varying Operating Condition. *Modern Applied Science* Vol.4, no. 3 March 2010.
- [98]. Shivakumar, P. Srinivasa Pai, B.R. Shrinivasa Rao. Artificial Neural Network based prediction of performance and emission characteristics of a variable compression ratio CI engine using WCO as a biodiesel at different injection timings. *Applied Energy* 88 (2011) 2344–2354.
- [99]. Yusuf Çay, Adem Çiçek, Fuat Kara, Selami Sagiroglu. Prediction of engine performance for an alternative fuel using artificial neural network. *Applied Thermal Engineering* 37 (2012) 217-225.
- [100]. Ismail H.M, Hoon Kiat N, Cheen Wei Queck, Suyin Gan. Artificial neural networks modelling of engine-out responses for a light-duty diesel engine fuelled with biodiesel blends. *Applied Energy* 92 (2012) 769–777.
- [101]. H. Sharon, R. Jayaprakash, M. Karthigai selvan, D.R. Soban kumar, A. Sundaresan, K. Karuppasamy. Biodiesel production and prediction of

- engine performance using SIMULINK model of trained neural network. Fuel 99 (2012) 197–203.
- [102]. M. H. Shojaeefard, M. M. Etghani, M. Tahani, M. Akbari. Artificial Neural Network Based Multi-Objective Evolutionary Optimization of a Heavy-Duty Diesel Engine. International Journal of Automotive Engineering Vol. 2, Number 4, Oct 2012.
- [103]. Thomas Renald C.J, Somasundaram P. Experimental Investigation on Attenuation of Emission with Optimized LPG Jet Induction in a Dual Fuel Diesel Engine and Prediction by ANN Model. Energy Procedia 14 (2012) 1427 – 1438.
- [104]. Vinay Kumar. D, Ravi Kumar. P, M.Santosha Kumari. Prediction of Performance and Emissions of a Biodiesel Fueled Lanthanum Zirconate Coated Direct Injection Diesel engine using Artificial Neural Networks. Procedure Engineering 64 (2013) 993–1002.
- [105]. Yusuf Cay. Prediction of a gasoline engine performance with artificial neural network. Fuel xxx (2013) xxx–xxx.
- [106]. Shiva Kumar, Srinivas Pai P and Shrinivasa Rao B. R. Influence of injection timings on performance and emissions of a biodiesel engine operated on blends of Honge methyl ester and prediction using artificial neural network. Journal of Mechanical Engineering Research Vol. 5 (1), pp. 5-20, January 2013.
- [107]. Tushar M Patel. Artificial Neural Network Based Prediction of Performance Characteristic of Single Cylinder Diesel Engine for Pyrolysis Oil and Diesel Blend. The International Journal of Computer Science & Applications (TIJCSA) Volume 2, No. 03, May 2013 ISSN – 2278-1080.

- [108]. Kannan, K. R. Balasubramanian and R. Anand. Artificial neural network approach to study the effect of injection pressure and timing on diesel engine performance fueled with biodiesel. *International Journal of Automotive Technology*, Vol. 14, No. 4 (2013), pp. 507-519.
- [109]. Sumit Roy, Rahul Banerjee, Probir Kumar Bose. Performance and exhaust emissions prediction of a CRDI assisted single cylinder diesel engine coupled with EGR using artificial neural network. *Applied Energy* 119 (2014) 330–340.
- [110]. Sumit Roy, Rahul Banerjee, Ajoy Kumar Das, Probir Kumar Bose. Development of an ANN based system identification tool to estimate the performance-emission characteristics of a CRDI assisted CNG dual fuel diesel engine. *Journal of Natural Gas Science and Engineering* 21 (2014) 147-158.
- [111]. Kamyar Nikzadfar, Amir H. Shamekhi. Investigating the relative contribution of operational parameters on performance and emissions of a common-rail diesel engine using neural network. *Fuel* 125 (2014) 116–128.

APPENDIX

Table A 4.1 Normalized data for Variable Injection Timing

IT	Blend	Load	BSFC	BTE	BMEP	EGT	CO	UHC	CO ₂	NOx	Smoke
0.1	0.1	0.1	0.85294	0.11081	0.13593	0.19137	0.59333	0.74066	0.15714	0.10366	0.28105
0.1	0.1	0.3	0.38235	0.41256	0.35563	0.33048	0.42	0.69419	0.31429	0.12634	0.56737
0.1	0.1	0.5	0.26471	0.56668	0.5129	0.50042	0.37333	0.59129	0.48571	0.1695	0.77368
0.1	0.1	0.7	0.19412	0.68119	0.70177	0.68974	0.44667	0.41535	0.71429	0.21998	0.86211
0.1	0.1	0.9	0.14706	0.75826	0.71637	0.80933	0.63333	0.21286	0.9	0.27412	0.89368
0.1	0.36667	0.1	0.80588	0.15073	0.10223	0.18069	0.56667	0.89668	0.14286	0.10512	0.29579
0.1	0.36667	0.3	0.35882	0.45341	0.3514	0.33135	0.46	0.67095	0.3	0.12451	0.54211
0.1	0.36667	0.5	0.24118	0.60692	0.53776	0.49741	0.38	0.57469	0.47143	0.16292	0.74316
0.1	0.36667	0.7	0.17059	0.72328	0.71406	0.69665	0.53333	0.40207	0.65714	0.22035	0.85263
0.1	0.36667	0.9	0.14706	0.78332	0.85447	0.9	0.9	0.2029	0.87143	0.27888	0.87474
0.1	0.63333	0.1	0.82941	0.13588	0.17658	0.18067	0.57333	0.65768	0.14286	0.10293	0.33263
0.1	0.63333	0.3	0.38235	0.46177	0.2775	0.34959	0.48	0.63444	0.3	0.12305	0.55368
0.1	0.63333	0.5	0.26471	0.58587	0.52131	0.52706	0.38	0.47842	0.47143	0.16548	0.76737
0.1	0.63333	0.7	0.17059	0.75114	0.58601	0.64399	0.45333	0.39876	0.68571	0.21559	0.84842
0.1	0.63333	0.9	0.14706	0.79973	0.73976	0.80604	0.7	0.17967	0.9	0.27997	0.87684
0.1	0.9	0.1	0.9	0.13124	0.17704	0.1866	0.58667	0.57801	0.14286	0.1	0.43579
0.1	0.9	0.3	0.40588	0.44753	0.27571	0.31226	0.43333	0.63776	0.28571	0.12414	0.59474
0.1	0.9	0.5	0.26471	0.61342	0.52539	0.48712	0.36667	0.36556	0.44286	0.1717	0.80316
0.1	0.9	0.7	0.17059	0.76414	0.58009	0.66182	0.44667	0.30581	0.65714	0.21962	0.87158
0.1	0.9	0.9	0.14706	0.81365	0.89347	0.8464	0.7	0.15643	0.88571	0.29643	0.9
0.3	0.1	0.1	0.73529	0.11483	0.18986	0.12151	0.54	0.72407	0.11429	0.11902	0.17474
0.3	0.1	0.3	0.31176	0.40451	0.28067	0.29807	0.38667	0.67427	0.27143	0.1556	0.46
0.3	0.1	0.5	0.19412	0.58618	0.44275	0.44502	0.30667	0.57469	0.42857	0.22254	0.60632
0.3	0.1	0.7	0.14706	0.66015	0.67398	0.61647	0.36667	0.40871	0.61429	0.32533	0.76316
0.3	0.1	0.9	0.12353	0.714	0.87398	0.77813	0.56667	0.19959	0.8	0.45409	0.84526
0.3	0.36667	0.1	0.71176	0.18261	0.18996	0.12662	0.5	0.89004	0.11429	0.11866	0.17053
0.3	0.36667	0.3	0.31176	0.48745	0.35725	0.24908	0.38	0.65768	0.25714	0.15853	0.41579
0.3	0.36667	0.5	0.21765	0.67562	0.52281	0.40583	0.3	0.55809	0.41429	0.23132	0.59474
0.3	0.36667	0.7	0.12353	0.78673	0.68885	0.57239	0.46	0.39212	0.58571	0.33484	0.76316
0.3	0.36667	0.9	0.12353	0.81087	0.88885	0.73404	0.83333	0.19295	0.8	0.45007	0.81579
0.3	0.63333	0.1	0.66471	0.21604	0.16914	0.12257	0.51333	0.64108	0.11429	0.11902	0.19474
0.3	0.63333	0.3	0.31176	0.52274	0.33941	0.25129	0.36667	0.62448	0.25714	0.15743	0.37474
0.3	0.63333	0.5	0.19412	0.67593	0.52149	0.43033	0.32	0.45851	0.42857	0.22876	0.63684

0.3	0.63333	0.7	0.12353	0.81644	0.59071	0.58778	0.36667	0.37552	0.62857	0.31728	0.77368
0.3	0.63333	0.9	0.1	0.9	0.7342	0.74888	0.63333	0.16639	0.82857	0.44934	0.84
0.3	0.9	0.1	0.71176	0.20768	0.19219	0.12527	0.5	0.55809	0.11429	0.11866	0.24737
0.3	0.9	0.3	0.31176	0.53295	0.27844	0.26378	0.40667	0.60788	0.27143	0.15524	0.43684
0.3	0.9	0.5	0.19412	0.70905	0.52156	0.41073	0.32667	0.34232	0.44286	0.22327	0.65789
0.3	0.9	0.7	0.14706	0.82634	0.68067	0.58708	0.38667	0.29253	0.58571	0.33118	0.78421
0.3	0.9	0.9	0.12353	0.85543	0.85613	0.75909	0.63333	0.14315	0.85714	0.46982	0.83684
0.5	0.1	0.1	0.9	0.1	0.1789	0.14482	0.3	0.68091	0.15714	0.15706	0.27895
0.5	0.1	0.3	0.38235	0.41813	0.34788	0.26356	0.16667	0.63112	0.3	0.21779	0.54316
0.5	0.1	0.5	0.24118	0.59392	0.52188	0.40242	0.1	0.53154	0.47143	0.35935	0.67895
0.5	0.1	0.7	0.17869	0.6911	0.69552	0.56059	0.16667	0.36556	0.62857	0.51555	0.78316
0.5	0.1	0.9	0.14706	0.75176	0.71151	0.79384	0.36667	0.15643	0.87143	0.74234	0.84105
0.5	0.36667	0.1	0.77928	0.17302	0.17939	0.10604	0.3	0.84689	0.12857	0.14792	0.23789
0.5	0.36667	0.3	0.33529	0.48312	0.27885	0.24908	0.16667	0.61452	0.27143	0.21267	0.42632
0.5	0.36667	0.5	0.21765	0.662	0.51288	0.38472	0.1	0.51494	0.42857	0.33594	0.68632
0.5	0.36667	0.7	0.14873	0.78142	0.73348	0.56259	0.23333	0.34896	0.6	0.50201	0.80526
0.5	0.36667	0.9	0.12353	0.85203	0.89824	0.72196	0.63333	0.14979	0.81429	0.69991	0.86105
0.5	0.63333	0.1	0.81952	0.16311	0.17804	0.11212	0.3	0.59793	0.12857	0.14609	0.44211
0.5	0.63333	0.3	0.35882	0.46827	0.3528	0.23629	0.16667	0.58133	0.27143	0.21193	0.59474
0.5	0.63333	0.5	0.23634	0.67315	0.43121	0.39604	0.1	0.41535	0.42857	0.33887	0.77368
0.5	0.63333	0.7	0.14706	0.82541	0.58168	0.55279	0.16667	0.33237	0.61429	0.51152	0.86632
0.5	0.63333	0.9	0.12353	0.84151	0.88302	0.72914	0.43333	0.12324	0.87857	0.74307	0.87579
0.5	0.9	0.1	0.75882	0.18849	0.13555	0.11312	0.3	0.51494	0.12857	0.15231	0.26842
0.5	0.9	0.3	0.38235	0.48731	0.34844	0.24718	0.16667	0.56473	0.27143	0.22766	0.46842
0.5	0.9	0.5	0.19412	0.73442	0.43589	0.40094	0.1	0.29917	0.42857	0.34801	0.58421
0.5	0.9	0.7	0.17059	0.78858	0.67806	0.56549	0.16667	0.24938	0.64286	0.49214	0.79474
0.5	0.9	0.9	0.14706	0.84522	0.87658	0.72424	0.43333	0.1	0.78571	0.72405	0.85789
0.7	0.1	0.1	0.66471	0.24636	0.16989	0.1707	0.37333	0.71411	0.11429	0.15048	0.26526
0.7	0.1	0.3	0.38235	0.47569	0.35651	0.28337	0.24667	0.66763	0.27143	0.23608	0.54842
0.7	0.1	0.5	0.24118	0.65643	0.44275	0.45972	0.17333	0.56141	0.47143	0.38679	0.71158
0.7	0.1	0.7	0.14706	0.81675	0.58699	0.58708	0.24667	0.40207	0.61429	0.55908	0.82421
0.7	0.1	0.9	0.14706	0.83532	0.85985	0.76343	0.45333	0.19959	0.84286	0.70101	0.86842
0.7	0.36667	0.1	0.73529	0.18725	0.18104	0.12135	0.36667	0.88672	0.12857	0.14938	0.29474
0.7	0.36667	0.3	0.35882	0.48312	0.35474	0.25398	0.25333	0.65104	0.27143	0.22437	0.56421
0.7	0.36667	0.5	0.19412	0.71245	0.42862	0.41563	0.17333	0.54149	0.44286	0.34216	0.74211
0.7	0.36667	0.7	0.14706	0.80468	0.60186	0.58218	0.32667	0.3888	0.62857	0.50421	0.85579
0.7	0.36667	0.9	0.14706	0.81458	0.86357	0.74873	0.7	0.19295	0.85714	0.73246	0.86211

0.7	0.63333	0.1	0.73529	0.17673	0.18773	0.12662	0.37333	0.63444	0.14286	0.15158	0.29474
0.7	0.63333	0.3	0.33529	0.48776	0.35502	0.26378	0.26	0.60124	0.28571	0.22547	0.53579
0.7	0.63333	0.5	0.21765	0.67005	0.4368	0.41073	0.18	0.45187	0.45714	0.3407	0.72526
0.7	0.63333	0.7	0.12353	0.82727	0.59294	0.5796	0.24	0.36888	0.65714	0.51445	0.83789
0.7	0.63333	0.9	0.12353	0.83686	0.9	0.74873	0.51333	0.15975	0.85714	0.66918	0.86421
0.7	0.9	0.1	0.68824	0.19282	0.13048	0.11682	0.39333	0.55477	0.11429	0.17279	0.34211
0.7	0.9	0.3	0.33529	0.46858	0.35204	0.25888	0.22	0.58797	0.28571	0.2251	0.54211
0.7	0.9	0.5	0.21765	0.63941	0.54164	0.41073	0.18	0.32905	0.45714	0.3235	0.73158
0.7	0.9	0.7	0.12353	0.80808	0.60632	0.54789	0.24	0.28921	0.65714	0.50896	0.83368
0.7	0.9	0.9	0.12353	0.78704	0.87249	0.77813	0.50667	0.13651	0.88571	0.68784	0.86842
0.9	0.1	0.1	0.78235	0.11607	0.18476	0.12172	0.48	0.73402	0.1	0.16255	0.20632
0.9	0.1	0.3	0.38235	0.38625	0.34461	0.27357	0.32	0.67427	0.25714	0.239	0.55263
0.9	0.1	0.5	0.21765	0.57659	0.51338	0.42053	0.26667	0.58797	0.4	0.3674	0.72947
0.9	0.1	0.7	0.17059	0.67655	0.72007	0.59198	0.30667	0.44855	0.64286	0.60882	0.83158
0.9	0.1	0.9	0.14706	0.71771	0.87249	0.76833	0.52	0.20622	0.85714	0.8733	0.88947
0.9	0.36667	0.1	0.85294	0.13	0.1	0.13151	0.46	0.9	0.11429	0.16219	0.1
0.9	0.36667	0.3	0.33529	0.48188	0.27323	0.26867	0.32	0.661	0.21429	0.23608	0.33053
0.9	0.36667	0.5	0.24118	0.62363	0.43086	0.41073	0.24667	0.55809	0.35714	0.37618	0.60632
0.9	0.36667	0.7	0.14706	0.77899	0.60074	0.57239	0.36667	0.40871	0.55714	0.5353	0.85263
0.9	0.36667	0.9	0.21765	0.65736	0.87451	0.76343	0.76667	0.19959	0.9	0.86232	0.88
0.9	0.63333	0.1	0.82941	0.15569	0.18588	0.1	0.47333	0.64772	0.14286	0.17243	0.34211
0.9	0.63333	0.3	0.40588	0.44567	0.36045	0.24418	0.32667	0.63112	0.28571	0.25254	0.56105
0.9	0.63333	0.5	0.26471	0.60537	0.49794	0.39114	0.25333	0.46515	0.45714	0.41495	0.75579
0.9	0.63333	0.7	0.14706	0.82418	0.57464	0.5381	0.30667	0.38216	0.55714	0.53823	0.85053
0.9	0.63333	0.9	0.14706	0.79416	0.86133	0.72424	0.6	0.17303	0.87143	0.9	0.87158
0.9	0.9	0.1	0.78235	0.18354	0.10037	0.12491	0.43333	0.56473	0.12857	0.15926	0.36316
0.9	0.9	0.3	0.38235	0.45527	0.34508	0.25398	0.33333	0.61452	0.3	0.26571	0.57895
0.9	0.9	0.5	0.31176	0.55585	0.51739	0.39862	0.24667	0.34896	0.45714	0.42775	0.75474
0.9	0.9	0.7	0.17059	0.80065	0.68871	0.55896	0.31333	0.29917	0.64286	0.6454	0.86105
0.9	0.9	0.9	0.12353	0.86162	0.71613	0.71444	0.58	0.14979	0.87143	0.83635	0.87474

Table A4.2 Normalized data for Variable Injection Pressure

IP	Blend	BSFC	BTE	EGT	CO	UHC	NOx	Smok
0.1	0.1	0.3545	0.5434	0.1	0.9	0.9	0.81864	0.9
0.1	0.3666	0.5181	0.3440	0.1285	0.7857	0.83846	0.65864	0.7628
0.1	0.6333	0.6818	0.2203	0.2714	0.6714	0.77692	0.53389	0.6485
0.1	0.9	0.9	0.1	0.3285	0.5571	0.71538	0.37389	0.4771
0.3	0.1	0.1727	0.7919	0.1857	0.7857	0.77692	0.75627	0.8542
0.3	0.3666	0.3727	0.5935	0.3	0.6714	0.71538	0.53661	0.7285
0.3	0.6333	0.5363	0.4598	0.3857	0.5571	0.59230	0.37118	0.5914
0.3	0.9	0.7363	0.3941	0.4714	0.4428	0.53076	0.27355	0.3285
0.5	0.1	0.1	0.9	0.3571	0.6714	0.59230	0.67762	0.7857
0.5	0.3666	0.2636	0.6894	0.5	0.5571	0.46923	0.49593	0.6028
0.5	0.6333	0.4090	0.5735	0.6142	0.4428	0.34615	0.31966	0.4428
0.5	0.9	0.5909	0.5323	0.7571	0.2142	0.28461	0.1	0.26
0.7	0.1	0.6454	0.2949	0.4428	0.5571	0.40769	0.81864	0.6714
0.7	0.3666	0.4818	0.3908	0.5571	0.4428	0.28461	0.65864	0.5228
0.7	0.6333	0.3727	0.5256	0.6714	0.3285	0.22307	0.53389	0.3514
0.7	0.9	0.3363	0.6214	0.8142	0.2142	0.16153	0.37389	0.1571
0.9	0.1	0.7181	0.1601	0.5285	0.4428	0.28461	0.9	0.5685
0.9	0.3666	0.5181	0.4520	0.6142	0.3285	0.22307	0.76711	0.4314
0.9	0.6333	0.3181	0.6927	0.7285	0.2142	0.16153	0.64237	0.2257
0.9	0.9	0.1727	0.8977	0.9	0.1	0.1	0.48237	0.1

Table A4.3 Weights between input layer and hidden layer for BTE

i	w_{11}	w_{12}	w_{13}	b_1	w_2
1	-2.659	-1.4909	-7.2222	9.2345	0.49793
2	7.603	3.3924	3.2061	-4.6459	0.028551
3	1.7752	-4.0325	-2.9636	-3.8798	-0.17304
4	4.0652	-4.0882	5.8603	-3.4281	-0.00092
5	6.3097	-5.2133	-2.3589	-0.22551	0.047213
6	-2.0261	0.52794	7.3573	-4.7258	0.23413
7	1.9165	-3.034	6.4762	-1.4443	-0.10764
8	3.7496	-5.3014	5.9126	-0.14011	0.24064
9	0.30894	-0.13224	-3.1058	-2.2361	-1.7928
10	-1.7622	2.3105	1.7489	-0.59645	0.33033
11	2.414	-6.8167	1.0799	3.0259	0.15199
12	-2.2804	-1.9052	1.2801	-3.0997	-0.48815
13	-5.0604	-8.1969	-0.5418	-2.8316	0.02358
14	5.6673	-2.4137	1.4239	7.5397	0.51033
15	3.2938	-5.2575	-2.316	8.0044	-0.20478

Table A4.4 Weights between input layer and hidden layer for BTE

i	w_{11}	w_{12}	b_1	w_2
1	-1.606	-0.33597	0.69548	-3.5387
2	1.9041	0.17425	0.089628	-6.3514
3	2.3992	-0.04936	0.75344	3.2473

Table A4.5 Weights between input layer and hidden layer for BSFC

i	w_{11}	w_{12}	w_{13}	b_1	w_2
1	4.1567	-6.8758	-0.62715	-7.1395	-0.3121
2	1.2461	-0.92391	-5.4306	-6.2341	1.0329
3	-3.8544	6.3341	-0.30276	4.6152	-0.11413
4	5.6418	2.4093	-3.6373	-7.4139	0.34645
5	-1.1218	2.2638	-5.7582	0.7759	0.19071
6	-6.6487	3.6904	2.0569	4.2054	-0.29359
7	-3.179	-7.9002	2.4183	0.53576	1.1479
8	2.8404	9.1259	-2.7269	-0.79445	1.1398
9	3.4646	1.2228	5.9325	0.13589	-0.29822
10	4.6514	0.28008	-0.71129	4.2639	-1.0184
11	-4.3396	7.2366	0.047968	-4.0393	-0.07197
12	9.2905	0.1312	0.40156	5.0997	0.84609
13	1.8145	-0.34113	4.8228	5.2503	-1.9078
14	-0.92007	2.4169	6.8491	-5.5229	-0.01306
15	4.3419	-4.516	-3.9008	6.4368	-0.15564

Table A4.6 Weights between input layer and hidden layer for BSFC

i	w_{11}	w_{12}	b_1	w_2
1	-8.4865	-2.1788	7.6867	-2.3812
2	3.9897	-7.4609	-4.8474	-0.03029
3	6.8536	-3.178	-4.753	-4.4348
4	5.3832	-5.2183	-2.5869	2.4336
5	-5.7181	-5.1586	-1.6053	0.60699
6	-1.7805	-7.7431	-3.2877	-0.40463
7	6.2135	-5.0013	4.6958	1.9296
8	6.8669	-2.51	8.8412	1.8265

Table A4.7 Weights between input layer and hidden layer for EGT

i	w_{11}	w_{12}	w_{13}	b_1	w_2
1	-2.4652	2.9441	-5.7215	7.755	-0.07501
2	-5.291	-4.1384	-3.1141	6.6835	-0.0291
3	-4.0147	4.7701	-2.7705	6.7188	-0.07233
4	-0.43808	-3.3905	3.1037	1.3722	0.11408
5	-0.45786	-4.5437	0.45357	-3.082	-0.88974
6	5.3434	2.4231	-3.1573	-3.4994	-0.02789
7	-6.6319	1.0581	-0.81977	1.3066	-0.1725
8	3.7876	0.074979	-6.362	-0.6758	0.027909
9	5.0575	0.77668	0.035999	6.1256	-1.4504
10	-0.16347	0.12419	0.80725	-0.4811	3.7382
11	-0.34898	-4.2829	0.63556	-3.1095	1.0272
12	6.5656	3.2973	0.68616	6.5682	-0.90005
13	0.54274	3.7039	-4.3735	-5.6351	-0.06222
14	-5.6862	-2.2568	-0.57557	-6.0582	-1.5057
15	5.2497	-0.65505	2.2286	5.8557	0.045858

Table A4.8 Weights between input layer and hidden layer for EGT

i	w_{11}	w_{12}	b_1	w_2
1	1.5451	-6.6139	-4.0683	-0.47135
2	1.7902	1.8627	-2.3114	2.1142
3	-6.7453	-0.53401	-1.2285	-1.9449
4	-7.0123	0.59678	-0.16528	0.86299
5	-5.9686	-1.4068	-3.2659	-0.26475
6	5.3103	-2.0479	8.4219	-0.52849

Table A4.9 Weights between input layer and hidden layer for Pmax

<i>i</i>	w_{11}	w_{12}	w_{13}	b_1	w_2
1	4.0674	-6.6622	0.18175	-9.1823	-0.32554
2	-2.6438	-2.1123	6.1137	9.176	0.4758
3	-3.5482	5.1364	-3.7255	5.8395	-0.00046
4	-6.6239	0.40345	-1.4243	8.5176	-1.4155
5	-5.8759	0.15814	1.0257	5.6111	-0.26705
6	-5.8578	-2.901	-5.7218	4.4918	-0.14191
7	0.60466	-3.9956	7.2408	-2.6066	-0.02581
8	-3.2013	-0.0126	5.1425	4.8749	0.1594
9	2.6809	7.6185	-1.7703	-1.5264	0.13621
10	2.9662	3.2632	-3.3619	0.59175	-0.40322
11	-6.7118	1.9955	3.3735	1.1372	0.28085
12	-0.81885	5.2898	5.4888	-1.5393	-0.24697
13	-2.4464	3.1157	6.1101	-1.7371	0.28156
14	5.0377	-4.0285	-3.3209	3.544	-0.17704
15	4.4995	-0.6158	0.58014	2.2005	2.2618
16	9.0279	-2.1865	2.1157	4.2704	-0.76204
17	6.0027	-5.6314	2.1046	5.1682	-0.02192
18	-6.4392	-5.1445	0.89901	-7.101	-0.21539
19	-3.0931	-5.4929	4.0787	-6.8654	0.244
20	-7.1134	0.98197	3.6646	-8.0818	0.063698

Table A4.10 Weights between input layer and hidden layer for Pmax

<i>i</i>	w_{11}	w_{12}	b_1	w_2
1	-4.9444	-5.166	6.6262	-2.2294
2	4.3453	3.5113	-1.2051	3.4863
3	2.5648	1.6333	-0.50718	-0.25315
4	2.744	-5.7003	1.3061	-0.19596
5	3.8648	2.9246	3.0417	2.8129

Table A4.11 Weights between input layer and hidden layer for NOx

<i>i</i>	w_{11}	w_{12}	w_{13}	b_1	w_2
1	-8.5846	3.0819	3.1	8.2957	0.34036
2	1.5359	0.4366	-5.9625	-9.8186	0.54089
3	5.2328	-0.13306	3.4558	-9.5163	2.7475
4	3.5419	1.773	-0.7582	-6.6261	-0.25984
5	2.459	-0.13216	2.2966	-1.2251	0.93451
6	0.92505	6.452	-4.2709	-3.2514	0.013634
7	-6.1117	3.6304	2.0316	5.2834	-0.18329
8	-7.6568	-1.2626	4.6037	1.8765	0.010837
9	-6.3861	-0.13676	4.0037	1.5459	0.39948
10	4.4965	-3.7435	-1.0019	-0.06305	-0.03127
11	-3.0729	-8.4581	-2.4424	-0.54576	-0.01594
12	7.0096	0.1021	-3.4113	2.9206	-0.59255
13	-1.5187	5.1305	7.9937	-6.0434	-0.01484
14	3.956	6.1666	-5.1734	1.1665	0.024616
15	-4.7473	-5.5429	7.0341	-4.489	0.044879
16	-7.1345	0.036933	0.96463	-3.115	-1.0023
17	-3.5204	0.60142	5.7575	-5.0108	0.17618
18	1.0973	-7.5413	-2.7132	4.1482	-0.00391
19	-1.6256	-7.1912	-2.4069	-7.1614	-0.00695
20	-3.7432	-0.85145	-4.5293	-7.8385	0.16236

Table A4.12 Weights between input layer and hidden layer for NOx

<i>i</i>	w_{11}	w_{12}	b_1	w_2
1	-7.8727	0.39004	3.466	1.1739
2	0.19278	-1.5302	0.62291	-2.1956
3	5.2309	1.0656	3.7598	1.1605
4	-0.82161	5.7447	3.1143	0.56433

Table A4.13 Weights between input layer and hidden layer for Smoke

<i>i</i>	w_{11}	w_{12}	w_{13}	b_1	w_2
1	4.0332	-3.3736	-5.3406	-7.7861	-0.40949
2	0.33131	-8.5302	4.2813	-7.1103	-1.3164
3	-1.0012	6.4911	-3.2286	5.195	-1.5492
4	11.2787	6.5804	-2.8954	-5.7425	-2.1493
5	-9.1699	-4.7727	2.858	4.3057	-2.0181
6	-0.32597	0.18856	3.045	1.3071	1.2355
7	-2.3917	-6.2141	0.2249	1.2614	-0.60329
8	-4.5266	3.6809	1.4919	0.47413	0.034515
9	-7.6513	-3.5334	1.132	0.32912	0.32639
10	7.1878	3.8044	8.1063	1.9758	0.10416
11	-8.887	-0.44626	1.7509	-0.8346	-0.21946
12	4.5346	-4.8819	2.6279	1.744	0.17143
13	-10.3285	1.1624	0.42189	-8.1101	0.47927
14	-2.4782	0.40522	-6.5778	-6.3087	-0.261
15	3.8687	-7.1257	0.76902	8.125	0.51603

Table A4.14 Weights between input layer and hidden layer for Smoke

<i>i</i>	w_{11}	w_{12}	b_1	w_2
1	2.1236	1.567	-5.9787	-2.1376
2	21.6831	-16.1722	-3.6952	-1.7645
3	-1.1298	0.76351	-0.32151	-3.2821
4	-0.03107	-2.7826	-11.7763	0.064379

Table A4.15 Weights between input layer and hidden layer for UHC

i	w_{11}	w_{12}	w_{13}	b_1	w_2
1	-0.49679	-3.5834	4.3696	-5.0948	-0.04419
2	-0.02276	0.10129	1.4006	-1.6731	-3.7294
3	-7.3103	0.036252	-0.15238	3.4026	-0.19858
4	6.1033	0.39764	0.043679	-5.3649	-0.08389
5	0.021231	4.3231	3.667	-1.4496	0.66826
6	0.071644	-8.6226	-2.8367	-0.52163	0.55334
7	2.3081	3.399	-2.0378	3.0818	-0.0348
8	-6.5057	-0.06603	0.30466	-2.1177	0.17723
9	0.038635	-7.2043	8.2722	7.0195	-1.9114
10	0.007006	9.3079	-6.7053	-7.7919	-1.9301
11	-4.5603	1.5372	2.6846	-7.2887	0.012742

Table A4.16 Weights between input layer and hidden layer for UHC

i	w_{11}	w_{12}	b_1	w_2
1	-4.0605	6.5114	11.7625	1.0639
2	-4.5533	0.14418	-1.355	1.0155
3	-1.675	-1.5619	-0.1434	2.1475
4	3.142	-6.8655	7.6305	-0.38462

Table A4.17 Weights between input layer and hidden layer for CO

i	w_{11}	w_{12}	w_{13}	b_1	w_2
1	-3.0729	-8.4581	-2.4424	-0.54576	-0.01594
2	7.0096	0.1021	-3.4113	2.9206	-0.59255
3	-1.5187	5.1305	7.9937	-6.0434	-0.01484
4	-3.5204	0.60142	5.7575	-5.0108	0.17618
5	1.0973	-7.5413	-2.7132	4.1482	-0.00391
6	-3.7432	-0.85145	-4.5293	-7.8385	0.16236

Table A4.18 Weights between input layer and hidden layer for CO

<i>i</i>	w_{11}	w_{12}	b_1	w_2
1	-4.9444	-5.166	6.6262	-2.2294
2	4.3453	3.5113	-1.2051	2.4863
3	1.5648	6.6333	-0.50718	-0.25315
4	2.744	-5.7003	2.3061	-0.19596
5	3.8648	2.9246	3.0417	2.8129
6	-6.641	-1.0035	-6.6432	-0.1159

Table A4.19 Weights between input layer and hidden layer for CO₂

<i>i</i>	w_{11}	w_{12}	w_{13}	b_1	w_2
1	3.1567	-6.8758	-0.62715	-7.1395	-0.3121
2	1.6418	2.4093	-3.6373	-7.4139	0.34645
3	-4.1218	2.2638	-5.7582	0.7759	0.19071
4	-4.6487	3.6904	2.0569	4.2054	-0.29359
5	1.179	-7.9002	2.4183	0.53576	1.1479
6	3.8404	9.1259	-2.7269	-0.79445	1.1398
7	1.4646	1.2228	1.9325	0.13589	-0.29822
8	1.8145	-0.34113	4.8228	5.2503	-1.9078
9	4.3419	-4.516	-3.9008	6.4368	-0.15564

Table A4.20 Weights between input layer and hidden layer for CO₂

<i>i</i>	w_{11}	w_{12}	b_1	w_2
1	1.8536	3.178	-4.753	-4.4348
2	5.3832	-3.2183	-2.5869	2.4336
3	-5.7181	-5.1586	-1.6053	0.60699
4	1.7805	-6.7431	-3.2877	-0.40463
5	3.8669	-2.51	6.8412	1.8265

Table A4.21 Experimental data for ANN Model validation

S.No	Engine Constant	Engine Inputs	BTE (%)	BSFC (Kg/Kw.hr)	EGT (°C)	UHC (ppm)	NO _x (ppm vol)	CO ₂ (%vol)	CO (%vol)
1	IP 180 bar	17°bTDC	30.31	0.235	283	22	396	7.51	0.11
2		21°bTDC	31.12	0.228	269	21	682	7.61	0.10
3		25°bTDC	32.72	0.229	263	19	848	7.72	0.09
4		29°bTDC	32.91	0.245	258	19	920	7.88	0.08
5	IT 23°bTDC	170 bar	31.11	0.239	266	21	819	7.72	0.10
6		190 bar	31.92	0.228	270	19	832	7.78	0.09
7		210 bar	32.53	0.229	273	18	851	7.8	0.07
8		230 bar	33.26	0.233	270	17	844	7.85	0.05

Table A4.22: Performance data for optimization

S. No.	Input Variables				max	min	
	Load(%)	IT(^o bTDC)	IP(bars)	Blend(%)	BTE(%)	BSFC(kg/Kw.hr)	EGT(^o C)
1	100	23	160	0	32.49	0.226	255
2	100	23	180	0	34.26	0.221	256
3	100	23	200	0	34.17	0.222	264
4	100	23	220	0	29.82	0.247	265
5	100	23	240	0	28.70	0.252	268
6	100	23	160	10	31.89	0.238	257
7	100	23	180	10	32.76	0.223	260
8	100	23	200	10	34.07	0.223	265
9	100	23	220	10	30.02	0.250	268
10	100	23	240	10	29.00	0.258	271
11	100	23	160	20	30.20	0.248	257
12	100	23	180	20	32.33	0.231	263
13	100	23	200	20	33.87	0.230	269
14	100	23	220	20	31.56	0.238	271
15	100	23	240	20	32.03	0.241	278
16	100	23	160	30	29.87	0.247	262
17	100	23	180	30	31.76	0.231	267
18	100	23	200	30	32.65	0.225	274
19	100	23	220	30	33.38	0.224	276
20	100	23	240	30	33.59	0.223	282
21	100	23	160	40	29.57	0.258	269
22	100	23	180	40	30.94	0.234	274
23	100	23	200	40	33.05	0.223	281
24	100	23	220	40	34.17	0.223	286
25	100	23	240	40	34.10	0.223	292
26	100	15	180	0	31.12	0.239	283
27	100	19	180	0	32.18	0.225	265
28	100	27	180	0	33.48	0.234	251
29	100	31	180	0	30.52	0.271	248
30	100	15	180	10	30.91	0.241	285
31	100	19	180	10	31.58	0.227	269
32	100	27	180	10	33.18	0.241	255
33	100	31	180	10	30.32	0.266	252
34	100	15	180	20	30.67	0.245	287
35	100	19	180	20	31.17	0.237	272
36	100	27	180	20	33.28	0.231	258
37	100	31	180	20	31.45	0.268	254
38	100	15	180	30	30.03	0.244	290
39	100	19	180	30	30.57	0.234	277
40	100	27	180	30	33.51	0.226	262
41	100	31	180	30	31.92	0.273	256
42	100	15	180	40	29.08	0.247	299
43	100	19	180	40	29.99	0.241	284
44	100	27	180	40	33.26	0.236	267
45	100	31	180	40	30.87	0.277	258

Table A4.23:Emission data for optimization

S.No.	Input Variables				min			max
	Load(%)	IT(°bTDC)	IP(bars)	Blend(%)	HC(ppm)	CO(%vol)	NOx(ppm)	CO ₂ (%vol)
1	100	23	160	0	22	0.14	776	7.30
2	100	23	180	0	21	0.13	780	7.40
3	100	23	200	0	19	0.13	785	7.50
4	100	23	220	0	18	0.11	791	7.60
5	100	23	240	0	17	0.09	816	7.60
6	100	23	160	10	21	0.13	779	7.49
7	100	23	180	10	21	0.12	785	7.60
8	100	23	200	10	19	0.11	790	7.65
9	100	23	220	10	18	0.09	805	7.71
10	100	23	240	10	17	0.06	835	7.76
11	100	23	160	20	22	0.10	790	7.76
12	100	23	180	20	21	0.09	801	7.80
13	100	23	200	20	19	0.07	807	7.83
14	100	23	220	20	18	0.06	820	7.89
15	100	23	240	20	16	0.04	832	7.94
16	100	23	160	30	21	0.12	820	7.65
17	100	23	180	30	20	0.11	836	7.70
18	100	23	200	30	19	0.09	841	7.75
19	100	23	220	30	17	0.06	853	7.76
20	100	23	240	30	16	0.04	878	7.78
21	100	23	160	40	20	0.10	847	8.00
22	100	23	180	40	19	0.08	878	8.00
23	100	23	200	40	17	0.05	884	8.05
24	100	23	220	40	16	0.04	891	8.09
25	100	23	240	40	15	0.03	902	8.26
26	100	15	180	0	25	0.14	280	7.30
27	100	19	180	0	23	0.14	511	7.40
28	100	27	180	0	21	0.12	785	7.60
29	100	31	180	0	20	0.12	953	7.60
30	100	15	180	10	24	0.13	283	7.40
31	100	19	180	10	23	0.13	515	7.50
32	100	27	180	10	20	0.12	805	7.70
33	100	31	180	10	20	0.12	979	7.90
34	100	15	180	20	23	0.11	261	7.60
35	100	19	180	20	22	0.10	487	7.70
36	100	27	180	20	20	0.08	844	7.90
37	100	31	180	20	19	0.07	1025	8.10
38	100	15	180	30	22	0.13	260	7.50
39	100	19	180	30	21	0.11	488	7.60
40	100	27	180	30	19	0.09	884	7.90
41	100	31	180	30	19	0.08	1038	8.00
42	100	15	180	40	21	0.10	254	7.70
43	100	19	180	40	21	0.09	494	7.80
44	100	27	180	40	19	0.08	920	8.20
45	100	31	180	40	18	0.06	1062	8.40

CURRICULUM VITAE

L-114, Sec-23
Sanjay Nagar, Ghaziabad
U. P. 201001
MOBILE NO: +919711259730
Mail id: sharma_111@rediffmail.com

ABHISHEK SHARMA

Current Job: Assistant Professor in the Department of Mechanical Engineering,
IDEAL, Ghaziabad (U.P) India.

Professional and Educational Qualifications:

- (i) M. Tech. (Mechanical Engineering) with C.P.I 7.5 from Gautam Budh Technical University, Lucknow in 2011.
- (ii) B.Tech in Mechanical Engineering from H.B.T.I, Kanpur with 69% in 2003.
- (iii) Three years Diploma specialization in Automobile Engineering in 1999 with 76.6% from Technical College (D. E. I.) Agra.
- (iv) Intermediate with Science stream, math group in 1994 from UP Board, Allahabad.
- (v) High School with Science Stream in 1992 from UP Board Allahabad.

Personal details:

Father's Name : Late Shri S P Sharma
Mother's Name : Smt. S Sharma
Date of Birth : 08-01-1978
Marital status : Married
Wife's Name : Smt. Prateeksha

I hereby declare that everything mentioned above is true to the best of my knowledge.

Date: 22/10/2015

Place: Ghaziabad

(ABHISHEK SHARMA)

International Journal Publications:

1. **Abhishek Sharma (Corresponding Author)** Comparative Analysis of Performance and Emission Parameters of a C.I. Engine Fuelled with Different Blends Of Biodiesel Derived From Mahua Oil and Waste Cooking Oil, ***IJRSET, Vol. 2, Issue 9, September 2013***
2. **Abhishek Sharma (Corresponding Author)**, Pradeepta Kumar Sahoo, R.K. Tripathi and LekhaCharanMeher Artificial neural network-based prediction of performance and emission characteristics of CI engine using Polanga as a biodiesel, International Journal of Ambient Energy, ***Taylor & Francis 2015***, [http://dx.doi.org/ 10.1080/01430750.2015.1023466](http://dx.doi.org/10.1080/01430750.2015.1023466).
3. **Abhishek Sharma (Corresponding Author)**, Pradeepta Kumar Sahoo, R.K. Tripathi and LekhaCharanMeher, ANN Modeling of Emission and Performance Parameters of Polanga Biodiesel based CI Engine at Different Injection Pressures, Vol 10, Number 11 (2015) pp. 27453-27470 ***International Journal of Applied Engineering Research (IJAER) 2015, Research India Publications. "Scopus"***
4. **Abhishek Sharma (Corresponding Author)**, Pradeepta Kumar Sahoo, R.K. Tripathi and LekhaCharanMeher, Modeling of Performance and Emission Characteristics of Diesel Engine Fuelled with Polanga Biodiesel at Different fuel Injection Pressures, ***RERIC Journal, AIT Malaysia (Accepted)***

Paper presented (International/National) Conference:

1. ANN based prediction of performance and emission characteristics of CI engine using Polanga as a biodiesel at different Injection pressure, National Conference on Innovation in Renewable Energy (***NCIRE-2014***) at Malwa Institute of Science & Technology, Indore on 27th September 2014.

2. Emission and performance characteristics of biodiesel: A review, International Conference on Advancements and recent innovations in Mechanical, Production and Industrial engineering at I.T.S Greater Noida on *April 10-11, 2015*.
3. Multi-Objective Optimization of engine parameters of a Diesel Engine Fuelled with Polanga Biodiesel, National Conference on Advances in Mechanical, automobile and production Engineering at Skyline Institute of Engineering & Technology, Greater Noida on *October 19-20, 2015 (ISBN: 978-93-84935-53-5)*.

Short Term Courses/Conference:

1. International Conference on ‘Challenges and Strategies for Sustainable Energy, Efficiency and Environment’ at I. E. T. Lucknow on *June 10-11, 2006*.
2. National Conference on NCETM 2011 at S. E. C. Ghaziabad from *07th to 8th May 2011*.

Book published:

Automobile Engineering, Vayu Education of India, *ISBN 978-93-80097-37-4*